Deutsches GeoForschungsZentrum GFZ, Helmholtz-Zentrum Potsdam,

Sektion 5.3 Geomikrobiologie

Phylogenetic and physiological characterization of deep-biosphere microorganisms in El'gygytgyn Crater Lake sediments

---

DISSERTATION

zur Erlangung des Grades eines Doktors der Naturwissenschaften

"doctor rerum naturalium"

– Dr. rer. nat. –

in der Wissenschaftsdisziplin "Mikrobiologie"

Eingereicht an der

Mathematisch-Naturwissenschaftlichen Fakultät

der Universität Potsdam

von

Janine Heise

geb. Görsch

Potsdam, Februar 2017

Published online at the
Institutional Repository of the University of Potsdam:
URN urn:nbn:de:kobv:517-opus4-403436
http://nbn-resolving.de/urn:nbn:de:kobv:517-opus4-403436

Preface

This work was funded by the German Research Foundation (DFG) in the framework of the priority program SPP 1006 - International continental scientific drilling program (ICDP) by grants to Dirk Wagner (WA-1554/14-1+2) and is primarily focused on the microbiological characterization of the deep-biosphere of El'gygytgyn Crater Lake sediments dated to be up to 3.6 million years old.

Sediments of the El'gygytgyn Crater Lake were retrieved during the ICDP Lake El'gygytgyn Drilling project in 2008 and 2009. Subsampling was done in the University of Cologne/ Institute of Geology and Mineralogy. The laboratory and evaluating work was mainly performed at the German Research Centre for Geosciences in Potsdam and partially in Copenhagen/Denmark as part of a research visit (grant of the German Academic Exchange Service, DAAD, Kurzstipendium für Doktoranden, Referat 313) at the Center for Permafrost (CENPERM) and the Geological Survey of Denmark and Greenland (GEUS). Half a year of the research period was funded by a scholarship of the University of Potsdam/Coordination Office for Equal Opportunities (Brückenprogramm zur Förderung des Promotionsabschlusses).

The following thesis is written in English and presented as a monograph to the Faculty of Mathematics and Natural Science at the University of Potsdam. The materials and methods and the results are framed by a general introduction including the description of the study site, the scientific background as well as the objectives of the study. They are followed by a final synthesis encompassing a general conclusion, the most important results, and the critical remarks.

Table of Content

List of Abbreviations

16S rRNA	ribosomal ribonucleic acid of the small subunit
BLAST	Basic Local Alignment Search Tool
BP	before present
bp	base pairs
BSA	bovines serumalbumin
cDNA	complementary DNA
$\delta^{18}O$	ratio of ^{18}O to ^{16}O, used as temperature proxy
DFG	German Research Foundation (Deutsche Forschungsgemeinschaft)
DGGE	denaturing gradient gel electrophoresis
DNA	desoxyribonucleic acid
dNTP	deoxynucleotide triphosphates
DOC	dissolved organic carbon
dw	dry weight
eDNA	extracellular DNA
EMA	ethidium monoazide
ENA	European Nucleotide Archive
et al.	et alii (and others)
EW	Extreme arctic warmth
FA	fulvic acid
FISH	fluorescence in situ hybridization
G	glacial period
GuaHCL	guanidine hydrochloride
HA	humic acid
I	interglacial period
ICDP	International Continental Scientific Drilling Program
iDNA	intracellular DNA
ka	thousand years
LC	Largest cooling in Pliocene
LED	light-emitting diode
Ma	million years

mcrA gene	gene encoding methyl coenzyme-M reductase
MIS	Marine Isotopic Stage
mRNA	messenger ribonucleic acid
MTWM	mean temperature of the warmest month
NaP	sodium phosphate
NASA	National Aeronautics and Space Administration
NCBI	National Center for Biotechnology Information
NMDS	non-metric multidimensional scaling analysis
nt	nucleotide
NTU	Nephelometer Turbidity Unit
OD	optical density
ODP	Ocean Drilling Program
OTU	operational taxonomic unit
PANN	mean annual precipitation
PCR	polymerase chain reaction
PI	propidium iodide
PMA	propidium monoazide
PPW	Pliocene-Pleistocene warmth
PVPP	polyvinylpolypyrrolidon
QIIME	Quantitative Insights Into Microbial Ecology (open-source bioinformatics pipeline)
qPCR	quantitative (real time) PCR
R^2	coefficient of determination
RDA	redundancy analysis
rpm	revolutions per minute
rRNA	ribosomal ribonucleic acid
Si	silica
TC	total carbon
tDNA	total DNA
TOC	total organic carbon
TSS	total suspended solids
VBNC	viable but non-culturable cells
ww	wet weight
XRF	X-ray fluorescence

Summary

The existence of diverse and active microbial ecosystems in the deep subsurface – a biosphere that was originally considered devoid of life – was discovered in multiple microbiological studies. However, most of the studies are restricted to marine ecosystems, while our knowledge about the microbial communities in the deep subsurface of lake systems and their potentials to adapt to changing environmental conditions is still fragmentary. This doctoral thesis aims to build up a unique data basis for providing the first detailed high-throughput characterization of the deep biosphere of lacustrine sediments and to emphasize how important it is to differentiate between the living and the dead microbial community in deep biosphere studies.

In this thesis, up to 3.6 Ma old sediments (up to 317 m deep) of the El'gygytgyn Crater Lake were examined, which represents the oldest terrestrial climate record of the Arctic. Combining next generation sequencing with detailed geochemical characteristics and other environmental parameters, the microbial community composition was analyzed in regard to changing climatic conditions within the last 3.6 Ma to 1.0 Ma (Pliocene and Pleistocene). DNA from all investigated sediments was successfully extracted and a surprisingly diverse (6,910 OTUs) and abundant microbial community in the El'gygytgyn deep sediments were revealed. The bacterial abundance (10^{3}-10^{6} 16S rRNA copies g^{-1} sediment) was up to two orders of magnitudes higher than the archaeal abundance (10^{1}-10^{5}) and fluctuates with the Pleistocene glacial/interglacial cyclicality. Interestingly, a strong increase in the microbial diversity with depth was observed (approximately 2.5 times higher diversity in Pliocene sediments compared to Pleistocene sediments). The increase in diversity with depth in the Lake El'gygytgyn is most probably caused by higher sedimentary temperatures towards the deep sediment layers as well as an enhanced temperature-induced intra-lake bioproductivity and higher input of allochthonous organic-rich material during Pliocene climatic conditions. Moreover, the microbial richness parameters follow the general trends of the paleoclimatic parameters, such as the paleo-temperature and paleo-precipitation. The most abundant bacterial representatives in the El'gygytgyn deep biosphere are affiliated with the phyla *Proteobacteria*, *Actinobacteria*, *Bacteroidetes*, and *Acidobacteria*, which are also commonly distributed in the surrounding permafrost habitats. The predominated taxon was the halotolerant genus *Halomonas* (in average 60% of the total reads per sample).

Additionally, this doctoral thesis focuses on the live/dead differentiation of microbes in cultures and environmental samples. While established methods (e.g., fluorescence in situ hybridization, RNA analyses) are not applicable to the challenging El'gygytgyn sediments, two newer methods were adapted to distinguish between DNA from live cells and free (extracellular, dead) DNA: the propidium monoazide (PMA) treatment and the cell separation adapted for low amounts of DNA. The applicability of the DNA-intercalating dye PMA was successfully evaluated to mask free DNA of different cultures of methanogenic archaea, which play a major role in the global carbon cycle. Moreover, an optimal procedure to simultaneously treat bacteria and archaea was developed using 130 µM PMA and 5 min of photo-activation with blue LED light, which is also applicable on sandy environmental samples with a particle load of ≤ 200 mg mL^{-1}. It was demonstrated that the soil texture has a strong influence on the PMA treatment in particle-rich samples and that in particular silt and clay-rich samples (e.g., El'gygytgyn sediments) lead to an insufficient shielding of free DNA by PMA. Therefore, a cell separation protocol was used to distinguish between DNA from live cells (intracellular DNA) and extracellular DNA in the El'gygytgyn sediments. While comparing these two DNA pools with a total DNA pool extracted with a commercial kit, significant differences in the microbial composition of all three pools (mean distance of relative abundance: 24.1%, mean distance of OTUs: 84.0%) was discovered. In particular, the total DNA pool covers significantly fewer taxa than the cell-separated DNA pools and only inadequately represents the living community. Moreover, individual redundancy analyses revealed that the microbial community of the intra- and extracellular DNA pool are driven by different environmental factors. The living community is mainly influenced by life-dependent parameters (e.g., sedimentary matrix, water availability), while the extracellular DNA is dependent on the biogenic silica content. The different community-shaping parameters and the fact, that a redundancy analysis of the total DNA pool explains significantly less variance of the microbial community, indicate that the total DNA represents a mixture of signals of the live and dead microbial community.

This work provides the first fundamental data basis of the diversity and distribution of microbial deep biosphere communities of a lake system over several million years. Moreover, it demonstrates the substantial importance of extracellular DNA in old sediments. These findings may strongly influence future environmental community analyses, where applications of live/dead differentiation avoid incorrect interpretations due to a failed extraction of the living microbial community or an overestimation of the past community diversity in the course of total DNA extraction approaches.

Zusammenfassung

Innerhalb der letzten 20 Jahre wurden diverse und aktive mikrobielle Gemeinschaften in zahlreichen Habitaten der tiefen Biosphäre gefunden, in denen zuvor kein Leben denkbar war. Die mikrobiologischen Untersuchungen beschränken sich dabei meist auf marine Ökosysteme, wohingegen das Wissen über die tiefe Biosphäre von Seesystemen und die Anpassung der Mikroorganismen an sich ändernde klimatische Bedingungen noch sehr eingeschränkt ist. Ziel dieser Arbeit ist es, die mikrobielle Gemeinschaftsstruktur der tiefen Biosphäre des El'gygytgyn Kratersees in Hinblick auf klimatische Veränderungen der vergangenen 1,0 bis 3,6 Millionen Jahre zu charakterisieren, beeinflussende Umweltparameter zu detektieren und dabei zwischen der lebenden und toten mikrobiellen Gemeinschaft zu differenzieren. Die Seesedimente (43-317 m tief) weisen eine erstaunlich hohe Diversität (6910 OTUs) und Mikrobenfülle (10^{3}-10^{6} bakterielle, 10^{1}-10^{5} archaeale 16S rRNA Kopien g^{-1} Sediment) auf, wobei eine 2,5-fach höhere Diversität in den pliozänen Sedimenten im Vergleich zu den jüngeren pleistozänen Sedimenten detektiert werden konnte. Der Diversitätsanstieg mit zunehmendem Sedimentalter (und Tiefe) basiert höchstwahrscheinlich auf die erhöhte temperaturinduzierte Bioaktivität im See und dem erhöhten Eintrag von Organik reichen Material innerhalb des Pliozäns (feucht und warm).

Die Unterscheidung zwischen der DNA lebender Mikroben (intrazellulare DNA) und freier DNA (extrazellulare DNA, meist von toten Mikroben) wurde durch die Adaption von zwei Extraktionsmethoden, der Behandlung mit Propidium-Monoazid (PMA) und der Zellseparation, erreicht. Dabei wurde ein PMA-Protokoll (130 µM PMA, 5 Min Lichtaktivierung mit blauen LEDs) zur erfolgreichen Behandlung von Reinkulturen methanogener Archaeen etabliert, das auch für sandige Umweltproben (Partikelbeladung ≤ 200 mg mL^{-1}) nutzbar ist. Für die feinporigeren Seesedimente des El'gygytgyn Kratersees wurden die zellseparierten DNA-Pools der iDNA und eDNA mit dem Gesamt-DNA-Extrakt (kommerzielles Kit) verglichen, wobei die DNA-Pools starke Unterschiede in ihrer Zusammensetzung aufzeigten (24,1% Distanz basierend auf relative Häufigkeiten) und der Gesamt-DNA-Extrakt die lebende mikrobielle Gemeinschaft nur unzureichend widerspiegeln konnte. Individuelle Redundanzanalysen (RDA) zeigten, dass die mikrobielle Gemeinschaft der iDNA von lebensbeeinflussenden Parametern abhängig ist (u.a. Sedimentmatrix,

Wasserverfügbarkeit), wohingegen die der eDNA maßgeblich durch den Anteil an biogener Kieselerde (silica) beeinflusst wird.

Diese Arbeit stellt die erste umfangreiche Datenbasis der Diversität und Verteilung von Mikroorganismengemeinschaften in der tiefen Biosphäre eines Seesystems über mehrere Millionen Jahre dar. Zusätzlich zeigt die Studie, dass die Lebend/Tot-Unterscheidung, mit dem ein höherer Anteil der Varianz innerhalb der Gemeinschaft durch Umweltparameter erklärt werden kann, im Vergleich zur Gesamt-DNA-Extraktion ein wesentlicher Schritt zur genauen Widerspiegelung der mikrobiellen Gemeinschaft und deren Funktion in der Tiefen Biosphäre ist.

1 Introduction

The focus of this thesis is the microbiological investigation of deep sediments of the El'gygytgyn Crater Lake, one of a few study sites in the field of the deep biosphere of a lake system. The overall aim is to analyze microbial communities in up to 3.6 million years old sediments and to find the main community shaping environmental parameters. Next to the community analyses, the thesis emphasizes the differentiation between live and dead microorganisms in pure cultures of archaea and in environmental samples.

1.1 Microbial life in the deep biosphere

Microbiological studies over the last two decades have increasingly focused on life in the deep biosphere (Kallmeyer and Wagner, 2014). Deep biosphere habitats are physically located below the surface of continents and the bottom of the ocean (Edwards et al., 2012) and represent the most voluminous part of the biosphere (Kerr, 2002). Despite the lack of nutrients and strong biophysical challenges, the marine deep biosphere is expected to be occupied by living and metabolically active microorganisms (D'Hondt et al., 2004; Kallmeyer et al., 2012; Lomstein et al., 2012; Parkes et al., 1994). Microbes could be detected in hostile places, such as in 1500 meters deep water in Columbia River basalt lava, in 3.2 kilometers deep rocks of South African gold mines, or preserved even for more than 250 million years in ancient brine pockets in subterranean salt (Kerr, 2002). Life in the deep biosphere is characterized by extreme environmental conditions such as the absence of sunlight and limited oxygen penetration. Although microorganisms are exposed to a limited nutrient supply and strong stress conditions, such as high temperatures and pressures, a surprisingly high microbial abundance has been observed in the depth. Sub-seafloor sedimentary microbial abundance, for example, varied between $2.9 \cdot 10^{29}$ and $35.5 \cdot 10^{29}$ cells in dependence of the study (Kallmeyer et al., 2012; Whitman et al., 1998). This thesis investigates the lacustrine deep biosphere, instead of the much better researched marine and terrestrial deep biosphere.

For the marine subsurface microbiology, a decisive technical progress resulted from the deep coring in the frame of the Ocean Drilling Program (ODP) and later the Integrated Ocean Drilling Program (IODP), which replaced not only shallow sampling techniques but also enabled the examination of microbial life in sediments hundreds of meters to kilometers below the ocean

floor (Edwards et al., 2012). Since then, researchers have demonstrated in multiple cases the existence of diverse and active microbial ecosystems in the deep subsurface (D'Hondt et al. 2002; Edwards et al. 2012; Lomstein et al. 2012) and have confirmed a fundamental role of deep biosphere microorganisms in the global biogeochemical cycle over short and long time scales (Hoehler and Jørgensen, 2013; Schippers et al., 2010). Moreover, it is known that metabolic rates of sub-seafloor biospheres are orders of magnitudes lower than those of life on Earth's surface and that the inherent microbial community is adapted to an extraordinary low metabolic activity (D'Hondt et al., 2002). It has been suggested that deep biosphere microbes manage their lives in extreme slow motion in the way that they repair macromolecular damage but often are in a state of dormancy (Price and Sowers, 2004), or with an extremely long doubling time (once every 100-2,000 years, Biddle et al. 2006; or every 1,000 years, Jørgensen 2011).

In contrast to studies of marine deep biosphere, studies of the terrestrial deep biosphere are mostly use-case driven (Edwards et al., 2012; Fredrickson and Balkwill, 2006). A large portion of these studies examine the interaction between the microbial community and precious resources such as bacterial oil degradation in the underground (Bailey et al., 1973; Head et al., 2003) or microbial life in deep gold mines (Moser et al., 2005; Takai et al., 2001). Economically important topics are fossil energy sources, utilization of geothermal energy, and limited minerals and metals as well as the storage of gases (e.g., carbon dioxide or hydrogen) in the deep biosphere. Here, an increasing number of studies explore the groundwater (Ino et al., 2016) and hydrothermal waters microbiology (Dick et al., 2013; Schulze-Makuch and Kennedy, 2000) or consider the effect of various contaminations on subsurface microbial diversity or radioactive waste in deep repositories (De Lipthay et al., 2004; Fredrickson et al., 2004; Williams et al., 2013).

Our knowledge of the microbial composition and abundance in deep subsurface sediments of lakes is currently lacking. There is no comprehension about the lacustrine deep biosphere microorganisms and their possibility to adapt to changing environmental conditions. Previous studies are mostly limited to upper lake sediments of the Arctic (0.25-60 m, He et al. 2012; Comeau et al. 2012; Crump et al. 2012) or Antarctic environments (0.2-0.6 m, Peeters et al. 2012; Chen et al. 2005). For instance, He et al. (2012) demonstrated the response of methanotrophs of Arctic lake sediments to different incubation temperatures and showed that methylotrophs are also abundant in 0.20 m deep sediments at low temperatures (4°C and 10°C).

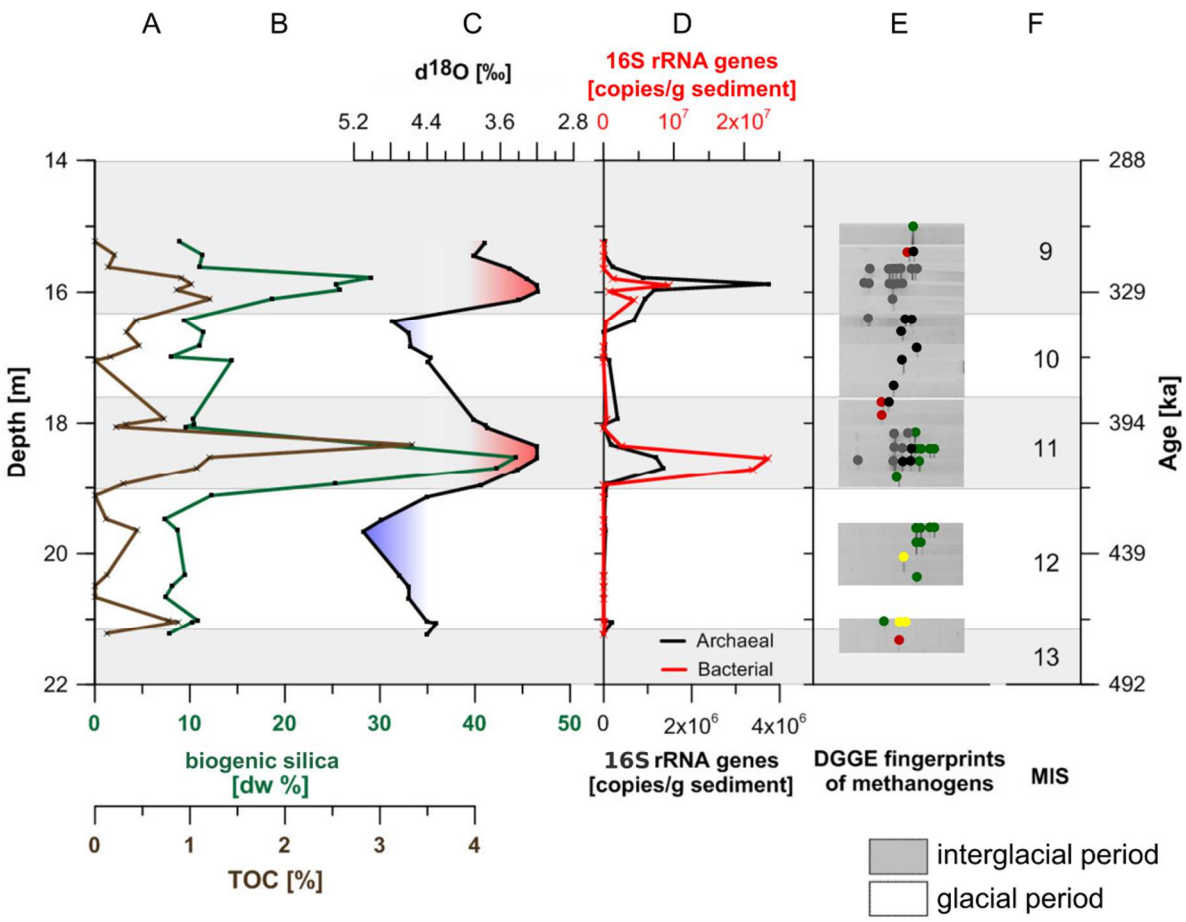

Figure 1.1: Depth profile of the upper 15-21 m of El'gygytgyn Crater Lake sediments with (**A**) the total organic carbon (TOC) in %, (**B**) the amount of biogenic silica as a measure of the bioproductivity in a lake (after Rosén et al. 2009), (**C**) the benthic $d^{18}O$ stack as a temperature proxy (Lisiecki and Raymo, 2005), (**D**) the bacterial (red) and archaeal (black) 16S rRNA genes in copies g^{-1} sediment ww, (**E**) the diversity pattern of denaturing gradient gel electrophoresis (DGGE) fingerprints of methanogenic archaea (*mcrA* gen), and (**F**) the corresponding marine isotope stages (MIS), whereby interglacial periods are highlighted in light-grey and glacial periods in white. The age-depth model of the sediments is based on Nowaczyk et al. 2013. DNA sequences of the DGGE bands were re-amplified and assigned to their next taxonomical neighbor *Methanosarcinales* (green), *Methanomicrobiales* (yellow), *Methanocellales* (red), methanogenic archaea (black) or *Crenarchaeota* (grey). Figure according to Görsch 2011.

There are also several studies evaluating the upper layers of the surrounding permafrost, focusing on methanogenic archaea (Allan et al., 2014; Ganzert et al., 2007), methanotrophic bacteria (Liebner and Wagner, 2007; Liebner et al., 2009), or the general bacterial community (0.28-28 m, Steven et al. 2007; Hinsa-Leasure et al. 2010; Yergeau et al. 2010).

The International Continental Scientific Drilling Program ICDP 5011-1 in 2008/09 retrieved up to 317 m deep sediments of the El'gygytgyn Crater Lake – which correspond to a maximal age

of 3.6 Ma – and facilitates for the first time a detailed microbial analysis of the lacustrine deep biosphere. Thereby, the previous master thesis (Görsch 2011) showed the following promising results on the microbial composition of the upper 20 m of the sediments. Firstly, the abundance and diversity of methanogens is increasing in interglacial periods (MIS 9 and 11) compared to glacial periods (MIS 10 and 12). Secondly, an indirect response of the microbial community to climate phases was observed caused by a better availability of nutrients within temperature-induced algae blooms and by higher bioactivity (Figure 1.1, modified after Görsch 2011). Following up, this thesis analyzes the microbial community of the deeper sediments (up to 317 m ≙ 3.6 Ma old) and performs correlation analyses with all relevant environmental parameters.

1.2 The El'gygytgyn Crater Lake and its climate history

The El'gygytgyn impact crater is located in the North East Russian Arctic (67.5° N, 172° E) (Figure 1.2, 1.3A) and was formed by a meteorite impact 3.6 million years ago. After the meteorite impact, the crater (18 km in diameter) was filled by a lake with a diameter of 12 km and a water depth of 170 m. The Crater Lake is one of the best preserved impact structures of the Earth (Layer, 2000) and it is the only known terrestrial impact structure that has formed in siliceous volcanic rocks (Gurov et al., 2005). It is described by a five-layer model (Figure 1.3B) including a water layer, two upper sedimentary layers, and two layers out of breccia material (Gebhardt et al., 2006). Since its formation, the lake was not superimposed by a glacier (Gebhardt et al., 2006) and thus a continuous accumulation of lake sediments with a total thickness of 317 m was possible. The resulting oldest continuous terrestrial climate record in the Arctic (Nolan and Brigham-Grette, 2007) contains information about the earlier climate history and the evolution of life since the meteorite impact.

The main sedimentation rates (Figure 1.3.1A) range between 4-5 cm ka^{-1} (youngest sediment material) to 45 cm ka^{-1} (3.6 to 3.3 Ma old sediment) (Nowaczyk et al. 2013). Today, the lake is surrounded by continuous permafrost with a mean thickness of approximately 340 m (Mottaghy et al., 2013). Frost weathering, slope dynamics, and fluvial outwash are the main drivers of erosion in the ~300 km^2 catchment area (Nolan and Brigham-Grette, 2007). The 50 seasonally active inlet streams cause a sediment transport of approximately 350 t per year into the lake, whereby the aeolian input contributes only to 2-5% of the total input (Fedorov et al., 2013). A single outlet, the Enmyvaam River, is located on the southeastern edge of the lake.

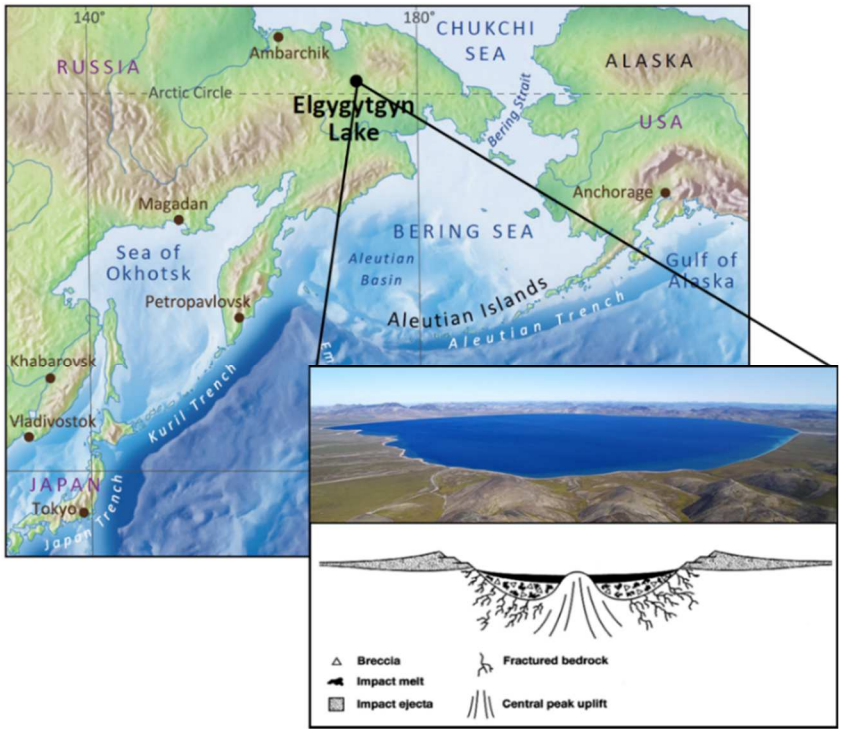

Figure 1.2: Location of the Lake El'gygytgyn (67.5°N, 172°E) in the North East Russian Arctic. The complex crater was formed by an impact 3.6 million years ago. The schematic view of the crater complex is inferred from NASA (http://craters.gsfc.nasa.gov/crater_diagram.html).

The current climate of the lake surroundings is cold, dry, and windy with a mean annual air temperature of -10.3 °C at 3 m above the ground (Nolan and Brigham-Grette, 2007), extreme temperatures of -40 °C in the winter and up to +26 °C in the summer, and a mean annual ground temperature of -6 °C at 20 m depth (Mottaghy et al., 2013). In a 2.5-year-long record between 2000 and 2003 (Nolan and Brigham-Grette, 2007), the water temperature of this (ultra)-oligotrophic, monomictic lake never exceeded 4 °C. The sediment temperature increases linearly with the depth, ranging from 6 °C at the water sediment interface to nearly 24 °C at bottom (5 °C/100 m, Mottaghy et al. 2013). Between mid-October and early- or mid-July, the lake is ice-covered (Nolan et al., 2002) and thermally stratified with partial oxygen-depletion, whereas the water column is fully mixed after the snowmelt in late summer. The vegetation of the Holocene is dominated by a herb tundra community of *Cyperaceae* and *Poaceae* with some *Betula* and *Salix* (Andreev et al., 2012).

Sediments of the El'gygytgyn Crater Lake were retrieved during an International Continental Scientific Drilling Program (ICDP, 5011-1) named "Scientific Drilling in El'gygytgyn Crater Lake" in autumn 2008 and spring 2009 (Melles et al., 2011). The drilling project resulted in a 317 m long composite profile, which consists of three sediment cores (Figure 1.3B, 5011-1 A-C) and covers the Arctic climate archive of the Pliocene and Pleistocene.

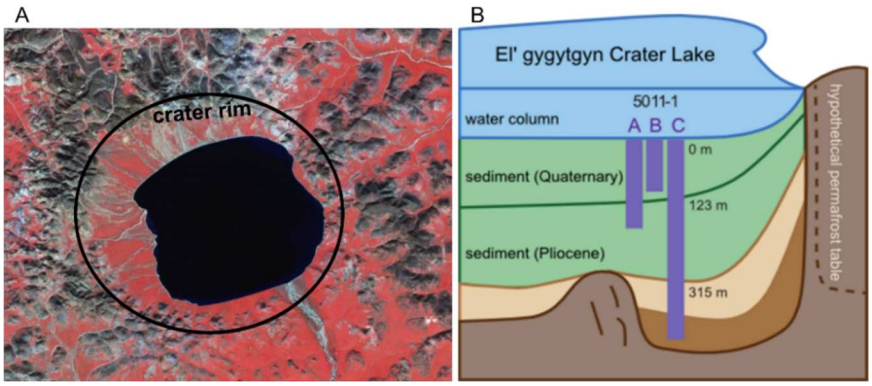

Figure 1.3: Characteristic of the El'gygytgyn Crater Lake showed as (**A**) Landsat 7 image (NASA) with indicated crater rim and (**B**) schematic image with marked drilling locations and hypothetical permafrost table (GFZ Potsdam).

The climate history within the last 3.6 Ma of the Arctic is characterized by different climate scenarios (Brigham-Grette et al., 2013; Melles et al., 2012), which also influenced the vegetation of the lake catchment area (Figure 1.4):

Extreme Arctic warmth (3.6 to 3.4 Ma, EW Zone I and II). During the time of lake formation in the late-Pliocene interval, the reconstructed mean temperature of the warmest month (MTWM) was +15-16 °C and the annual precipitation (PANN) was ~600 mm/a, which is approximately 7-8 °C warmer and 400 mm wetter than today (Brigham-Grette et al., 2013). Similarly warm and wet conditions could be reconstructed for the Pleistocene super interglacial of the marine isotope stage (MIS) 11 (430-390 ka BP), which is also considered to be an analogue for the Holocene and future climate conditions (Tzedakis, 2010). The pollen-based reconstruction of the vegetation of the late-Pliocene revealed the presence of taxon-rich taiga and cool conifer forest biomes prior to the MIS MG6, indicated by a mixture of boreal and temperate tree taxa (Tarasov et al. 2013) with a dominance of spruce-larch-fir-hemlock forests (Andreev et al., 2014). After this relatively cool interval of MG6, which was characterized by minimal summer insolation rates and maxima of marine oxygen isotope records, the biome of cool mixed forest additionally occurred within the EW II.

Largest cooling of the mid-Pliocene (3.31 to 3.28 Ma, LC). The largest cooling of the mid-Pliocene (MIS M2) was characterized by a global cooling event (De Schepper et al., 2009) resulting in a sudden drop of the global temperature and atmospheric humidity (Figure 1.4C, D), as well as by low lake levels (Andreev et al., 2014) and a perennial lake ice blanket of the Crater lake. The number of detected tree pollen in the El'gygytgyn vicinity also declined rapidly, which is indicated by the absence of the taiga, cool mixed, and cool conifer forest biomes. In contrast, the pre-dominant biomes were the open vegetation types tundra and cold- and drought-tolerant steppe, which consisted of boreal or Arctic herb and shrub communities (Tarasov et al. 2013). However, the climatic conditions were different from glacial conditions, and the temperatures were as warm as the Holocene average (around 9 °C) or even higher (Brigham-Grette et al., 2013). Moreover, the detection of high values of coprophilous (dung-preferring) fungi spores indirectly suggests the presence of large grazing herds (e.g., mammoth, horse, bison) around the lake (Andreev et al., 2014).

Pliocene-Pleistocene warmth (3.26 to 2.2 Ma, PPW). The time period of 3.26 to 2.2 Ma BP, showed ~3-6 °C warmer and 100-200 mm wetter conditions than today with a gradual decrease in both atmospheric parameters (Brigham-Grette et al. 2013, Figure 1.4C, D). Summers cooler than today occurred only in the last 2.5 Ma (except during the M2 cooling event). The gradual transition of the generally warmer/wetter environments of the mid- to late-Pliocene to colder/dryer environments of the early-Pleistocene was accompanied by a change in the forest composition followed by a replacement of the forest-dominated environments prior to 2.7 Ma by treeless and shrubby environments at the beginning of the Pleistocene (2.6 Ma BP) (Figure 1.4A). In the course of this transition, the degree of openness of the lake catchment area was continuously increasing (Figure 1.4B). The frequent occurrence of high abundances of green algae colonies (*Botryococcus*) coinciding with *Artemisia* and *Poaceae* pollen implies shallow water levels in the Crater Lake, most probably caused by the drier climate (Andreev et al., 2014).

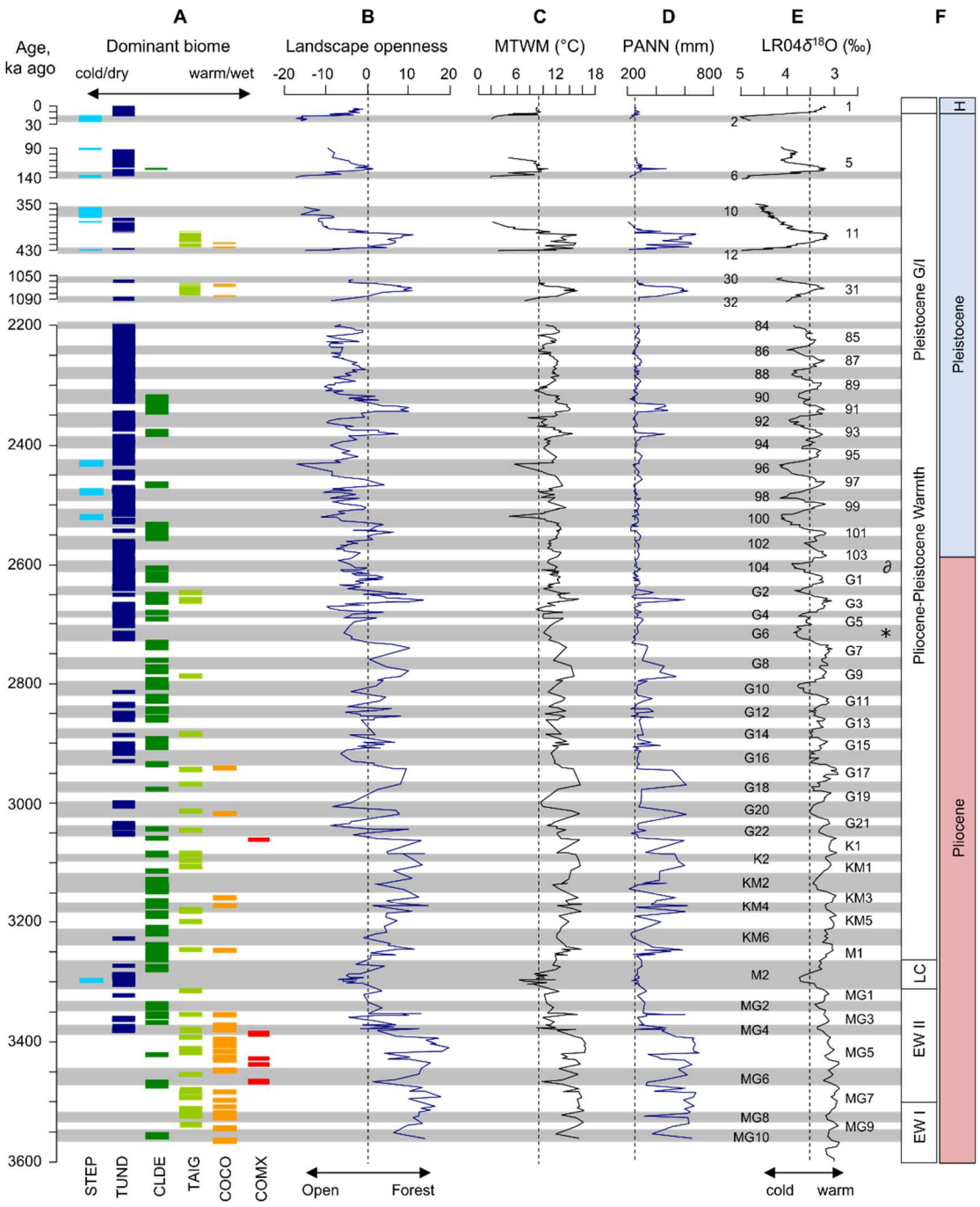

Figure 1.4: Paleo-environmental conditions and pollen-based biome reconstruction of the Arctic within the last 3.6 Ma (figure modified after Tarasov et al. 2013) showing the (**A**) dominant vegetation types (biomes; STEP = cold steppe, TUND = tundra, CLDE = cold deciduous forest, TAIG = taiga, COCO = cool conifer forest, COMX = cool mixed forest), (**B**) measure of landscape openness, (**C, D**) reconstructed mean temperature of the warmest month (MTWM) in °C and annual precipitation (PANN) in mm a^{-1} based on pollen spectra (after Melles et al. 2012; Brigham-Grette et al. 2013), (**E**) global marine isotope stack in ‰ ($\delta^{18}O$, after Lisiecki & Raymo 2005) with corresponding marine isotope stages (MIS), whereby warm isotope periods are highlighted in white and cold isotope periods in grey, (**F**) associated climate phases of the Pliocene and Pleistocene. EW: Extreme Arctic warmth, LC: Largest cooling in Pliocene, G/I: Changing glacial and interglacial periods in Pleistocene, * = onset of northern hemisphere glaciation, ∂ = first glacial and formation of permafrost.

Pleistocene glacial and interglacial cycles (2.6 Ma to 11.7 ka, G/I). In the course of the Pliocene-Pleistocene transition and the onset of the northern hemisphere glaciation (2.7 Ma BP), the first glacial period appeared during the MIS 104 (2.6 Ma BP), which was attended by the formation of permafrost (Figure 1.4E *, ∂). Next to the increased importance of a cold/dry adapted vegetation in the Pleistocene, which was dominated by the tundra biome (caused in an increased albedo effect), the vegetation responded rapidly to warmer and colder global climate conditions of the Pleistocene glacial and interglacial periods (Tarasov et al. 2013). Thereby, especially noticeable is the almost exclusive occurrence of the steppe biome during glacial periods (MIS 100, 98, 94, 12, 10, 6, and 2) and the enhanced presence of the cold-deciduous forest during interglacial periods of the early- to mid-Pleistocene (MIS 101, 97, 93, and 91) (Figure 1.4A). Glacial periods were characterized by heavy global marine isotopic values, low regional July insolation, the occurrence of perennial lake ice, and a relatively low primary production in the lake. In contrast, interglacial periods coincided with light values in the global marine isotope record, high regional July insolation, and a high intra-lake bioactivity (Melles et al., 2012), whereby super interglacial phases (MIS 93, 91, 87, 77, 55, 49, 31 and 11) exhibited extremely high summer temperatures and annual precipitation.

It is especially important to examine the older sediments that reflect the climate history of the last 3.6 to 1.0 Ma, because there is no other record of the Arctic reaching into the late-Pliocene and thus this time period has not been microbiological investigated so far. The microbiological analysis of such old and deep sediments of the El'gygytgyn Crater Lake provides the unique possibility to study the deep biosphere of a lake. Thereby, the Crater Lake represents one of the first investigation sites for the lacustrine deep biosphere.

1.3 Sources of microorganisms of the El'gygytgyn Crater Lake

Based on the last 3.6 Ma of climate history of the Arctic, the climatic conditions of the Pliocene and Pleistocene were characterized by significant differences (Section 1.2). Most probably, changing climatic conditions affected the autochthonous bioproductivity and microbial community structure in the water column and consequently the microbial community at the bottom of the lake. Additionally, they mainly influence the allochthonous input of organic material and associated microorganisms from the catchment into the El'gygytgyn Crater Lake.

Different studies revealed an impact of increased temperatures on the ecological reorganization of algal communities (Smol et al., 2005), increased nutrient concentrations, and primary production (Quayle et al., 2002) in polar lakes. Changes in the bioproductivity in turn influence the species distribution (Parmesan and Yohe, 2003) and food-web dynamics (Perkins et al., 2010) within the lake. Further, the availability of light affects significantly the photosynthetic community: In deeper lakes, benthic mats of filamentous cyanobacteria dominate the littoral zone where light conditions are relatively high (Hodgson et al., 2004), whereas diatoms control the primary production under low light conditions. Palaeoecological studies of Arctic lakes demonstrated that warmth and a strong solar irradiance resulted in an enhanced pelagic related to benthic algal production (Smol et al., 2005) and a formation of more complex communities and trophic structures. Thereby, the community structure of the phytoplankton directly affects the microbial loop in polar lakes, including the primary production and production of dissolved organic carbon (DOC) by planktonic organisms as well as the uptake of DOC by bacteria and its transfer to higher trophic levels (Vincent et al., 2008). Additionally, the nutrient supply has a decisive influence of the bioproductivity and depends on intra-lake and extra-lake processes. Within the lake, the vertical transport of nutrients from the bottom waters to the zone of photosynthesis can be inhibited under cold conditions by a limited wind-induced mixing of the water column (Vincent et al., 2008).

Apart from the intra-lake processes, the nutrient delivery is mainly influenced by the allochthonous input of organic material from the lake surroundings. Thereby, the taxon-rich tree biomes of the Arctic during the warm and wet Pliocene suggest a significantly higher amount of organic-rich detritus produced in the lake catchment area and therefore a higher input of microorganisms into the Crater Lake. Additionally, the input could also be enhanced by wetter climate conditions, which most probably leads to a larger inflow than the 350 t sediments per year nowadays. Thereby, Jeppesen et al. (2014) indicated that enhanced net precipitations can be accompanied by a higher nutrient delivery from the catchment into a lake and can positively influence the amount of DOC in dependence of the terrestrial vegetation cover. Due to the lack of studies dealing with the microbial community composition in Arctic Pliocene samples during this epoch, there is almost no knowledge about the potential microbial community structure that could be a source of the microorganisms in the lake sediments.

In contrast to the Pliocene microbial community, there are several studies about Arctic microbial life in permafrost-influenced soils/sediments of the Pleistocene and of the Holocene. Because of the large annual sediment input into the lake, an influence on the lacustrine deep

biosphere sediments must be expected by the original permafrost microbial community. Compared to the Pliocene, the microbial input during the early-Pleistocene should have a distinct community composition because of the significantly colder and drier climate and the formation of permafrost. Vincent et al. (2008) described that low temperatures, low moistures, and freezing conditions limit the activity of soil microbes, decrease soil-weathering, and lead to low rates of nutrient delivery for biological production. Moreover, cold conditions inhibit the vegetation development, which results in a smaller amount of root biomass and associated rhizospheric microbes as well as a low amount of organic matter (Schwartzman, 1999).

In detail, microbial life in the Arctic permafrost has adapted to extreme conditions. Approximately 23% of the landscape north of the equator is permafrost (i.e., ~26 million km^2, Walsh et al. 2005), where permafrost is defined as layers of stone, soil, or sediment that remained 0 °C or lower in at least two consecutive years (Van Everdingen 2005). Permafrost can be divided by its density: Continuous permafrost (90-100% of the area is permafrost) transitions into discontinuous (35-90%) and eventually sporadic (5-35%) permafrost towards the equator (Figure 1.5).

For microorganisms, life in permafrost implies a multifaceted degree of challenges including low temperature, low water availability as well as low thermal energy and a loss of cell membrane fluidity and impeded nutrient transport (Jansson and Taş, 2014). Moreover, permafrost microorganisms have to cope among others with high temperature fluctuations between seasons (e.g., Siberian air temperature change between +26 °C to -40 °C, Nolan & Brigham-Grette 2007), repeating freeze/thaw cycles, high UV-light radiation, and high salt concentration (e.g., in liquid brine veins).

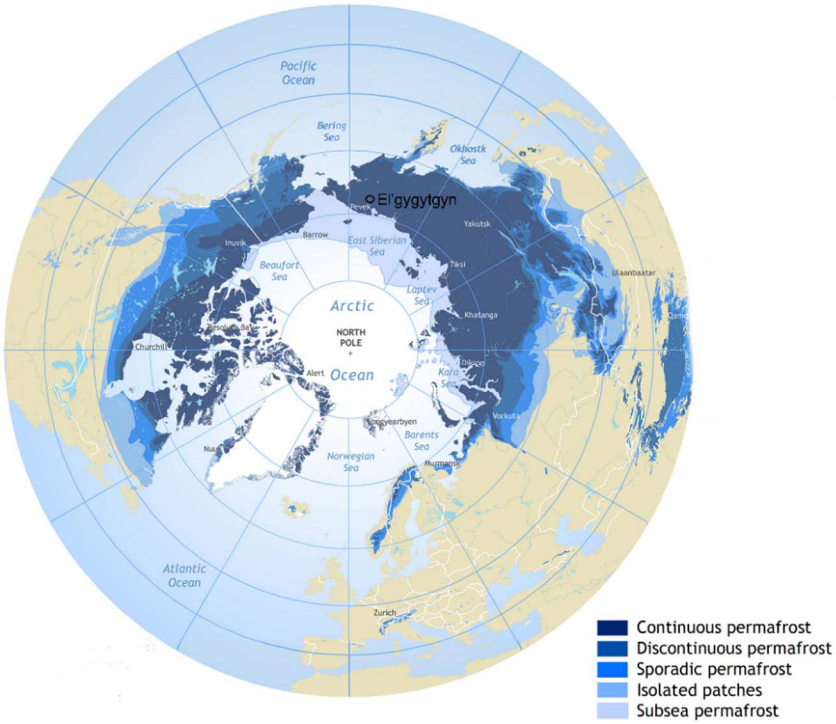

Figure 1.5: Distribution of permafrost and ground-ice on a circum-Arctic map (Brown et al., 1997). The black circle indicates the study site of this PhD thesis – the El'gygytgyn Crater Lake – surrounded by Siberian continuous permafrost.

Despite these harsh conditions, the microbial biosphere of the permafrost is highly diverse due to different adaption strategies of the microbes. Steven et al. (2007) were able to cultivate bacterial strains of the phyla *Firmicutes*, *Actinobacteria,* and *Proteobacteria*, whereby the majority of isolates belonged to psychrotolerant and halotolerant organisms. Additionally, they demonstrated the presence of halophilic archaeal DNA using a 16S rRNA gene clone library. Indeed, several studies emphasize the substantial adaption strategies of halophilic and halotolerant microorganisms in permafrost and other cold habitats: For example, *Virgibacillus arcticus* was isolated from the Canadian high Arctic (Niederberger et al., 2009), and *Halomonas glaciei* was found in a solid layer of fast ice in Antarctica (Reddy et al., 2003). Additionally, the phyla *Bacteriodetes, Acidobacteria, Cyanobacteria,* and several uncharacterized species were identified as frequently occurring bacteria in permafrost environments (Steven et al., 2013; Yergeau et al., 2010). Hinsa-Leasure et al. (2010) used a combined approach of culture-dependent and culture-independent methods to characterize the bacterial community in a Siberian seacoast permafrost and also revealed the phyla *Firmicutes*, *Actinobacteria,* and *Proteobacteria* as the main representatives, whereby 85% of the isolates are classified as the genera *Arthrobacter* and *Planococcus*. Interestingly, they identified the *icl* gene (encoding

isocitrate lyase, a marker for cold adaptation) in multiple isolates. Next to the expression of cold-shock proteins that entail benefits for protein folding, transcription, translation, and regulation of membrane fluidity under low temperatures (D'Amico et al., 2006), a successful strategy to adapt to permafrost condition is the transition into a dormant state with a low metabolic activity (Jansson and Taş, 2014).

Moreover, different aerobic methanotrophic bacteria of the phylum *Proteobacteria,* such as *Methylobacter*, *Methylosarcina*, *Methylocystis*, *Methylosinus*, and *Methylocapsa,* have been detected (Barbier et al., 2012; Liebner et al., 2009). The antagonistic group of methanogenic archaea also show a great diversity in northern permafrost regions, whereby species belonging mainly to the families *Methanomicrobiaceae*, *Methanosarcinaceae*, *Methanosaetaceae*, *Methanobacteriaceae*, *Methanocellaceae*, and *Methanospirillaceae* (Allan et al., 2014; Barbier et al., 2012; Ganzert et al., 2007) were identified. Apart from psychrotolerant strains of methanogenic archaea (Dong and Chen, 2012; Simankova et al., 2003), many permafrost methanogens are characterized by increased survival potentials against high salinities, desiccation, presence of oxygen, and long-term freezing (Morozova and Wagner, 2007; Wagner et al., 2013). Thereby, methanogenic archaea in permafrost play an important role in the global carbon cycle (Wagner and Liebner, 2009) (Figure 1.6, modified after Graham et al. 2012), when considering that the northern permafrost region stores approximately 50% of the global below ground organic carbon (≙ 1672 Pg, Tarnocai et al. 2009), much more than previously expected (Gorham, 1991). In the course of a climate change-driven thawing of the permafrost and an intensified microbial carbon turnover, an increased emission of greenhouse gases is suggested (IPCC, 2013). Methane has an approximately 33 times higher 100-year global warming potential than carbon dioxide (Shindell et al. 2009). Especially, the methane emission into the atmosphere could increase significantly due to the enhanced formation of waterlogged low-oxygen environments (Schuur et al., 2013), which could be shown, for instance, by an increase of the total lake area (+12%) and lake number (+4%) in continuous permafrost between 1973 and 1997/98 (Smith et al. 2005).

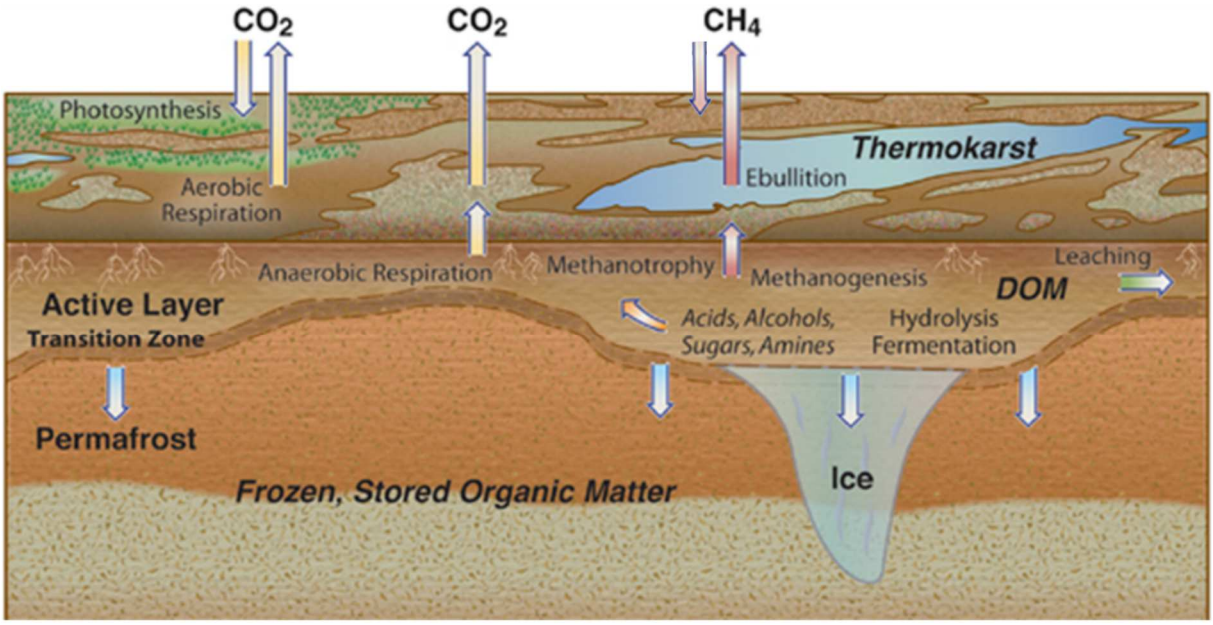

Figure 1.6: Influence of the microbial community on the permafrost carbon cycle under increased polar temperatures (modified after Graham et al. 2012). Thawing permafrost introduces previously unavailable organic matter into the expanded active layer and leads to an enhanced formation of waterlogged low-oxygen environments (e.g., also in form of lakes). Complex organic matter is converted into a mixture of organic acids, alcohols, sugars, and amines by hydrolysis and microbial fermentation. Next, methanogenic archaea are able to convert acetate or hydrogen and carbon dioxide into methane. In contrast to the methanogens, methanotrophs act as methane sink by oxidizing parts of the emitted methane into carbon dioxide.

1.4 Differentiation between live and dead microorganisms

Particularly with regard to the microbiological work in the deep biosphere, it is of paramount importance to distinguish between live (potential active) and dead microorganisms. The differentiation enables on the one hand the investigation of the active microbial community, which is indeed participating in the global material cycles, and on the other hand to disclose the microbial community of the past. Thereby, the concept of live/dead differentiation has its origin in the field of human pathology aiming to assess or dismiss medical risks (Barbau-Piednoir et al., 2014; Nkuipou-Kenfack et al., 2013; Yáñez et al., 2011). Over many decades, the gold standard was based on the cultivation method, although cultivation imposes certain requirements on the experimental setting, such as the correct chemical, nutritional, and physical prerequisites, which are often not known a priori (Eilers et al., 2000). Because of the risk of underestimation of living microorganisms (e.g., viable but non-culturable cells, VBNC, Li et al. 2014) and the fact that we are only able to cultivate a small fraction of the known bacterial species (Keller and Zengler, 2004), there is the need for new and fast methods of live/dead differentiation.

One approach is the usage of DNA intercalating dyes, which makes it possible to distinguish between live and membrane-compromised (dead) cells. The photoactive dye propidium monoazide (PMA) has a high affinity to DNA, but cannot pass through membranes of living cells. Under light activation it intercalates into free double-stranded DNA. Because these PMA-DNA aggregates are not amplifiable, a combination of PMA treatment and (q)PCR leads to a inhibition of free DNA, whereby the DNA from living cells will be amplified (Figure 1.7). Consequently, a comparison of a PMA-treated and PMA-untreated sample allows us to deduce the microbial composition of free DNA.

The PMA treatment represents a cost-effective and rapid technique that is well adapted to a wide range of Gram-positive and Gram-negative bacteria (Bae and Wuertz, 2012; Nocker and Camper, 2006; Nocker et al., 2006; Taylor et al., 2014). Nevertheless, PMA has been rarely used for the domain of archaea (Barth et al., 2012; Gagen et al., 2013) and has not been established for methanogenic archaea yet. Methanogenic archaea in Arctic soils/sediments are important players in the global carbon cycle (Allan et al., 2014) and contribute to the emission of greenhouse gases (Ganzert et al., 2007; Wuebbles and Hayhoe, 2000). To date, only a few PMA experiments have been conducted in archaea (e.g., Halobacterium salinarum, Barth et al.,

2012; miscellaneous crenarchaeotic group, Gagen et al., 2013). Due to the substantial differences in cellular structure between bacteria (e.g., peptidoglycan layer and ester lipids) and archaea (e.g., different cell wall polymers and ether lipids) (Barton, 2005; Konings et al., 2002), archaeal cells most likely exhibit other behaviors in response to PMA. For that reason, this thesis evaluates the PMA treatment for methanogenic archaea.

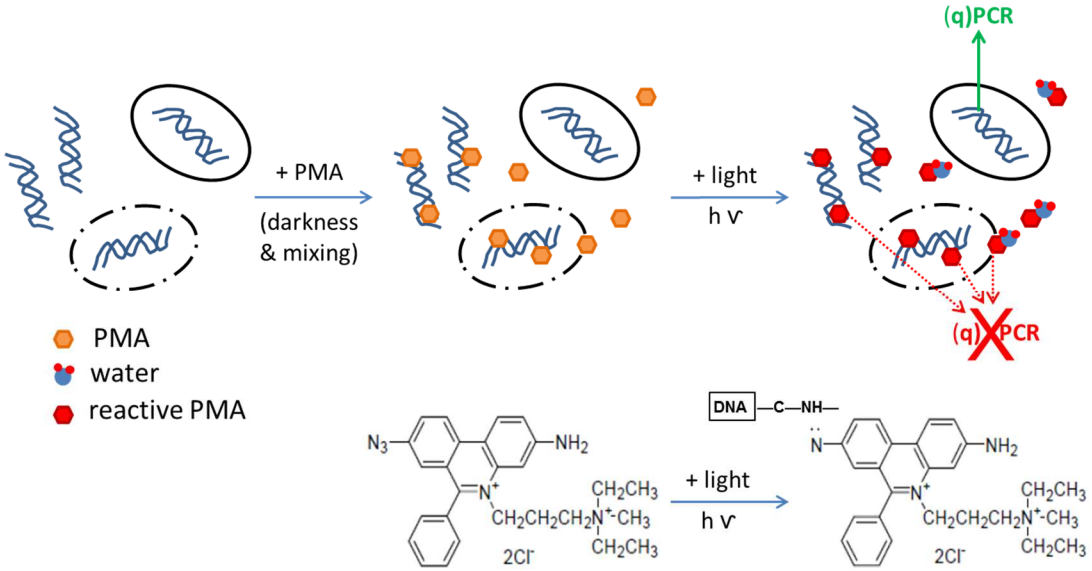

Figure 1.7: Mechanism of action of propidium monoazide: PMA is distributed in the sample by regular mixing in darkness. When exposed to light (e.g., blue LEDs or 500 W halogen lamp), the azide group of PMA converts into a highly reactive nitrene radical, which covalently binds to DNA molecules of damaged cells. The dye is able to bind to every fourth to fifth nucleotide, whereat the polymerase activity is inhibited and for the free DNA no product is generated during subsequent (q)PCR.

While the importance of live/dead differentiation has been acknowledged in the human pathogenic field and for cultures, most of the studies about community analyses in environmental samples build their interpretation on a total DNA (tDNA) extract. However, it is uncertain whether the extracted tDNA originates from the living community or might be an artifact of ancient communities or excreted DNA (Corinaldesi et al., 2011, 2005; Dell`Anno and Danovaro, 2005; Ogram et al., 1988) and therefore the interpretations about the current microbial community and their function in the habitat inherently have a high risk to be inexact or faulty (Dlott et al., 2015; Lombard et al., 2011). These observation are supported by recent studies showing that environmental samples contain a large amount of free (extracellular) DNA: Luna et al. (2002) identified 70-74% of cells in marine sediments as dead, whereby Dell`Anno & Danovaro (2005) classified the majority of 90% of the DNA in deep-sea ecosystems as extracellular DNA (eDNA, = free DNA). Even earlier in 1995, Zweifel & Hagström (1995)

revealed a high fraction of 68-98% of non-nucleoid-containing bacteria (ghosts) in seawater samples.

In general, we can assume that in the deep biosphere the amount of eDNA increases with the age of the samples, because the low bioactivity in the sample and the high binding capacity of the sedimentary matrix (e.g., negatively charged particles such as silica particles, clay, humic acids, and organic matter) (Crecchio & Stotzky 1998; Boom et al. 1990; Levy-Booth et al. 2007; Taberlet et al. 2012) can result in a long-term conservation of eDNA. Theoretical and empirical studies predicted a maximal survival time of DNA of a few thousand years in warm regions to approximately 1 million years in cold regions (Hofreiter et al., 2001; Poinar et al., 1996; Willerslev and Cooper, 2005). Especially, in samples encompassing geological time scales, and therefore in particular for sediments from the El'gygytgyn Crater Lake, it is an issue of paramount importance to differentiate between the DNA from living cells and dead cells. Next to the possibility to analyze the current microbial community and their metabolic activity, the eDNA pool has the potential to describe the past microbial community of the sample (Alawi et al., 2014; Corinaldesi et al., 2005).

To distinguish between live and dead microorganisms in environmental samples, there are different methods available (e.g., flow cytometry, mRNA analyses, fluorescence in situ hybridization (FISH)), but most of them require samples in a rather good quality (e.g., large cell numbers, large amounts of fresh material) or are insufficiently adapted to sediment or soil samples (e.g., background noise, interference with humic substances). Further, the detection of mRNA requires gene expression, which is dependent on stress conditions (Barbau-Piednoir et al., 2014) and environmental conditions. Preliminary studies revealed that RNA analyses and FISH are not suitable for the deep sediments of the El'gygytgyn Crater Lake due to detection limits.

Although PMA has been successfully applied to water samples (Alonso et al., 2014; Dieser et al., 2010; Nocker et al., 2007), there are limitations for particle-rich environmental samples (Bae and Wuertz, 2009; Fittipaldi et al., 2011; Luo et al., 2010). In particular, next to the lowering of dye concentration by chemical adsorption, particles may inhibit a light-activation of PMA by shielding, which is known as turbidity effect (Fittipaldi et al., 2012). A highly developed turbidity effect can lead to a dramatic overestimation of the living microbial community (false positive effect). This thesis evaluates a PMA treatment and a cell separation for environmental samples to simultaneously distinguish between live and dead bacteria and

archaea. Thereby, it explores the boundaries of a PMA treatment in respect to high amounts of humic substances and high particle loads.

The idea of a cell separation (distinction between extracellular and intracellular DNA (iDNA)) based on a sodium phosphate buffer originated already in 1987 (Ogram et al., 1987). Still, this technique is rarely used to efficiently recover DNA from environmental soil and sediment matrices. A major reason for the lack of usage might be the time-consuming protocol, which was displaced by the rapid spreading of commercial DNA extractions kits including all necessary substances and consumption articles. Even the bacterial iDNA represents only intact and potential active cells, the bacterial eDNA pool can originate from dead cells (cell lysis), or active extrusion of living cells (biofilm formation) (Levy-Booth et al., 2007; Okshevsky and Meyer, 2015; Torti et al., 2015). It is still a controversial topic to what extent ancient prokaryotic DNA can persist and which methods ensure the differentiation between the current and past microbial signal. However, most of the former microbiological studies could not sufficiently explain changes in the microbial community structure with measured environmental parameters. This thesis hypothesizes that the discrimination of eDNA and iDNA addresses these problems.

Recently, the cell separation protocol was further developed by Alawi et al. (2014) for oligotrophic sediments with low cell numbers and low amounts of DNA and incorporating a silica-particle based DNA precipitation and purification. The protocol by Alawi et al. (2014) was slightly modified for the El'gygytgyn sediments (e.g., silica amount, iDNA extraction protocol; Figure 1.8) to facilitate a gentle differentiation between the eDNA and iDNA pools without the usage of any aggressive substance. Thereby, the main advantages of the cell separation over PMA treatment are the lack of turbidity effect with respect to clay- and silt-rich sediments as well as the possibility that the cell separation allows downstream analyses of both DNA pools, such as direct high throughput sequencing.

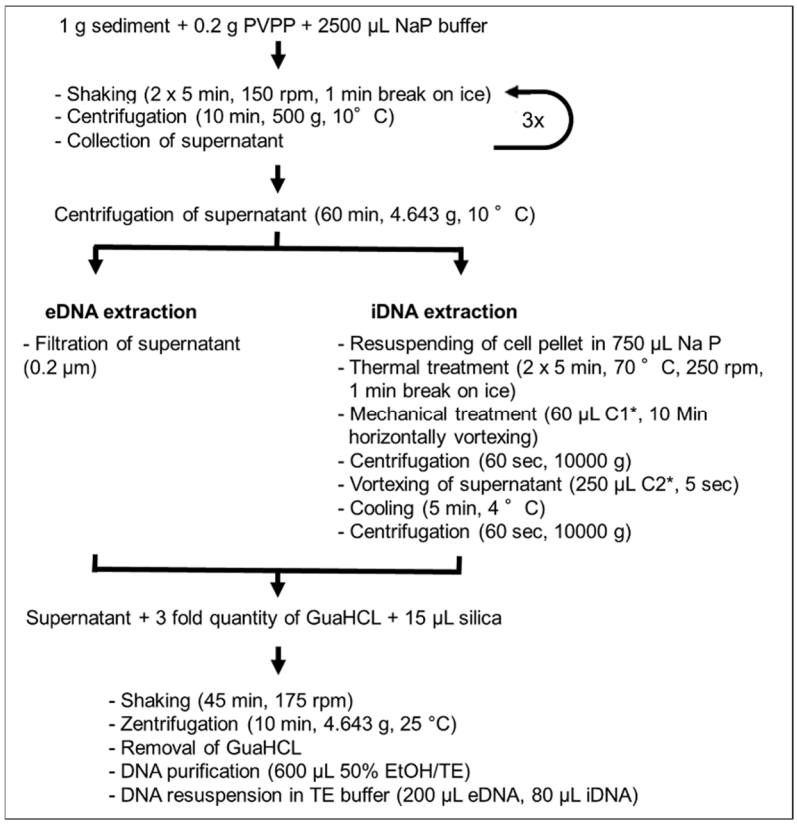

Figure 1.8: Workflow of cell separation protocol successfully used for the El'gygytgyn deep sediments (modified after Alawi et al, 2014). Briefly, iDNA and eDNA was sequentially washed from El'gygytgyn sediments with alkaline sodium phosphate buffer (NaP) and separated by centrifugation. Afterwards, the iDNA was extracted from the cell pellet by thermal and mechanical treatment and was bound to 15 µL silica particles, purified, and re-suspended in TE buffer, in the same way as the filtered eDNA.

1.5 Aims and objectives

The overall aim of this thesis is the first molecular microbiological investigation of up to 3.6 million years old lacustrine sediments at the example of the deep biosphere of the Lake El'gygytgyn, which contains the oldest terrestrial climate record of the Arctic. A detailed characterization of the microbial communities during different paleo-climatic conditions yields the first extensive database of the terrestrial deep biosphere of a lake system. Thereby, the microbiological examination is challenging due to the low amount of DNA and a large portion of cells being dormant, dead, or in a low activity state. The main hypotheses of this thesis are that 1) the microbial community composition and diversity of such deep lake sediments reflect the climatic history of the Arctic in the frame of the Pliocene-Pleistocene transition as well as during the Pleistocene glacial and interglacial cyclicity and that 2) molecular studies of the deep biosphere in general require to separately study nucleic acids from intact and compromised cells.

The following specific questions were addressed:

1. **What are the diversity, abundance and composition of the microbial communities and how does it change along the lake sediment chronosequence? (Section 3.1)**

The 16S rRNA gene copies for archaea and bacteria were determined with quantitative PCR. By using Illumina next generation sequencing technique, the microbial community composition in 57 sediment samples of the El'gygytgyn Crater Lake (3.6-1.0 Ma old, spanning Pliocene and Pleistocene) were characterized and multiple diversity indices were calculated to assess the α- and β-diversity.

2. **Which methods are appropriate to differentiate between the living and the dead microbial communities in environmental samples?**

On the one hand, the adjustment and evaluation of the propidium monoazide (PMA) treatment for environmental samples was carried out to distinguish between live and membrane-compromised (dead) cells in El'gygytgyn sediment and a reference soil sample (Section 3.2). On the other hand, a cell separation protocol for low amounts of DNA (Alawi et al., 2014) was adapted to the special requirements of the El'gygytgyn deep biosphere samples (Section 3.3).

2.1 Given that PMA was originally developed for bacteria, is it possible to also apply PMA to archaea? (Section 3.2)

The optimization of the PMA treatment to different strains of methanogenic archaea was conducted and the results were compared to a bacterial reference strain. Further, a special PMA treatment protocol that allows to distinguish between live and membrane-compromised (dead) cells of the domains archaea and bacteria at the same time was developed.

2.2 How appropriate is a total DNA extract for representing the living and past microbial community in the lacustrine deep biosphere? (Section 3.3)

For the first time, a 16S rRNA Illumina sequencing of 14 deep lake sediments was conducted separately for the intracellular (living) cell pool and for extracellular (free) DNA using a cell separation protocol optimized for samples with low amounts of DNA. Thereby, the extracellular DNA pool is expected to contain primarily DNA of the past microbial community and to a minor extent DNA of the recent microbial community. Both cell-separated DNA pools were compared with a DNA pool obtained by a commercial total DNA extraction kit. Indices for the taxonomic dissimilarity between the different DNA pools were calculated.

3. What are the environmental drivers behind changes of the microbial composition and what is the specific influence of the sediment age on microbial composition and diversity? (Section 3.4)

Sediment characteristics such as sediment moisture, grain size distribution, total (organic) carbon, and total nitrogen content were determined for 105 sediment samples of the El'gygytgyn Crater Lake. Additionally, externally determined climatic parameters, such as the global marine isotope stack (benthic $d^{18}O$), mean temperature of the warmest month (MTWA), mean annual precipitation (PANN), summer insolation, and elemental compositions (Si, Ti, Ca, K, Mn, Fe) were incorporated to conduct correlation analyses between the environmental parameters and the sediment age. Using non-metric multivariate scaling analysis (NMDS), the samples were clustered based on the similarity of the microbial community compositions for glacial and interglacial periods of the Pleistocene as well as the Pliocene. Redundancy analyses (RDA) were used to identify the key environmental parameters influencing the microbial community structure of the tDNA pool. Additionally, RDA analyses were performed individually for each cell-separated DNA pool to allow for a better explanation of the environmental drivers of each pool and the differences in microbial community composition between them.

2 Materials and Methods

This chapter briefly presents the study material and the methods to analyze it in the order of application. The first two sections include the analyses of the sediment properties. Section 2.3 describes the total DNA extraction of 57 sediment samples, whereas Section 2.4 presents the cell separation of 14 sediment samples. Section 2.5 summarizes the application of quantitative PCR. For all samples of both extraction methods, the Illumina sequencing was applied and the results were analyzed as it is described in Section 2.6-2.8. Additionally, the experiments for the PMA treatment are described in Section 2.9-2.15.

2.1 Sediment sampling and properties

Sediments of the El'gygytgyn Crater Lake were retrieved during the multi-national ICDP Lake El'gygytgyn Drilling project in 2008 and 2009 (in total 317 m of sediments and 200 m of underlying impact rocks, Melles et al. 2011). All molecular techniques of this study are based on inner coring sampling with a sterile spatula and sterile 15 mL falcon tubes. All samples were frozen at -20 °C until later analyses.

The percentage of total organic carbon (TOC) of the sediments was measured in duplicates for each freeze-dried, homogenized, and milled (PULVERISETTE 5, Fritsch Ltd, Germany) sample using an element analyzer (Elementar Vario MAX C, Hanau, Germany). The total carbon (TC) and total nitrogen (TN) were analyzed in duplicates with an element analyzer (Elementar Vario EL III, Hanau, Germany). The moisture content was determined by weighing the subsamples before and after freeze-drying. To determine the grain sizes, the samples were treated with acetic acid (10%) for 48 h to remove carbonate, and with H_2O_2 (35%) for 3 weeks to remove all organic material. The grain sizes were then measured after freeze-drying twice with a Coulter LS 200 laser particle size analyzer (Beckman Coulter, Brea, CA).

2.2 XRF scanning

The elemental composition of the cores was determined at a 2 mm resolution with an Itrax X-ray fluorescence (XRF) core scanner (Cox Analytical Systems; Croudace et al. 2006). Either a molybdenum (Mo) or a chromium (Cr) radiation source set to a tube voltage of 30 kV, a current

of 30 mA, and an exposure time of 10 s, were used to generate higher count rates and lower detection limits for heavier (Mn to U) and lighter elements (Al to Ti), respectively. To correct the Si data for the biasing effects of the sediment matrix (e.g., water content, organic matter), an empirically determined matrix-correction based on an exponential attenuation function between the ratio of wet and dry element intensities and the Itrax-derived ratio of Compton and Rayleigh scattering (inc/coh ratio) was applied (Melles et al., 2012; Wennrich et al., 2014).

2.3 Total DNA extraction

The total genomic microbial DNA (referred to as total DNA = tDNA) was extracted in triplicate out of 1 g material each with Power Soil™ DNA Isolation Kit (MO BIO Laboratories Inc., Carlsbad, CA) according to the manufacturer's protocol based on a cell disruption by chemical reagents (e.g., SDS) and by a horizontally vortex adapter. To increase the yield of DNA, the elution was performed with preheated elution buffer in two steps. The DNA triplicates were pooled for downstream analysis. The concentration of the extracted DNA was mainly under the detection limit of the NanoPhotometer™ P-360 (Implen).

2.4 Separation between extracellular and intracellular DNA by cell separation

Next to the tDNA extraction, a cell separation protocol adapted to very low amounts of DNA was used (Alawi et al., 2014) in triplicates per sample. Briefly, living cells (intracellular DNA = iDNA) and extracellular DNA (= eDNA) were sequentially washed from 1g sediment with 2500 µL alkaline sodium phosphate buffer and separated by centrifugation (Figure 1.8). The supernatants were centrifuged at 4,643 g and 10 °C for 60 min (SIGMA 4-16KS refrigerated centrifuge, swing out rotor). After separation of the cells, the iDNA was extracted from the cell pellet by heating two times (70 °C, 5 minutes), shaking horizontally with SDS containing C1 solution (MO BIO Laboratories Inc., Carlsbad, CA) for 10 minutes and removing non-DNA organic and inorganic material including humic substances and proteins by incubation with C2 solution (4 °C, 5 minutes). Afterwards, the iDNA was bound with guanidine hydrochloride to 15 µL silica particles, purified, and re-suspended in TE buffer, in the same way as the filtered eDNA (0.2 µm syringe filter). The DNA triplicates were pooled for downstream analysis of each DNA pool.

2.5 Bacterial and archaeal 16S rRNA gene copy number

Quantitative PCR was performed in triplicate 25 µL volumes using 12.5 µL iTaq Universal SYBR Green Supermix (Bio-Rad), 0.5 µL of each 20 mM primer, 5 µL (1:5 dilution) template,

and PCR-grade water to 25 µL on a CFX Connect Real-Time PCR Detection System (Bio-Rad). The primer pair Uni331F/Uni797R (Nadkarni et al., 2002) was used to amplify bacterial 16S rRNA genes, whereas the primer pair A571F/UA1406R (Baker et al., 2003) served to amplify archaeal 16S rRNA genes. Inhibition was checked by running qPCR on three consecutive dilutions and deemed non-existent if the dilutions yielded the same results. The cycling conditions were as follows: initial denaturation at 95 °C for 10 min, 40 cycles of denaturation at 95 °C for 30 s, annealing at 57 °C for 30 s, and elongation at 72 °C for 45 s (Uni331F/Uni797R) or 90 s (A571F/UA1204R), and subsequently a melting curve (65 °C to 95 °C, 1 °C each step). Standard curves for each qPCR assay were generated using tenfold serial dilutions of quantified (using 2100 Bioanalyzer with Agilent DNA 1000 Kit) linear standards of the target fragment amplified from *Bacillus subtilis* or *Methanosarcina vacuolata*. For all standards, near-perfect linear regressions (r2> 0.995; efficiency range of 0.9 to 1.0; slope range of -3.3 to -3.6) were obtained.

2.6 PCR amplification, amplicon library preparation and Illumina sequencing

The V4 region of the bacterial and archaeal 16S rDNA genes was amplified using the primers 515F (5'-GTGCCAGCMGCCGCGGTAA-3') and 806R (5'-GGACTACHVGGGTWTCTAAT-3') (Caporaso et al., 2011). The cycling conditions involved an initial 5 min denaturation step at 95 °C, followed by a 10-cycle touchdown protocol of 30 s at 94 °C, 45 s at 53 °C (-0.20 °C /step), and 60 s at 72 °C and subsequently 20 cycles of 30 s at 94 °C, 45 s at 50 °C, and 60 s at 72 °C. A final elongation step was conducted at 72 °C for 10 min. The PCR reactions were performed in duplicates containing the following: 5 µL 10x CoralLoad PCR Buffer (Qiagen, Germany), 200 µM of each dNTP, 1 µL of 50 mM $MgCl_2$, 0.25 µL of 20 mM primer mix, 2.5 U of HotStarTaq DNA polymerase (Qiagen, Germany), 0.3 µL BSA, and PCR-grade water to 50 µL. After gel purification, the amplicons served as a template for the second PCR performed under the same conditions as described above (50 °C annealing temperature), but for 16 cycles without touchdown. Primers for the second PCR consisted of the 515F or 806R primers extended by a 2-nt linker and a 4-6-nt barcode. Non-template controls were performed and were free of amplification products after both rounds of PCR. Duplicates were pooled and verified by agarose gel electrophoresis. Purification of the amplicons was conducted with HighPrep^{TM} PCR clean up system (MAGBIO, Gaithersburg, USA). The DNA concentration was quantified with the dsDNA HS assay of a Qubit® 2.0 Fluorometer (Life Technologies, Carlsbad, CA, 5 µL input). Samples were mixed equimolarly and Illumina adapter sequences were ligated on amplicons using TruSeq DNA PCR-Free LT Sample Prep Kit (Illumina). The

amplicon library (30% phiX DNA added) was subjected to sequencing on an Illumina MiSeq 2x250 bp paired-end platform in the National High-throughput DNA Sequencing Centre, Copenhagen.

2.7 Bioinformatics analysis

The 16S rDNA amplicons were analyzed using QIIME (version 1.8.0) (Caporaso et al. 2010; Navas-Molina et al. 2013). Raw paired-end reads were merged using PEAR (v0.9.4) (Zhang et al., 2014), and reads in the 3´-5´direction were reoriented into the 5´-3´direction using a custom-generated script (FASTX Toolkit 0.0.14 by A. Gordon). Merged reads were demultiplexed and quality-filtered. Low-quality sequences were removed from the dataset, including sequences that (i) had a stretch of 5 bp with a Phred quality score less than 25, (ii) contained ambiguous nucleotides (N), (iii) contained homopolymers longer than 6 bp, or (iv) exceeded a maximal sequence length of 320 bp. Quality-processed sequences were then checked for chimeras using USEARCH 6.1 (UCHIME algorithm) (Edgar et al., 2011) including both de-novo and reference-based chimera removal (using the CS Gold Database, http://drive5.com/uchime/gold.fa). Combined de novo- and reference-based chimera detection removed 1.6% of the sequences. The sequences were clustered using a de-novo UCLUST algorithm at a 97% similarity level and representative sequences were selected utilizing a cluster seed method (Edgar, 2010). The representative sequences were aligned using the PyNAST alignment algorithm (Caporaso et al. 2010) and taxonomically assigned using the default parameters in QIIME against the Greengene database (13_8-release) (DeSantis et al., 2006). The alignment was filtered with a lanemask file prior to the creation of a phylogenetic tree with FastTree (Price et al., 2009). OTU table was then trimmed by removing singletons (0.6% of the sequences) to reduce PCR or sequencing errors. Phylogenetic assignment of the 20 most abundant bacterial OTUs was processed additionally with NCBI BLAST (BLASTN 2.2.30+, nucleotide collection, January 2015) and compared to the Greengene database. All sequence data have been submitted to the European Nucleotide Archive (ENA) under accession number PRJEB9144.

2.8 Diversity analysis

Unless otherwise indicated, the statistical tests and the visualization of the data were performed in the R statistical environment (R Development Core Team, r-project.org) using the *vegan* (Oksanen et al., 2014) and *phyloseq* (McMurdie and Holmes, 2013) packages. For all analyses that are sensitive to absolute read counts, the dataset was rarefied with the function

rarefy_even_depth. Diversity indices (Shannon-Weaver, Chao1) were calculated with *estimate_richness*. The bubble plot depicting the abundance of dominant species was created using the R-package *rioja* (Juggins, 2014). To determine the dissimilarities between the samples based on their OTU compositions, non-metric multidimensional scaling (NMDS) plots were generated by normalizing the data with square root transformation and Wisconsin double standardization before applying the Bray-Curtis distances (*ordinate*, *plot_ordination)*. To investigate which environmental parameters could significantly explain the variation in the microbial community structure, a redundancy analysis (RDA) was calculated with CANOCO 5 (Ter Braak and Šmilauer, 2012) on arcsine-transformed and centered response data for each DNA pool. The significance of the relationship was assessed by Monte Carlo permutation tests (999 permutations).

The analysis of shared and exclusive OTUs per DNA pool was calculated and visualized with the help of the R package VennDiagram (Chen and Boutros, 2011). The Jaccard-distance (Jac_{dist}, emphasizing the rare biosphere) focuses on the presence/absence of OTUs between different DNA pools and is defined as a ratio of the common OTUs over all OTUs of the two comparative DNA pools. For two sets of OTUs $\mathbf{O_1}$, $\mathbf{O_2}$, the Jaccard-distance was calculated using the formula:

$$Jac_{dist}(O_1, O_2) = 1 - \frac{|O_1 \cap O_2|}{|O_1 \cup O_2|}.$$

For the Cosine-distance (Cos_{dist}), both DNA pools were interpreted as vectors $\mathbf{V_1}$, $\mathbf{V_2}$ where each component corresponds to the reads for a certain OTU. The complement of the Cosine-similarity in the positive space was used as the Cosine-distance as follows:

$$Cos_{dist}(V_1, V_2) = 1 - \frac{V_1 \cdot V_2}{\|V_1\| \|V_2\|}.$$

For the evaluation of the PMA treatment for methanogenic archaea and environmental samples, five experiments were performed as described in the following section. These experiments of the PMA part are published in Heise et al. 2016.

2.9 Cultivation of methanogens and preparation of membrane-compromised cells

The following strains of methanogenic archaea were used in this study: *Methanobacterium lacus* (DSM 24406), *Methanobacterium movilense* (DSM 26032, Schirmack et al., 2014), *Methanosarcina soligelidi* (DSM 26065, Wagner et al., 2013a; full genome Alawi et al., 2015), *Methanosarcina vacuolata* (DSM 1232) and *Methanosarcina barkeri* (DSM 800). The methanogenic cultures were grown at 28 °C in MB medium (*Mb. movilense*, *Mb. lacus*; for the media, see Schirmack et al., 2014), MW medium (*Ms. vacuolata*, *Ms. barkeri*, Ganzert et al., 2014), or OCM medium (*Ms. soligelidi,* Boone et al., 1989). The reference strain *Pseudomonas fluorescens* (DSM 50090) was cultivated on nutrient agar (5 g peptone, 3 g meat extract, if required, 15 g agar, 1000 mL distilled water, pH 7.0) at 28 °C. The growth of *P. fluorescens* was checked by measuring the optical density at 600 nm (OD600, NanoPhotometer™ P-360, Implen). Microbial growth of methanogens was checked by calculating the methane concentration using gas chromatography (GC Agilent 7890A) and by re-cultivation. To obtain membrane-compromised cells, 500 µL of each culture was treated with isopropanol (70% final concentration) for 40 min at room temperature. Isopropanol was removed by cell harvesting by centrifugation at 8,800 g for 30 min prior to re-suspension in 500 µL of the corresponding medium. The total cell counts were calculated in triplicates using Thoma cell counting chambers (counting at least 500 cells). Methanogens were harvested under anaerobic conditions in a glove box (Whitley MG 500, Meintrup DWS, England).

2.10 Experiment 1: Fluorescence microscopic examination of the membrane impermeability to PMA

To evaluate the membrane permeability of viable and membrane-compromised methanogenic archaea to PMA (Biotium® Inc., Hayward, CA), 500 µL of each sample (*Mb. lacus*, *Mb. movilense*, *Ms. barkeri*, *Ms. soligelidi*, bacterial reference strain *P. fluorescens*) was treated with SYTO 9 (stains all cells) and PMA (50 µM and 130 µM; stains membrane-compromised cells but not intact cells) and microscopically analyzed immediately and at regular intervals (≤ 20 min) (Leica DM 2000 with camera DFC 420C and filter system FI/RH). The LIVE/DEAD® BacLight™ kit (Molecular Probes®, Life Technologies, Germany) was used to confirm membrane integrity of viable cells and isopropanol-killed cells (Figure A.4). Before usage of the LIVE/DEAD® BacLight™, a fresh 1:1 mixture of the dyes SYTO 9 and propidium iodide (PI; stains membrane-compromised cells but not intact cells similarly to PMA) was

prepared, and 500 µL of each sample was incubated with 1.5 µL of dye mix for 15 min in the dark at room temperature before microscopy (filter system FI/RH).

2.11 Experiment 2: Evaluation of the PMA treatment for pure cultures by PMA-qPCR analyses

During this experiment, the parameters for an optimal light activation as well as the concentration and incubation time of PMA for *Ms. soligelidi*, *Mb. movilense*, and the reference strain *P. fluorescens* (each in triplicates) were adjusted. *Ms. soligelidi* and *Mb. movilense* were used to evaluate the applicability of a PMA treatment to the genera *Methanosarcina* and *Methanobacterium*, because they are characterized by a biochemically distinct cell wall structure. Different concentrations of PMA (50, 90, 130, and for *P. fluorescens* 200 µM) was added to equal amounts of intact or isopropanol-killed cells in the dark. Homogenized samples were incubated in the dark for 5 min with manual mixing every 60 s. Photo-induced cross-linking was conducted using blue-light-emitting diodes (LEDs) (two sets of 30 LEDs, 460 nm, 220-240 V ~50 Hz maximal 1 W, Centor, Germany). The light exposure was performed using a distance of 10 cm for 5, 8, 10, and 20 min with manual mixing every 60 s. Negative controls were assessed with and without PMA and light exposure. The genomic DNA extraction was performed using the UltraClean® Microbial DNA Isolation kit (MO BIO Laboratories, USA) following the manufacturer's instructions. The elution buffer was preheated to 55 °C and used in two steps (25 µL each). Quantitative PCR (qPCR) was performed in CFX Connect Real-Time PCR Detection System (Bio-Rad, CA, USA) in triplicates using iTaq Universal SYBR Green Supermix (Bio-Rad). The primer pair mlasF/mcrAR (Steinberg and Regan, 2008) was used to amplify the mcrA gene (methyl coenzyme-M reductase) of methanogenic archaea, whereas the universal bacterial primer pair Uni331F/Uni797R (Nadkarni et al., 2002) was used for the reference strain P. fluorescens. The cycling conditions were as follows: 95 °C for 10 min, 40 cycles of 95 °C for 30 s, 55 °C (mlasF/mcrAR) or 57 °C (Uni331F/Uni797R) for 30 s, 72 °C for 30 s, and a subsequent melting curve (65 °C to 95 °C, 1 °C increments). Standard curves for each qPCR assay were generated using tenfold serial dilutions of quantified (2100 Bioanalyzer, Agilent, USA) linear standards of the target fragment amplified from *Ms. barkeri* or *Bacillus subtilis*. For all standards, nearly perfect linear regressions ($R2 > 0.997$; efficiency range of 0.8 to 1.0; slope range of -3.3 to -3.8) were obtained. To verify the reproducibility of the quantification results, some samples were randomly re-evaluated in independent qPCR runs.

2.12 Experiment 3: Verification of the optimized PMA treatment by PCR coupled with denaturing gradient gel electrophoresis (PCR-DGGE)

Equal amounts of either living or isopropanol-killed cells of *Ms. vacuolata* and *Ms. soligelidi* (two close-related strains of the genus *Methanosarcin*a, which own similar sequences) were mixed and processed with the optimal light exposure time of 5 min and 130 µM PMA prior to a DNA extraction using the PowerSoil® DNA Isolation kit. Amplification of the archaeal 16S rRNA gene for subsequent DGGE was conducted using the primer pair GC_519F and 915R (Stahl and Amann, 1991). The DGGE analyses were conducted as described previously by Ganzert et al. (2007). If the DGGE method is applicable to separate between free DNA and DNA from living cells of two close-related strains, it is suggested to separate also more distantly-related strains.

2.13 Experiment 4: PMA treatment in the presence of humic substances

To investigate the interaction between PMA and humic substances, a humic acid standard (Suwannee River Humic Acid Standard II; HA) and a fulvic acid standard (Suwannee River Fulvic Acid Standard II; FA) from the International Humic Substances Society (IHSS, USA) was added at different concentrations (HA: 0.05 to 10 µg mL^{-1}, FA: 1.0 to 80 µg mL^{-1}) to 10 ng μL^{-1} of free DNA prior to treatment with 50 µM PMA. First, it was verified that 50 µM PMA successfully inhibited 10 ng μL^{-1} of free DNA without the addition of humic substances. Second, the concentrations of HA and FA (0.025 to 100 µg mL^{-1}) capable of inhibiting the polymerase activity were identified. Third, the effectiveness of PMA (50 µM, 1 min LED activation) to suppress the PCR amplification of DNA from membrane-compromised cells in the presence of different concentrations of humic substances was checked by standard PCR.

2.14 Experiment 5: PMA treatment with increased amounts of particle-rich environmental sample

Another vulnerability of the PMA treatment in environmental samples is the light activation of PMA. This experiment should clarify to which extent turbidity of the sample might reduce the effectiveness of the DNA masking of PMA (referred to as turbidity effect). PMA treatment of particle-rich environmental samples was evaluated using sediment material from El´gygytgyn Crater Lake (Far East Russian Arctic), which was retrieved during the ICDP Lake El'gygytgyn Drilling project in 2008 and 2009 (Melles et al., 2011). The clay and silt-rich sediment (16.3% clay, 47.0% silt, 36.7% sand; 0.11% total nitrogen; approximately 198 m deep and 3.3 Ma old)

(Nowaczyk et al., 2013a) is characterized by a low level of microbial activity and a low carbon value (0.24%). In comparison to the sediment material, sandy soil from Germany (2.8% clay, 14.8% silt, 82.4% sand; 0.21% total nitrogen) was used as an active and carbon-rich sample (2.96%). Thereby, the total carbon (TC) and total nitrogen (TN) were determined with an element analyzer (Elementar Vario EL III, Hanau, Germany), whereby the grain size was analyzed after removal of carbonate and organic material with a Coulter LS 200 laser particle size analyzer (Beckman Coulter, Brea, CA). Different amounts of double autoclaved soil (1,000, 600, 500, 200, 100, 50 mg mL^{-1}) and sediment (1,000, 600, 500, 200, 100, 50, 25, 10, 5, 1, 0.6 mg mL^{-1}) were added to 0.1% Diethylpyrocarbonate-treated water (nuclease-free, autoclaved, BioScience-Grade, Carl Roth, Germany) with 10 ng μL^{-1} DNA (genomic DNA of methanogens) before 50 µM or 130 µM PMA treatment. Negative controls (50 mg mL^{-1} of sediment or soil) consisted of samples without PMA or light exposure. The PMA treatment was performed similarly to the previous ones (Section 2.11). The total DNA was extracted using a PowerSoil® DNA Isolation kit (MO BIO Laboratories Inc., Carlsbad, CA) according to the manufacturer's protocol with preheated elution buffer. The PMA treatment was checked by PCR and qPCR analyses as described before.

2.15 Statistical analyses of PMA experiments

For comparison of PMA-treated and untreated samples, one-way ANOVA coupled with Tukey test (pairwise multiple comparison procedure) was conducted for normally distributed (passed Shapiro-Wilk normality test) and homoscedastic qPCR data (passed equal variance test). In the cases where the values in the groups do not show the same variances (= heteroscedastic) but are normally distributed, the Kruskal-Wallis one-way analysis of variance on ranks were used. Intact and membrane-compromised cells were analyzed separately and statistically significant differences ($p < 0.05$) were indicated by different letters (see Figure 3.7 and 3.8). To investigate the relation between the degree of false-negative results for living methanogens and the light exposure duration, linear regression analyses were performed with the software SigmaPlot 11.2.

3 Results

This chapter first examines the diversities and abundancies of total DNA extracts of 57 sediment samples in relation to changing climatic conditions within the last 3.6 Ma and especially for the Pliocene-Pleistocene transition. Secondly, this chapter focuses on the live/dead differentiation, where two newer methods are described, the PMA treatment and the cell separation (extracellular DNA, intracellular DNA). Finally, the environmental drivers are investigated which influence the three DNA pools.

3.1 Diversity, abundance and composition of the microbial communities along the lake sediment chronosequence

3.1.1 Bacterial and archaeal abundance

Based on their 16S rRNA genes, bacteria and archaea abundance were estimated every 100,000 years (approx. every 5 or 50 m, depending on the sedimentation rate, Figure 3.1A) using qPCR (Section 2.5 and Figure 3.1D) and compared with the Si/Ti (Figure 3.1B) and the total organic carbon (TOC) values (Figure 3.1C). In general, bacteria were approximately two orders of magnitude more abundant than archaea along the lake chronosequence. The bacterial abundance ranged from 1.2×10^3 to 1.8×10^6 (average 9.3×10^4) copies g^{-1} sediment (wet weight), and the archaeal abundance ranged from 2.9×10^1 to 1.2×10^5 (average 7.5×10^3) copies g^{-1} sediment. The maximal microbial abundance was associated with a depth of 141.5 m (Marine isotope stage MIS G15 with a moderate high amount of TOC). Within the youngest 2.6 Ma (MIS 23-104), the microbial abundance followed glacial/interglacial cyclicality. In the deeper sediment layers (MIS G5–MG12), the data revealed an almost constant microbial abundance, with an increase in the copy number for both archaeal and bacterial 16S rRNA genes, toward the deepest sediment layer.

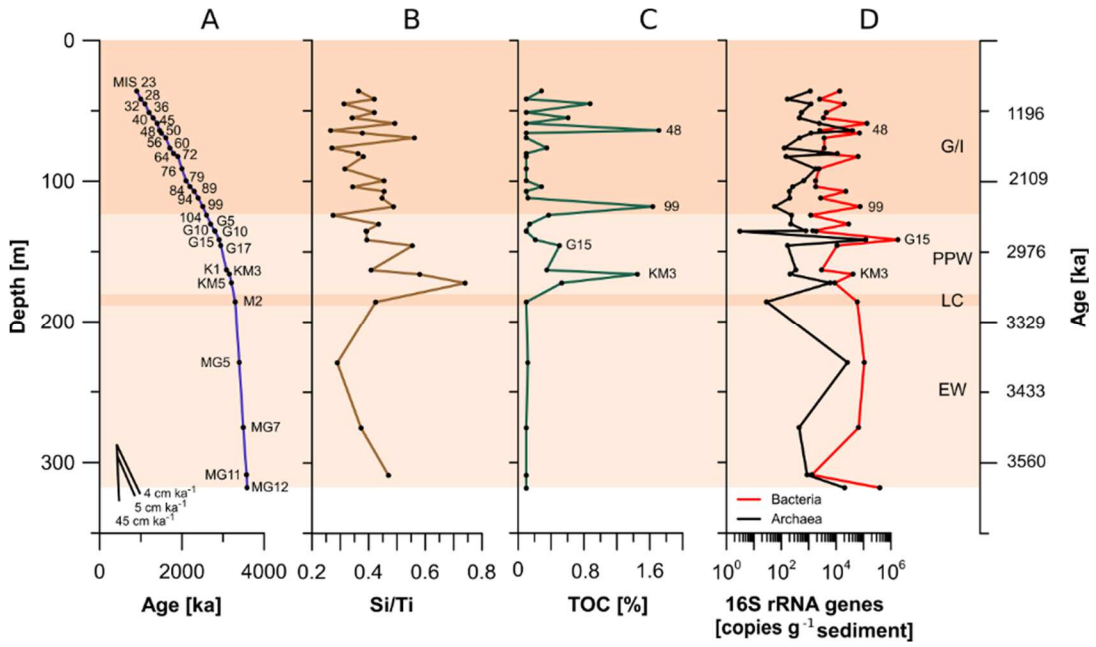

Figure 3.1: Vertical profile of Lake El'gygytgyn sediments between 36-317 m depth with **(A)** age-depth model of the sediments (Nowaczyk et al., 2013), indicating the sedimentation rates in cm ka^{-1}, **(B)** silica-titanium ratio reflecting the measure of biogenic silica, **(C)** total organic carbon (TOC) in %, and (**D**) abundance of bacterial (red line) and archaeal (black line) 16S rRNA genes in copies g^{-1} sediment (ww). The corresponding marine isotope stages (MIS, Lisiecki & Raymo, 2005) of each sample are indicated in (A). EW: Extreme arctic warmth, LC: Largest cooling in Pliocene, PPW: Pliocene-Pleistocene warmth, G/I: Changing glacial and interglacial periods in Pleistocene.

3.1.2 Quality of Illumina sequencing reads

After paired-end read merging and stringent quality filtering (e.g., no mismatch in the barcode or primer sequence, Phred quality score ≥ 25; Section 2.7), 68% of sequences with an average sequence length of 293 bp remained. A total of 5.59 million quality filtered reads from the 57 samples were ultimately further evaluated, between 3,971 and 225,527 reads per sample (Table A.2). The proportions of reads assigned to each taxonomic level differed by phylum (99.7%), class (99.7%), order (98.8%), family (95.0%), genus (77.5%), and species level (48.3%).

3.1.3 Microbial diversity and richness of the Lake El'gygytgyn deep biosphere

The mid- to late-Pliocene samples resulted in a significantly higher number of OTUs compared to the interglacial/glacial samples of the Pleistocene. All of the 5.59 million sequences clustered into 6,910 OTUs at a 97% similarity threshold (see Appendix Dataset 1). We received

171-1,197 OTUs (mean 634 OTUs) in the Pliocene (Figure 3.2G) but only 147-373 OTUs (mean interglacial: 238 OTUs, mean glacial: 266 OTUs) in the Pleistocene (Figure 3.3E). The approximately 2.5-fold higher microbial richness in the Pliocene sediments is mainly based on several rare taxa (< 100 reads). Thus, the OTUs of both sample series follow a power-law distribution: Almost all sediment layers are dominated by OTUs affiliated with *Halomonas* (*Gammaproteobacteria*, each 99% sequence similarity; see Figure 3.4), covering 2-94% (mean 60%) of the total reads per sample. Furthermore, 864 (12.5%) out of 6,910 OTUs incorporates a high abundance of ≥ 100 reads, whereas the main fraction of OTUs belonged to rare taxa.

Different diversity indices per sample can be found in Figure 3.2G, Figure 3.3E and Table A.2. The Chao 1 richness estimator and Shannon-Weaver diversity index (H) confirm a higher richness of the microbial communities within the Pliocene sediments (mean $Chao1_{Pliocene}$ = 1337, mean $Chao1_{Pleistocene}$ = 747; mean $H_{Pliocene}$ = 2.19, mean $H_{Pleistocene}$ = 1.47). Thereby, the Shannon-Weaver index classifies primarily the samples with the highest evenness as the most diverse, including samples of substantial disturbance, such as the formation of the lake ($H_{3585.5ka}$ = 3.57), largest cooling of mid-Pliocene ($H_{3298.0ka}$ = 5.01), or onset of Northern hemisphere glaciation ($H_{2698.8ka}$ = 4.14).

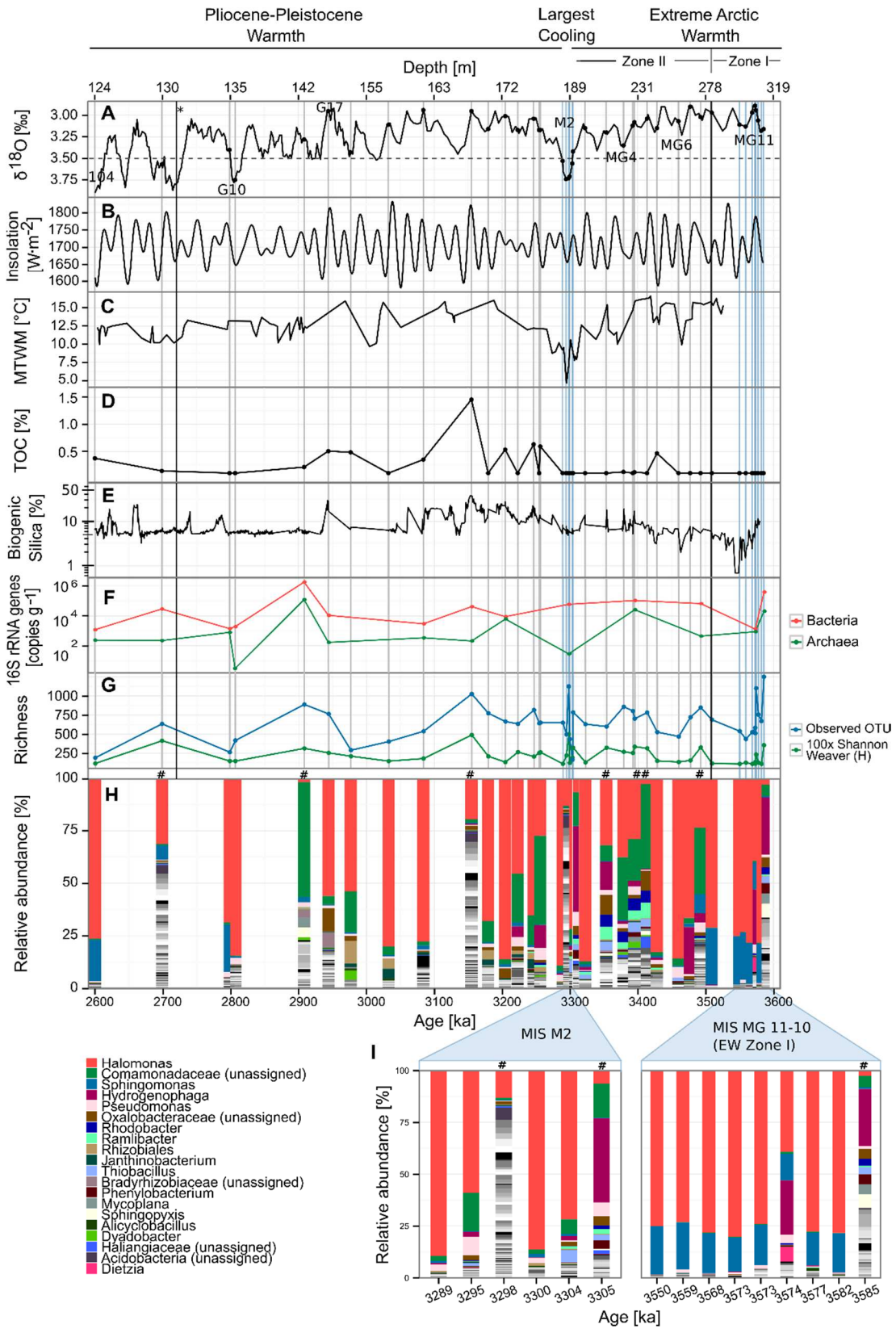

Figure 3.2: Mid- to late-Pliocene: Comparison of the microbial diversity and community composition, the reconstructed paleo-climatological conditions and other influencing environmental parameter with (**A**) global marine isotope stack in ‰ ($\delta^{18}O$, Lisiecki & Raymo 2005), M2 = Largest cooling in Pliocene, * = onset of northern hemisphere glaciation, 104 = first glacial, (**B**) 65°N summer insolation in W m^{-2} (Laskar et al, 2004), (**C**) reconstructed mean temperature of the warmest month (MTWM) in °C (within first 20 ka no pollen could be

detected and therefore no reconstruction of the MTWM is available), (**D**) total organic carbon (TOC) in %, (**E**) biogenic silica value in %; (**F**) bacterial (red line) and archaeal (green line) 16Sr RNA gene copies in copies per g wet weight, (**G**) diversity measurements expressed as observed OTU number, Chao1 richness estimates, and evenness-emphasizing Shannon-Weaver index, (**H**) relative abundance of microbial taxa (> 0.1% abundance; legend is sorted by frequency and shows the most abundant 20 taxa in color; additional taxa are shown in shades of grey), and (**I**) expanded view into microbial community of extreme Arctic warmth (MIS MG 11-10) and largest cooling in Pliocene (LC, MIS M2). Please note that all parameters are mapped to the age incorporating the specific sedimentation rates (up to 1 order of magnitude difference) of the age-depth model by Nowaczyk et al., 2013. Sediment layers with a Shannon-Weaver index above 3 and therefore an outstandingly high number of abundant OTUs (55-175 taxonomic categories above 0.1% of the total relative abundance) are indicated by pound signs.

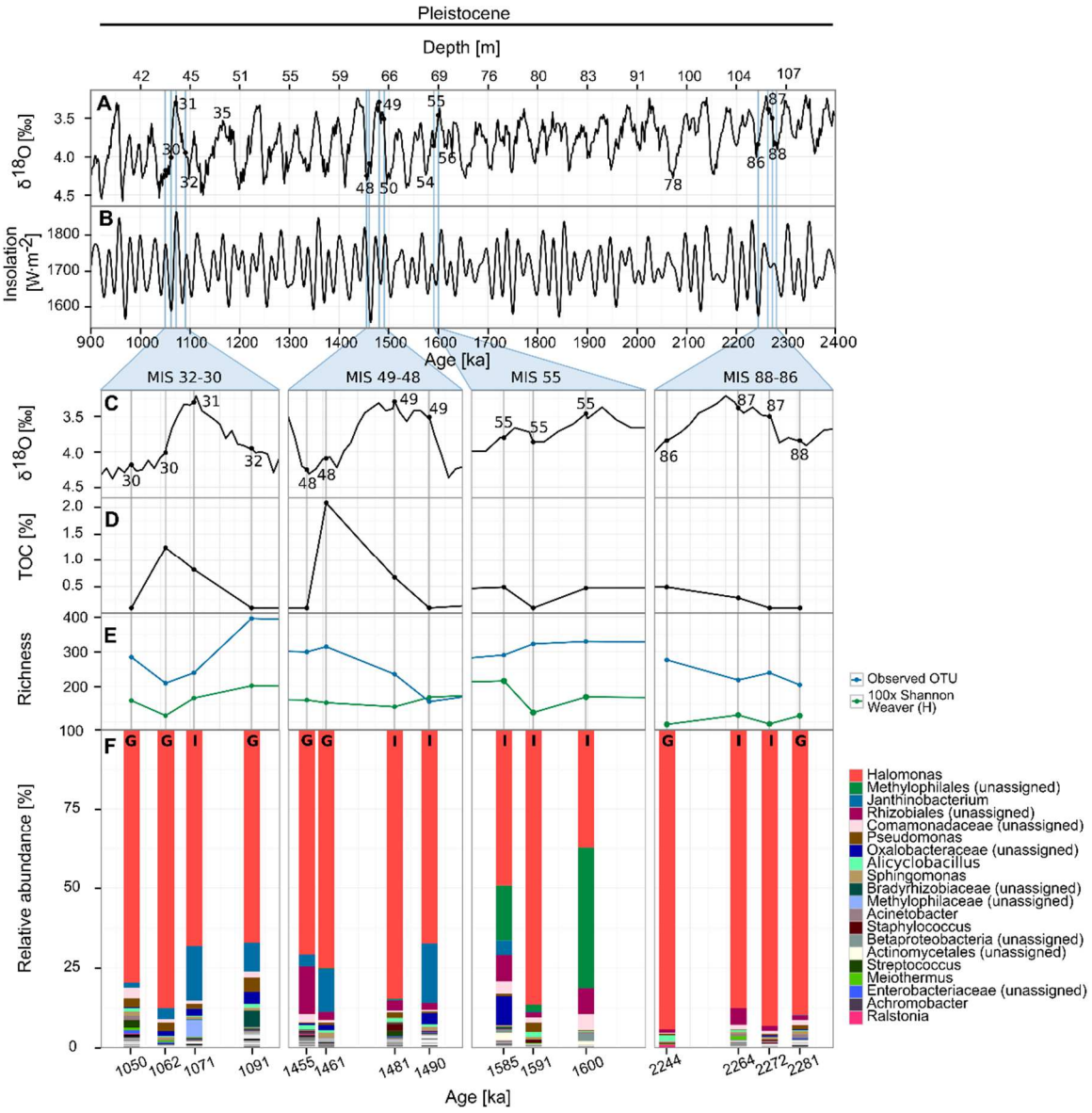

Figure 3.3: Interglacial/glacial cyclicity of the Pleistocene (super interglacial MIS 31, 49, 55, 87): Comparison of the microbial diversity and community composition, the reconstructed paleo-climatological conditions and other influencing environmental parameter with (**A**) global marine isotope stack in ‰ ($\delta^{18}O$, Lisiecki & Raymo 2005) (**B**) 65°N summer insolation in W m^{-2} (Laskar et al, 2004), (**C**) detailed view in global marine isotope stack in ‰, (**D**) total organic carbon (TOC) in %, (**E**) diversity measurements expressed as observed OTU number, Chao1 richness estimator, and evenness-emphasizing Shannon-Weaver index, and (**F**) relative abundance of microbial taxa (> 0.1% abundance; legend is sorted by frequency and shows the most abundant 20 taxa in color; additional taxa are shown in shades of grey). Please note that all parameter are mapped to the age incorporating the specific sedimentation rates (up to 1 order of magnitude difference) of the age-depth model by Nowaczyk et al., 2013. G: Glacial periods, I: Interglacial periods. Additional parameters, such as the reconstructed mean temperature of the warmest month (MTWM), are presented in supplementary information (Fig A2) due to missing pollen analysis for MIS 49 and MIS 55.

Due to the large differences in the abundance and richness of the Pliocene and Pleistocene sediments, both sample series are separately described in the following sections.

3.1.4 Microbial community composition in the mid- to late-Pliocene

The microbial communities are highly diverse and variable in the El'gygytgyn Lake sediments of the mid- to late-Pliocene. Ten sediment layers contained an outstandingly high number of abundant OTUs (Shannon-Weaver index above 3; 55-175 taxonomic categories above 0.1% of the total relative abundance; Figure 3.2H, I # and Figure 3.4 #). The microbial communities are dominated by *Proteobacteria* (90.8%), followed by *Actinobacteria* (2.3%), *Bacteroidetes* (2.1%), and *Acidobacteria* (0.75%). At a fine taxonomic level, the deep lake sediments are characterized by abundant families closely related to *Halomonadaceae*, *Sphingomonadaceae*, *Comamonadaceae*, and *Oxalobacteriaceae* (see also Table A.1 in Appendix for a comparison of the 20 most common taxonomic units and their coverage within different geological units).

In total, 67 unique archaeal OTUs were assigned to 16 different genera (obtained from < 0.1% of the total reads). The most abundant archaeal representative was *Candidatus Nitrososphaera* (*Thaumarchaeota*, *Nitrososphaeraceae*). Other archaeal sequences belonged mainly to *Halobacteriaceae*-related species *(Halobacterium*, *Haloarcula*, *Halonotius*, *Natronomonas*, *Halorubrum, Halolamina*, *and Haloquadratum), Methanobacterium* (*Methanobacteria*), as well as *Methanomicrobia (*methanogenic archaea *Methanosarcina* and *Methanosaeta).*

In Figure 3.2, the relative microbial abundance (Figure 3.2H, I genus level and if not identifiable, next higher taxonomical level), the reconstructed paleo-climatological conditions (Figure 3.2A-C) and the sedimentary characteristics of the Pliocene deposits (Figure 3.2D, E) are summarized. It is possible to divide the mid- to late-Pliocene into the following three climatic scenarios:

Extreme Arctic warmth (3.6 to 3.4 Ma, EW, Zone I and II). The oldest sediment sample (3.58 Ma) shows a high microbial abundance (measured by qPCR, Figure 3.2F) and a highly diverse microbial community (Figure 3.2H, I and Figure 3.4). The first 80 ka of lake sedimentation (Figure 3.2 Zone I of EW, MIS MG 11-10) are characterized by a quite similar composition mainly consisting of *Halomonas* und *Sphingomonas*, except for a rapid increase in the microbial diversity with maximal summer insolation, TOC value, and biogenic Si values ($Chao1_{3574.0ka}$ = 2360). After the initial colonization, we observed a much more diverse microbial composition while mean temperature of the warmest month (MTWM) (Figure 3.2C)

and annual precipitation (PANN) (see Figure A.1D) remained high (Figure 3.4, Zone II of EW). We revealed a decreasing ratio of *Sphingomonas*, but an increasing ratio of *Comamonadacea* (including *Hydrogenophaga*), and a strongly intensified appearance of *Thiobacillus*, *Rhodobacter*, *Cytophagaceae,* and *Ramlibacter*. Moreover, *Phyllobacteriaceae* (*Rhizobiales*) and *Bacteriovoraceae* (*Bdellovibrionales*) were present almost exclusively in Zone II of EW.

Largest cooling of the mid-Pliocene (3.31 to 3.28 Ma). The largest cooling of the mid-Pliocene (MIS M2) is characterized by a sudden drop in temperature (Figure 3.2A, C), low lake levels (see Figure A.1D), and a perennial lake ice blanket. The summer insolation variability had a lower amplitude, while MTMW, PANN, TOC, and biogenic Si exhibit a sharp decline (Figure 3.2 and Figure A.1). Within the rapid cooling phase, we also see a rapid decrease in diversity (mainly based on rare taxa with an abundance lower 1%), followed by a zone of maximal diversity (3298 ka; 90 taxa above 0.1%). The most abundant microbial communities mainly contain a similar composition as that within the last phases of extreme Arctic warmth, but with a decrease in *Rhodobacter* and *Hydrogenophaga* and an increase in *Rhizobiales* and *Mycoplana.*

Pliocene-Pleistocene warmth (3.26 to 2.2 Ma). The richness indices within the Pliocene-Pleistocene warmth are initially high. However, there is a fourphasic decrease in the OTU number and the Chao1 index toward the first glacial phases (MIS 104, 2.6 Ma). Along with *Halomonas* and *Sphingomonas*, we observed a high abundance of *Comamonadacea* and *Oxalobacteraeceae* as well as *Janthinobacterium*. There were three sediment layers with an outstandingly high number of abundant OTUs (Figure 3.2H, I #), whereby the sample with a high bacterial and archaeal gene copy number (2908 ka) had an extraordinary low amount of *Halomonas*, replaced by *Comamonadacea*.

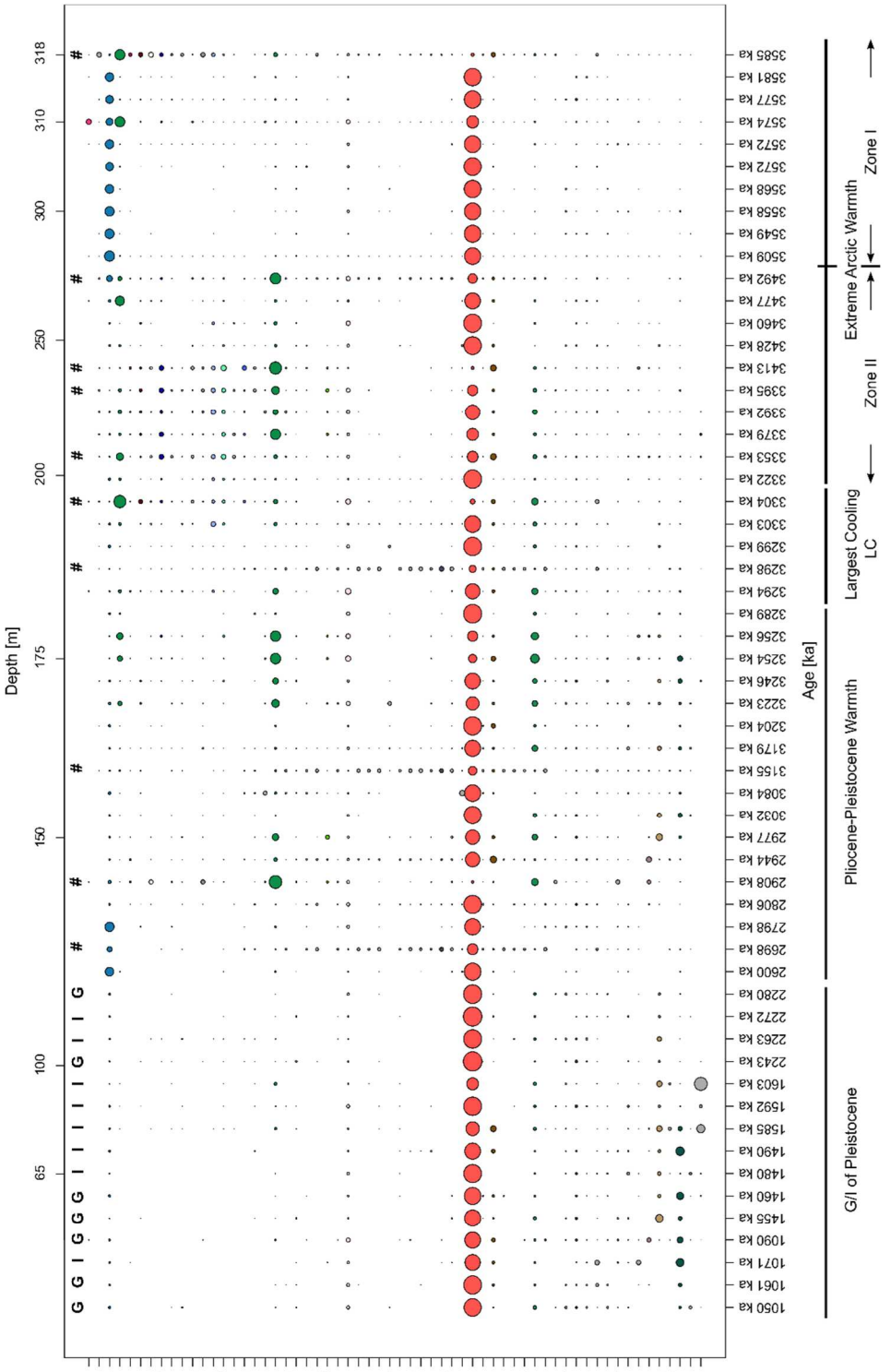

Figure 3.4: Bubble plot representing the distribution and relative abundance of the 60 most abundant taxa within the deep biosphere of the El'gygtgyn Crater Lake. For a better comparability, both Pleistocene and Pliocene deposits are included. Taxa are shown for genus level and if not identifiable in next higher taxonomical level, respectively. The most abundant 20 taxa are marked in color. Sediment layers with a Shannon-Weaver index above 3 and therefore an outstandingly high number of abundant OTUs (57-105 taxonomic categories above 0.1% of the total relative abundance) are indicated by pound signs. G: Glacial periods, I: Interglacial periods

Interestingly, the richness parameters Chao1, OTUs, and Shannon Weaver Index follow the general trend of the paleo-climate, which is illustrated in

Figure 3.5. In the warmer period of EW Zone I, the MG11, all richness parameter significantly increase. Here, it was possible to detect a microbial response to increasing temperatures (depleted $\delta^{18}O$-signals, high MTWM, high PANN) and increasing biogenic silica values, where a response of plant pollen (MTWM; PANN) was not demonstrable due to missing pollen in the deepest sediment layers. Especially noticeable are the richness values for cooler periods of the mid- to late Pliocene in the MIS MG6, M2 and G10, which follow the enriched $\delta^{18}O$-signals.

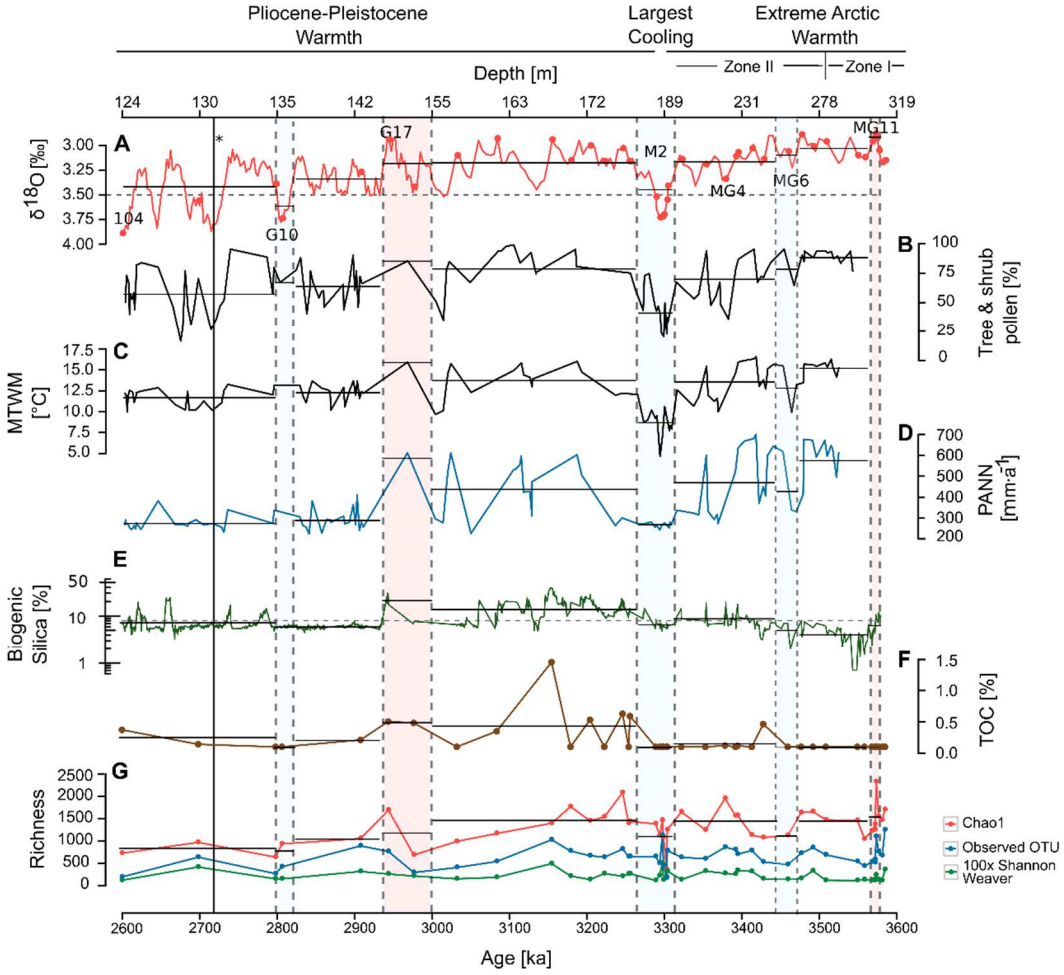

Figure 3.5: El'gygytgyn environmental parameter of the mid- to late-Pliocene are summarized and for each climatic interval the average is included for a better comparison of the dependencies with (**A**) global marine isotope stack in ‰ ($\delta^{18}O$, Lisiecki & Raymo (2005), M2 = Largest cooling in Pliocene, * = onset of northern hemisphere glaciation, 104 = first glacial, (**B**) Tree and shrub pollen in %, (**C, D**) reconstructed mean temperature of the warmest month (MTWM) in °C and annual precipitation (PANN) in mm a^{-1} (within first 20 ka no pollen could be detected and therefore no reconstruction of the MTWM and PANN is available), (**E**) biogenic silica value in %; (**F**) total organic carbon (TOC) in %, and (**G**) diversity measurements expressed as observed OTU number, Chao1 richness estimates, and evenness-emphasizing Shannon-Weaver index.

3.1.5 Microbial community composition of Pleistocene interglacial/glacial cycles

We also compared four super interglacial stages between 1.0 and 2.3 Ma (MIS 31, 49, 55, 87) (Melles et al., 2012) with their adjoining glacial periods. Interglacial periods are characterized by highly depleted $\delta^{18}O$-signals, which indicates warmer temperatures (Melles et al., 2012) in comparison to glacial periods. However, we could not find significant differences in the composition of the microbial community in the glacial and interglacial phases (Figure 3.3, Figure A.2,). The microbial community within one glacial/interglacial cycle was more similar than between different glacial/interglacial cycles.

We discovered a lower diversity in the interglacial/glacial sediments compared to the older layers of the chronosequence. The bacterial sequences were affiliated with the phyla *Proteobacteria* (mean 96.0%, based on *Alpha-*, *Beta-*, *Gamma-*, and *Deltaproteobacteria*), *Firmicutes* (1.6%), and *Actinobacteria* (0.7%), but had a significantly lower number of taxa. Additionally, the archaeal assemblage was less diverse: The sequences belong exclusively to *Euryarchaeota* and split into different representatives (e.g., *Halobacterium*, *Haloarcula and Halonotius*) of the family *Halobacteriaceae*. Compared to samples from the Pliocene, the Pleistocene interglacial/glacial period samples comprise much higher ratios of *Methylophilales*, *Janthinobacterium lividum*, and *Rhizobiales*. In contrast, the majority of OTUs (e.g., *Hydrogenophaga*, *Thiobacillus*, *Rhodobacter* and *Ramlibacter*) are restricted to the deep sediment layers (Figure 3.4, Table A.1).

3.2 Propidium monoazide treatment to distinguish between live and dead methanogens in pure cultures and environmental samples

Next to the investigation of the microbial abundance and composition of deep biosphere sediments, this thesis investigates the differentiation between the live and dead microbial communities. Within this section and the next section, results of the adaption of two newer methods to differentiate between intact cells (intracellular DNA, live) and free DNA (extracellular DNA, mainly dead) are shown. This section refers to the evaluation and adaption of the intercalating dye propidium monoazide (PMA) to methanogenic archaea and environmental samples (Section 2.9-2.15), whereas Section 3.3 demonstrates the results of a cell separation (Section 2.4 and Section 2.6-2.8).

All results of this section are derived from the following accepted publication:

Heise, J., Nega, M., Alawi, M., Wagner, D., 2015. Propidium monoazide treatment to distinguish between live and dead methanogens in pure cultures and environmental samples. J. of Microbiol. Methods 121: 11-23 http://dx.doi.org/10.1016/ j.mimet.2015.12.002

3.2.1 Experiment 1: Fluorescence microscopic examination of the membrane impermeability to PMA

With the use of the LIVE/DEAD® BacLight™ kit, it was possible to examine the membrane integrity of viable methanogenic cells and isopropanol-killed cells (dead cells) (Figure A.4). Neither concentration of PMA penetrated the membranes of intact methanogens (Figure 3.6 shows examples of *Mb. movilense* and *Ms. barkeri*). For instance, in a well grown culture of *Mb. movilense*, a negligible quantity of 2 out of 72 cells were stained with 130 µM PMA after a 10-min incubation (compare arrows in Figure 3.6A). In the exceptional case of *Ms. soligelidi*, a comprehensive cell bursting effect was observed under microscopic conditions, which led to complete staining with 130 µM PMA after cell collapse. However, such a destructive effect was not observed by PMA-qPCR (Experiment 2, Figure 3.8A). Moreover, PMA was able to penetrate all of the isopropanol-treated cells of *Mb. lacus*, *Mb. movilense*, *Ms. barkeri*, and *Ms. soligelidi*. A PMA concentration of 130 µM resulted in faster and more intensive staining of damaged cells in comparison to 50 µM (not shown).

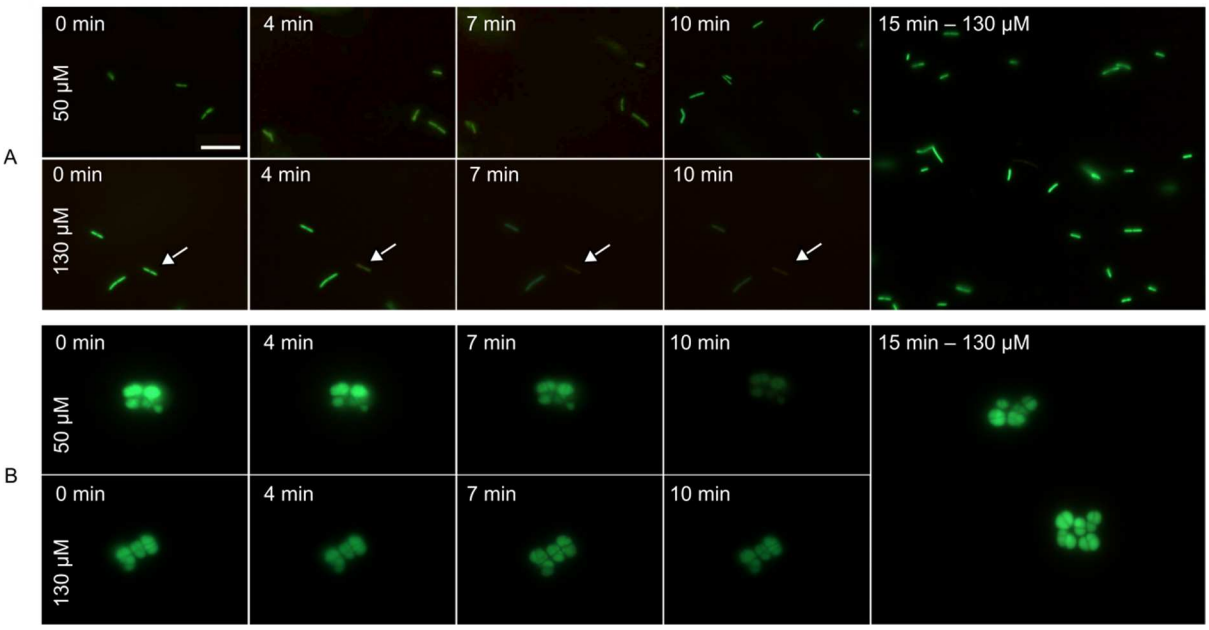

Figure 3.6: Microscopic examination of the effect of PMA (50 µM and 130 µM; red) on the membrane integrity of methanogenic archaeal cells. Intact cells of (**A**) *Methanobacterium movilense* and (**B**) *Methanosarcina barkeri* were assessed for different incubation durations. All of the samples were pre-stained with SYTO 9 (green) as a reference. The absence of PMA staining in the micrographs indicates that PMA does not infiltrate intact methanogenic cells. Bar, 10 µm.

3.2.2 Experiment 2: Evaluation of the PMA treatment for pure cultures by PMA-qPCR analyses

All data passed the normality test of Shapiro-Wilk ($P > 0.05$). In comparison to the negative control without any addition of PMA or light (Figure 3.7, NK), we observed significant lower archaeal gene copy numbers for all PMA controls ($p_{Tukey} < 0.05$) with the exception of the dead cells of *Mb. movilense* and *Ms. soligelidi* (Figure 3.7A and B right panel). The light exposure controls (LED) without PMA addition seemed to result in a negligible reduction of the qPCR signal, with the exception of those of intact *Mb. movilense* cells (reduction by 0.39 log = 59.20%). The control reactions revealed a significantly smaller effect on intact cells (reduction by maximal 0.2 log = 35.33% for *P. fluorescens*; or maximal 0.47 log = 66.22% for methanogens) (Figure 3.7 left panel) than on membrane-compromised cells (reduction by ≤ 1.2 log = 93.72% for *Ms. soligelidi*; or 4.4 log = 99.99% for *P. fluorescens*) (Figure 3.7 right panel).

In comparison to the control reactions, the signal reduction of intact and membrane-compromised cells was even higher after a proper PMA treatment (addition of PMA and light activation) (Figure 3.8). Complete suppression of free DNA was possible for *Ms. soligelidi* and *P. fluorescens* for all of the tested PMA concentrations (Figure 3.8A and C right panel),

whereas for *Mb. movilense* exclusively, a PMA concentration of 130 µM (≥ 5 min of light activation) was suitable (Figure 3.8B right panel). Thus, the PMA concentrations of 50 µM and 90 µM only led to an average signal reduction of 0.94 log (84.39%) for membrane-compromised *Mb. movilense*, with no significant effect of a longer duration of light exposure ($p_{t\text{-}test}$ = 0.15-0.85). Moreover, we revealed strong false-negative results for living methanogens (Figure 3.8A, B left panel), which resulted in an underestimation of the number of living cells (average signal reduction by 0.97 log = 87.32% for *Ms. soligelidi*; or 0.99 log = 89.98% for *Mb. movilense*). The degree of false-negative results for living methanogens was enhanced by a longer light exposure duration (linear regression $R^2_{adjusted,\ Ms.\ soligelidi}$ = 0.95-0.82, p-value = 0.007-0.051; $R^2_{adjusted,\ Mb.\ movilense}$ = 0.90-0.88, p-value = 0.001-0.024). In contrast, no strong reduction of living *P. fluorescens* cells by the PMA treatment was identified in terms of either the PMA concentration ($p_{t\text{-}test,\ 50\ \mu M}$ = 0.61, $p_{t\text{-}test,\ 200\ \mu M}$ = 0.04) or the light exposure duration ($p_{t\text{-}test,\ 50\ \mu M}$ = 0.45 , $p_{t\text{-}test,\ 200\ \mu M}$ = 0.41). Validation of the qPCR signal for living cells was performed by microscopy using a Thoma cell counting chamber. On average, qPCR and cell counting, respectively, revealed 2.4 x 10^4 +/- 2.3 x 10^3 copies μL^{-1} and 3.1 x 10^4 +/- 3.8 x 10^2 cells μL^{-1} for *Mb. movilense*, and 3.8 x 10^5 +/- 2.8 x 10^5 copies μL^{-1} and 1.3 x 10^5 +/- 5.3 x 10^3 cells μL^{-1} for *Ms. soligelidi*.

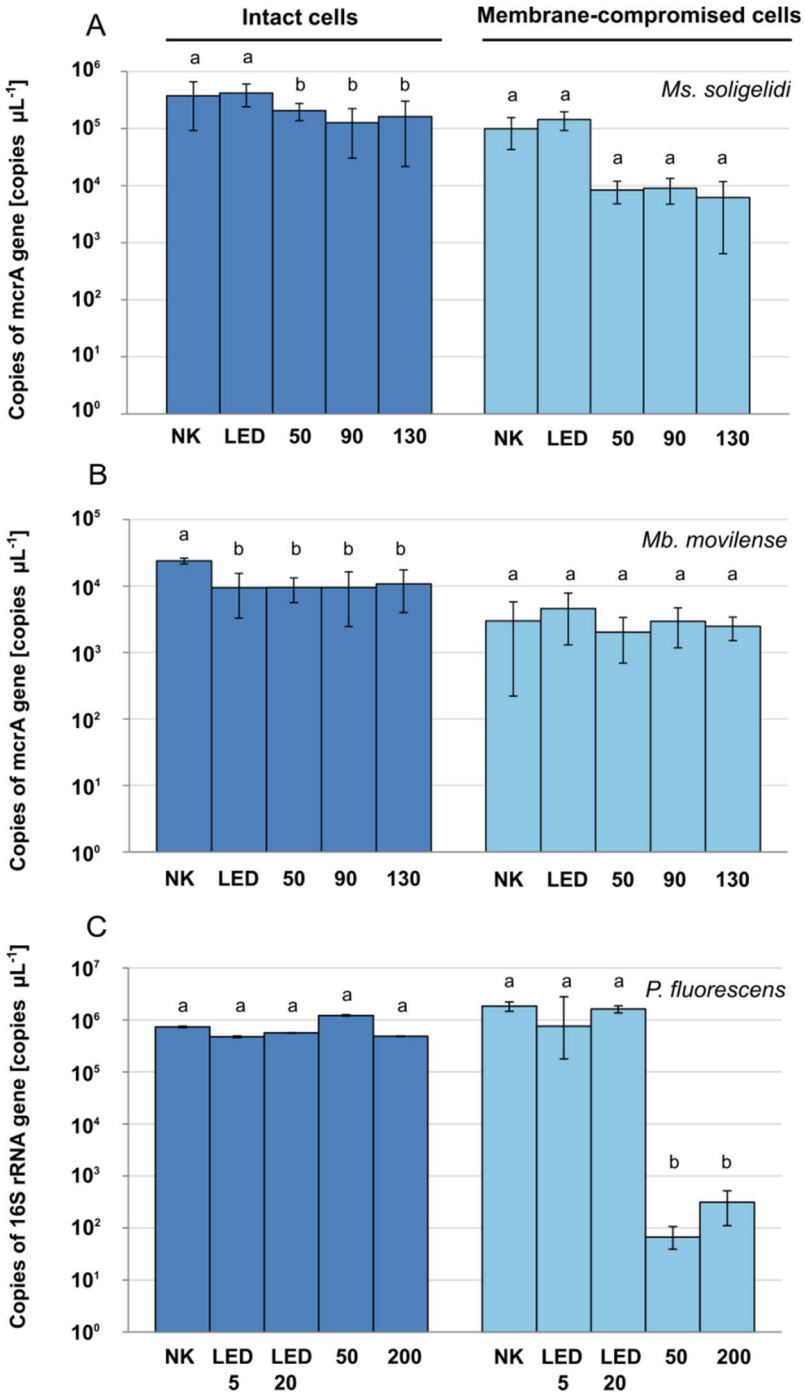

Figure 3.7: Overview of the different control reactions used to analyze the effects of the experimental parameters on measurable gene copies via qPCR. (**A**) *Methanosarcina soligelidi*, (**B**) *Methanobacterium movilense*, and (**C**) the reference strain *Pseudomonas fluorescens*. NK: without PMA and light exposure; LED: without PMA but with 10 min LED exposure; LED 5 or 20: without PMA but with 5 or 20 min LED exposure; 50-200: with 50-200 µM PMA but without any light exposure. Error bars indicate the standard deviation of the sample triplicates in PMA treatment. Statistically significant differences in measurable gene copies are shown by different letters (one-way ANOVA and Tukey test, $p < 0.05$) and are calculated separately for intact and membrane-compromised cells. For heteroscedastic data (membrane-compromised cells of *Ms. soligelidi* and *Mb. movilense*) the Kruskal-Wallis one-way analysis of variance on rank was used.

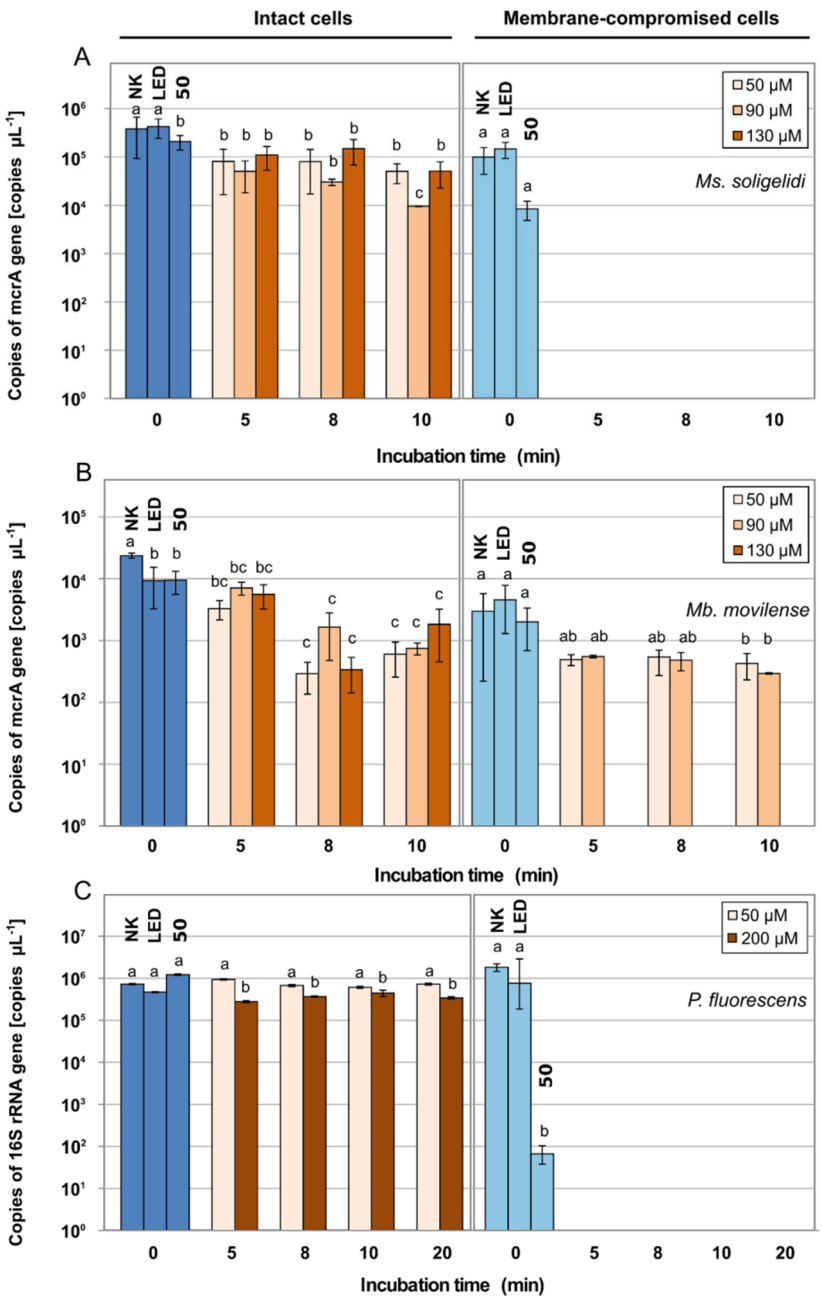

Figure 3.8: Application of PMA-qPCR for (**A**) *Methanosarcina soligelidi*, (**B**) *Methanobacterium movilense*, and (**C**) *Pseudomonas fluorescens*. Intact and membrane-compromised cells were treated in triplicates with PMA (50 µM to 200 µM) and photo-activated with LED light using different incubation times (5 to 20 min). The mcrA gene copies per µL (methanogens) or the 16S rRNA gene copies per µL (reference strain) resulting from the qPCR are shown. To evaluate the effect of a single experimental factor, different controls were evaluated (NK: without PMA and light exposure; LED: without PMA but with LED exposure; 50: with 50 µM PMA but without light exposure). Error bars indicate the standard deviation of the sample triplicates in PMA treatment. Statistically significant differences in measurable gene copies are shown by different letters (one-way ANOVA and Tukey test, $p < 0.05$) and are calculated separately for intact and membrane-compromised cells. For heteroscedastic data (membrane-compromised cells of *Ms. soligelidi* and *Mb. movilense*) the Kruskal-Wallis one-way analysis of variance on rank was used.

3.2.3 Experiment 3: Verification of the optimized PMA treatment by PCR coupled with denaturing gradient gel electrophoresis (PCR-DGGE)

By analyzing a mixture of either living or killed cells of two close-related methanogens, it was possible to suppress the amplification signal of the killed strain using the PMA-PCR technique (130 µM PMA) as evidenced by a reduction of the amplification product by approximately half (Figure 3.9A; additionally checked by qPCR lane 1: 8.0 x 10^8 +/- 6.40 x 10^6 copies μL^{-1}, lanes 2 and 3: 5.0 x 10^8 +/- 4.97 x 10^6 and 3.0 x 10^8 +/- 1.13 x 10^6 copies μL^{-1}). Using the DGGE fingerprint technique to separate DNA fragments of equal length according to their sequence, it was not only possible to differentiate between both methanogens (Figure 3.9B, lane 1: both strains, lane 2: *Ms. vacuolata*, lane 3: *Ms. soligelidi*) in separate DGGE bands but also to fully suppress the killed strains with a 130 µM PMA treatment (Figure 3.9B, lane 4: both strains are dead and the free DNA is PMA-masked).

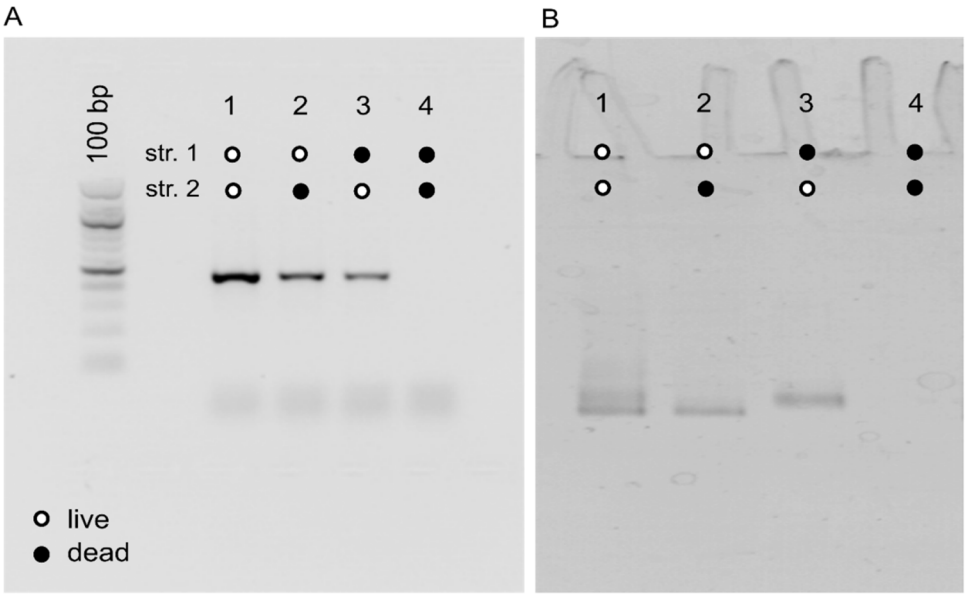

Figure 3.9: A mixture of either intact or dead cells of two methanogenic archaeal strains (str. 1 = *Ms. vacuolata*, str. 2 = *Ms. soligelidi*) after PMA treatment. The amplification products of the archaeal 16S rRNA gene were visualized in an agarose gel (**A**) and as DGGE fingerprints in a polyacrylamide gel (**B**). PMA was able to selectively suppress the amplification of free DNA in the isopropanol-killed pure cultures, indicated by qPCR-quantified amplification products with lane 1: 8.0 x 10^8 copies μL^{-1}, lanes 2 and 3: 5.0 x 10^8 and 3.0 x 10^8 copies μL^{-1}. Ladder: Quick Load 100 bp (New England Biolabs).

3.2.4 Experiment 4: PMA treatment in the presence of humic substances

We revealed a high efficiency of iTaq polymerase, even in the presence of relatively high concentrations of humic acid (amplification between 0.025-5 µg mL^{-1}, no amplification between 10 and 100 µg mL^{-1}) or fulvic acid (amplification between 0.025-80 µg mL^{-1}, no amplification for 100 µg mL^{-1}) (Figure A.5). Moreover, we did not observe an inhibitory effect of humic substances on PMA: free DNA was successfully suppressed by PMA in the presence of all investigated concentrations of humic substances (HA: 0.05-10 µg mL^{-1}; FA: 1-80 µg mL^{-1}) (Figure A.6).

3.2.5 Experiment 5: PMA treatment with increased amounts of particle-rich environmental sample

For both types of particle-rich samples, 50 µM PMA was not sufficient to completely inhibit the DNA of the dead cells (DNA in solution) (Figure A.7A, B right panel). Using 130 µM PMA, complete inhibition of the free DNA was not possible in the presence of silt and clay-rich sediments (Figure A.7A left panel). A visible reduction of the PCR amplification was observed for very low particle loads (≤ 10 mg mL-1) (Figure A.7A Nos. 1-4), but the qPCR results yielded, on average, 2.74 x 102 +/- 4.54 x 101 false-positive gene copies µL-1 (Figure 3.10 left panel). With an increased particle density, the measurable gene copy number rose (higher turbidity effects; maximal of 4.81 x 103 +/- 1.12 x 103 gene copies µL-1) and then declined again (inhibition of polymerase; minimal 7.44 x 101 +/- 1.2 x 101 gene copies µL-1, extremely small ΔCT values). For sandy soils (Figure A.7B and Figure 3.10 right panel), sufficient suppression of free DNA by PMA was possible until a particle load of 200 mg mL^{-1}. However, in the presence of a greater particle load, a substantial number of false-positive signals were detected.

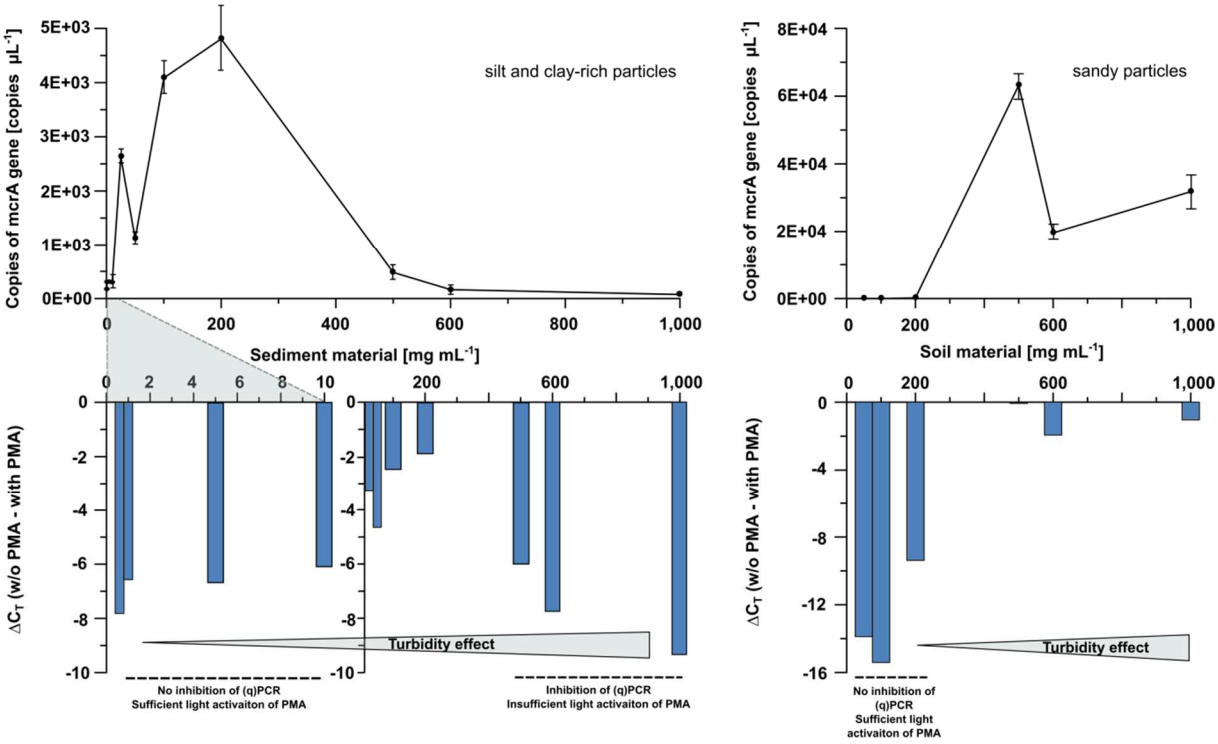

Figure 3.10: Influence of the sediment/soil matrix on PMA treatment (130 µM; 10 ng µL^{-1} DNA in solution) represented as measurable mcrA gene copies and ΔC_T values ($C_{T\_without\ PMA}$ minus $C_{T\_with\ PMA}$) obtained by qPCR. Inadequate activation of PMA was observed for all silt and clay-rich sediment (left panel). For sandy soils (right panel), sufficient suppression of the free DNA by PMA was possible up to a particle load of 200 mg mL^{-1}. Error bars indicate the standard deviation of the triplicates. Low amplification and therefore highly negative ΔC_T values at higher particle loads are caused by polymerase inhibition and not by PMA deactivation of extracellular (free) DNA.

3.3 Cell separation of deep biosphere sediments to differentiate between extracellular and intracellular DNA

The results of the PMA treatment on particle-rich samples show a strong dependence of the sediment texture and a distinct false positive effect for silt and clay-rich samples, such as the El'gygytgyn sediments. Therefore, we have chosen a cell separation over a PMA treatment to differentiate between intra- and extracellular DNA for the El'gygytgyn sediments. The results of the cell separation are presented in this section.

3.3.1 Separation of eDNA and iDNA in up to 3.6 million years old sediment samples

All analysis of cell separation were performed on 14 deep sediment samples of the El'gygytgyn Crater Lake (43-315 m deep, 1.0-3.6 Ma old) obtained during the International Continental Scientific Drilling Program (ICDP, core 5011-1, Melles et al. 2011). The eDNA and iDNA was extracted using a cell separation protocol adapted to very low amounts of DNA according to Alawi et al. 2014. The amount of extractable iDNA in the El'gygytgyn Crater Lake (Ø 0.78 ng per gram) is significantly lower (12-26 folds lower) than the amount of eDNA (Ø 18.8 ng per gram). Both DNA pools were completely separated from each other during the extraction procedure, indicated by their significantly different DNA quality (i.e., DNA fragment size). We revealed highly distinct genomic DNA (≥ 23000 bp) in the iDNA pool, whereas the eDNA is characterized by fragmented DNA of different sizes (500 to ~15000 bp) caused by degradation over time (Figure 3.11). The distinct DNA quality indicates different origins of the DNA molecules and different ages of the DNA pools. Furthermore, the mild treatment of the cell separation procedure is shown by an un-sheared DNA ladder after the entire treatment (Figure 3.11, lane L_{after}).

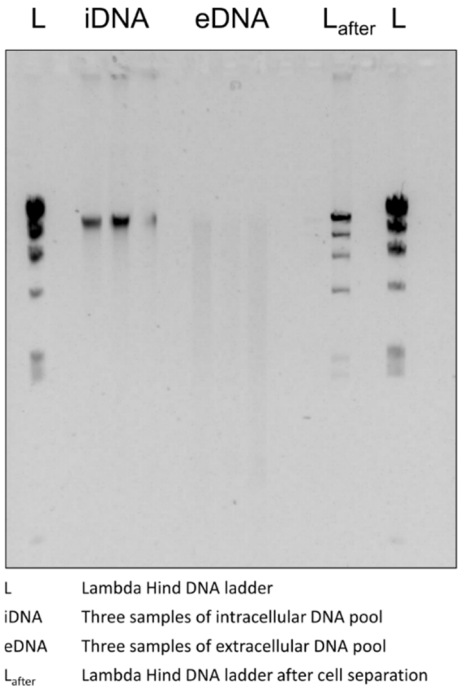

Figure 3.11: Gel-electrophoresis image of intra-and extracellular DNA extracts as well as λ Hind DNA ladder after cell separation (L_{after}). The eDNA shows smaller fragment size regarding to degradation over time. In contrast, the iDNA shows distinct bands of genomic DNA. The ladder indicates no shearing during the cell separation protocol, emphasizing the mild treatment of the used cell separation protocol. λ Hind DNA ladder: 7 lanes with 23130 bp, 9416 bp, 6557 bp, 4361 bp, 2322 bp, 2027 bp, and 564 bp.

3.3.2 Illumina MiSeq sequencing of total, e- and i- DNA pools

The good quality of the obtained high-throughput sequencing reads ensured the comparability of the different DNA pools, where a high percentages of 68% of sequences remained after paired-end read merging and stringent quality filtering (i.e., no mismatch in the barcode or primer sequence; Phred quality score ≥ 25; 1.6% of sequences identified as chimera). Thus, a total of 3.38 million quality filtered reads from 42 samples (tDNA, eDNA, and iDNA pool of 14 sediment depths) were further evaluated with 14,220 to 225,569 reads per sample (Table A.4).

3.3.3 Abundance and diversity of total, e- and i- DNA pools

The number of bacterial operational taxonomic units (OTUs) per sample ranged between 157 and 1102, whereby the number of archaeal or unassigned OTUs is negligible (up to 9 OTUs per sample) (Table A.4). The deeper sediment layers (3.6-2.9 Ma old) contain significantly more OTUs (Ø $OTUs_{Pliocene}$ = 629) than the younger layers (1.5-1.0 Ma old, Ø $OTUs_{Pleistocene}$ = 256),

indicating a bacterial diversity which is more than twice as high (similar to Section 3.1.3, based on 57 sediment samples).

Simultaneously, both the total number of OTUs and the Chao 1 diversity index ($Chao1_{min}$ = 343, $Chao1_{max}$ = 2360) consistently increase with sediment depth for all three DNA pools (linear correlation, R^2 = 0.56-0.84, p-value = <0.001-0.002) with approximately equal inclinations per diversity index ($m_{observed\ OTUs}$ = 0.30-0.54; m_{Chao1} = 0.17-0.26) (Figure 3.12). In contrast, the Shannon-Weaver index (H', additionally measure of the evenness) shows no dependence on the sediment depth (linear correlation, R^2 = 0.0008-0.059, p-value = 0.76-0.92) and exhibits punctual extremes in different sediment depths, while remarkably high values are also present in deep sediments (e.g., $H'_{44.4m}$ = 2.0-2.8, $H'_{141.5m}$ = 2.2-3.2, $H'_{309.7m}$ = 2.3-2.7, $H'_{315.3m;\ iDNA}$ = 2.9, Table A.3, A.4).

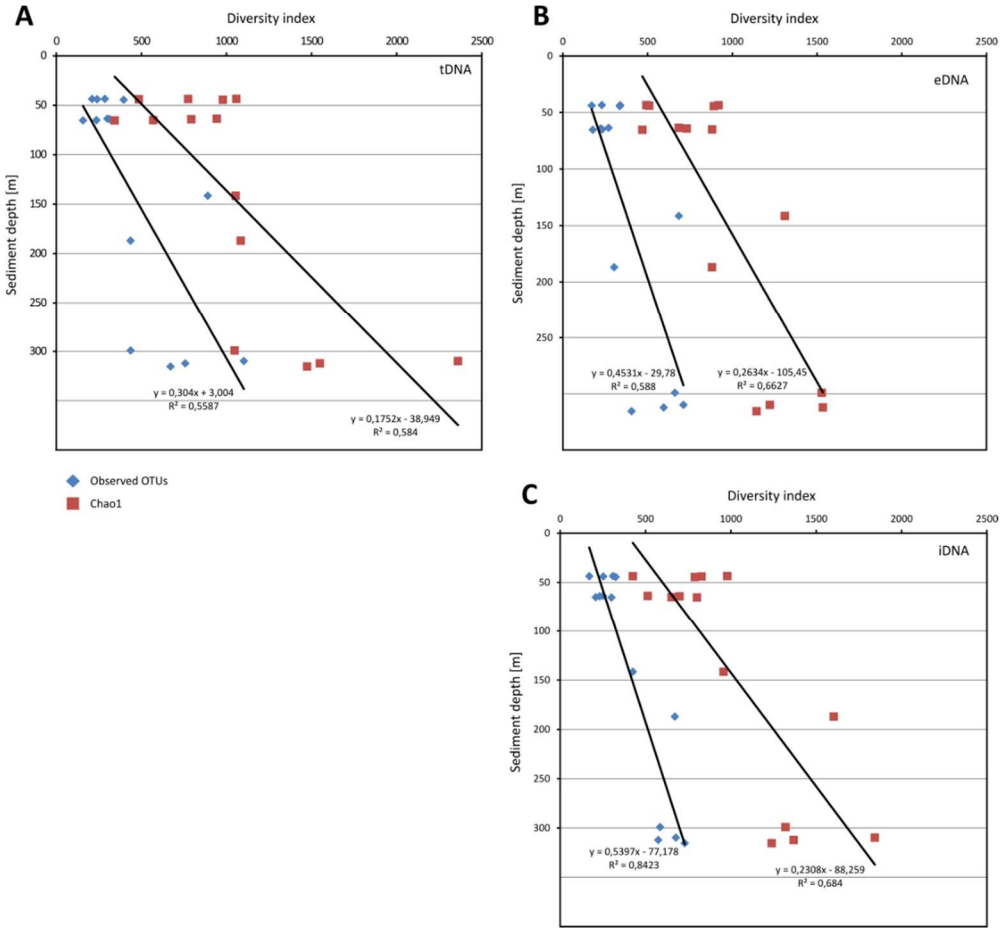

Figure 3.12: Diversity indices (Observed number of OTUs, Chao 1 index) dependent on the sediment depth for the total DNA pool (**A**), as well as the extra- (**B**) and intracellular DNA pool (**C**). Both diversity indices significantly increase with depth for all three DNA pools (linear correlation R^2 = 0.56-0.84, p-value = <0.001-0.002) and show no significantly different inclinations ($m_{observed\ OTUs}$ = 0.30-0.54; m_{Choa1} = 0.17-0.26) within one diversity index. In contrast, the Shannon Weaver index shows no dependence on the depth (linear correlation R^2 = 0.0008-0.059, p-value = 0.76-0.92, data not shown in graphs) and exhibits punctual extremes in different sediment depths.

Using the cell separation approach, it was possible to identify in each case more OTUs than using the common tDNA extraction (25% to 200% more OTUs, Figure 3.14B, Table A.4). Indeed, the cell-separated DNA pools contain together in average two times more OTUs per sediment (Ø $OTUs_{eDNA}$ = 381, $OTUs_{iDNA}$ = 407) than the tDNA (Ø $OTUs_{tDNA}$ = 460) (Figure 3.14B, Figure A.8B and Table A.4), even though theoretically the tDNA pool should cover both the eDNA and the iDNA pool.

Examining the cell-separated DNA pools, many sediment depths show a similar number of OTUs in the eDNA and the iDNA pool (Figure 3.13), whereas three sediment depths are characterized by a different behavior: the 43.6 m deep sediment sample (M6) contains twice as many OTUs in the eDNA pool, and the samples in 186.9 m (B10) and 315.3 m (B28) depths contain significantly more OTUs in the iDNA pool (Figure 3.13). Although, many samples did not differ in the OTU number between eDNA and iDNA pool, the OTUs in both DNA pools are taxonomical different to a large extent (Figure 3.14A, Figure A.8A and Appendix Dataset 2).

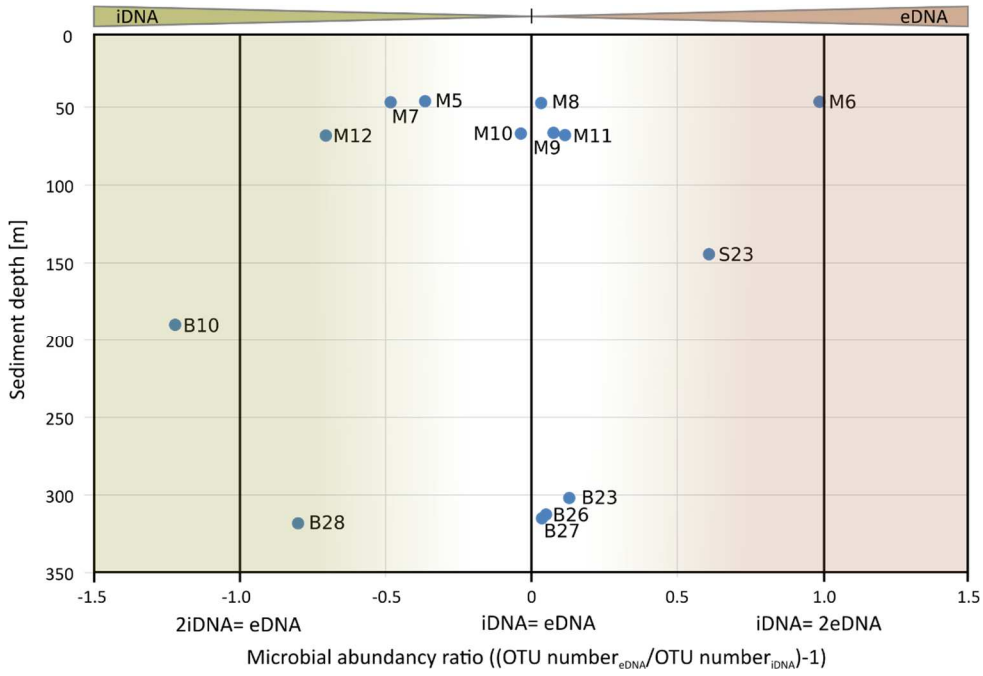

Figure 3.13: Ratios between the microbial abundance in the extracellular and intracellular DNA pool in dependence of the sediment depth. Most of the sediment samples exhibit only small differences in the number of OTUs between the eDNA and iDNA pool (value of the x-axis is near zero), whereas for example the upper sediment sample M6 contains twice as many OTUs in the eDNA pool than in the iDNA pool (value of the x-axis is 1).

In general, we found remarkable differences in the taxonomic composition of the common tDNA extraction and the cell-separated DNA pools. We observed in almost half of the

investigated samples (6 out of 14) a significant different composition of the iDNA in comparison to the eDNA and tDNA, even at the phylogenetic order-level (Figure 3.14A, Figure A.8A), and in particular at the OTU level (Appendix Dataset 2). This difference indicates that the tDNA pool do not cover a large proportion of taxa originating from the living microbial community but has a huge similarity with the eDNA pool. With a measure for the taxonomic disparity of the DNA pools based on all DNA pool-distinct OTUs (Table 3.1 Jaccard-distance, emphasizing the rare biosphere), we observed a median distance of 84.0% between two DNA pools. All DNA pools exhibit an almost similar Jaccard-distance (Jac_{dist_max} = 92.0%, Jac_{dist_min} = 72.0%) indicating a similarly high number of unique OTUs per DNA pool.

Table 3.1: Dissimilarity indices of the three different DNA pools for each investigated sediment sample of the El'gygytgyn Crater Lake. The Jaccard-distance emphasizes rare OTUs because of the comparison of the presence/absence information of each OTU and DNA pool. The Cosine-distance compares the distribution of the reads per OTU of two DNA pools. In general a dissimilarity of 0 means that both DNA pools have exactly the same OTUs or read distribution, and 1 that they have no common OTU or an orthogonal distribution. The abbreviations *t-e, t-i, e-i* stands for a dissimilarity index between the tDNA (t), iDNA (i) and eDNA (e) pool. Samples that show a similar distribution of the reads per OTU in the eDNA and tDNA pool are marked in bold letters.

Sample_ID	**Sample Age [ka]**	**Jaccard-distance over the OTUs**			**Cosine-distance over the reads**		
		t-e	**t-i**	**e-i**	**t-e**	**t-i**	**e-i**
M5	1050.3	0.917	0.879	0.829	0.973	0.340	0.465
M6	1061.8	0.840	0.900	0.868	**0.009**	**0.258**	**0.224**
M7	1071.3	0.908	0.881	0.874	0.348	0.284	0.047
M8	1090.6	0.794	0.839	0.794	0.267	0.263	0.152
M9	1455.4	0.820	0.861	0.876	**0.042**	**0.446**	**0.478**
M10	1460.9	0.896	0.895	0.777	0.579	0.624	0.047
M11	1480.5	0.863	0.884	0.852	**0.053**	**0.347**	**0.262**
M12	1490.5	0.860	0.876	0.846	0.136	0.110	0.023
S23	2908.4	0.718	0.804	0.762	0.714	0.744	0.494
B10	3299.5	0.840	0.823	0.853	**0.002**	**0.064**	**0.058**
B23	3559.0	0.822	0.829	0.799	0.116	0.047	0.025
B26	3574.0	0.727	0.755	0.729	0.422	0.041	0.312
B27	3577.4	0.748	0.729	0.758	**0.002**	**0.012**	**0.010**
B28	3581.8	0.776	0.890	0.863	**0.005**	**0.658**	**0.628**
	median	0.822	0.868	0.838	0.126	0.273	0.188

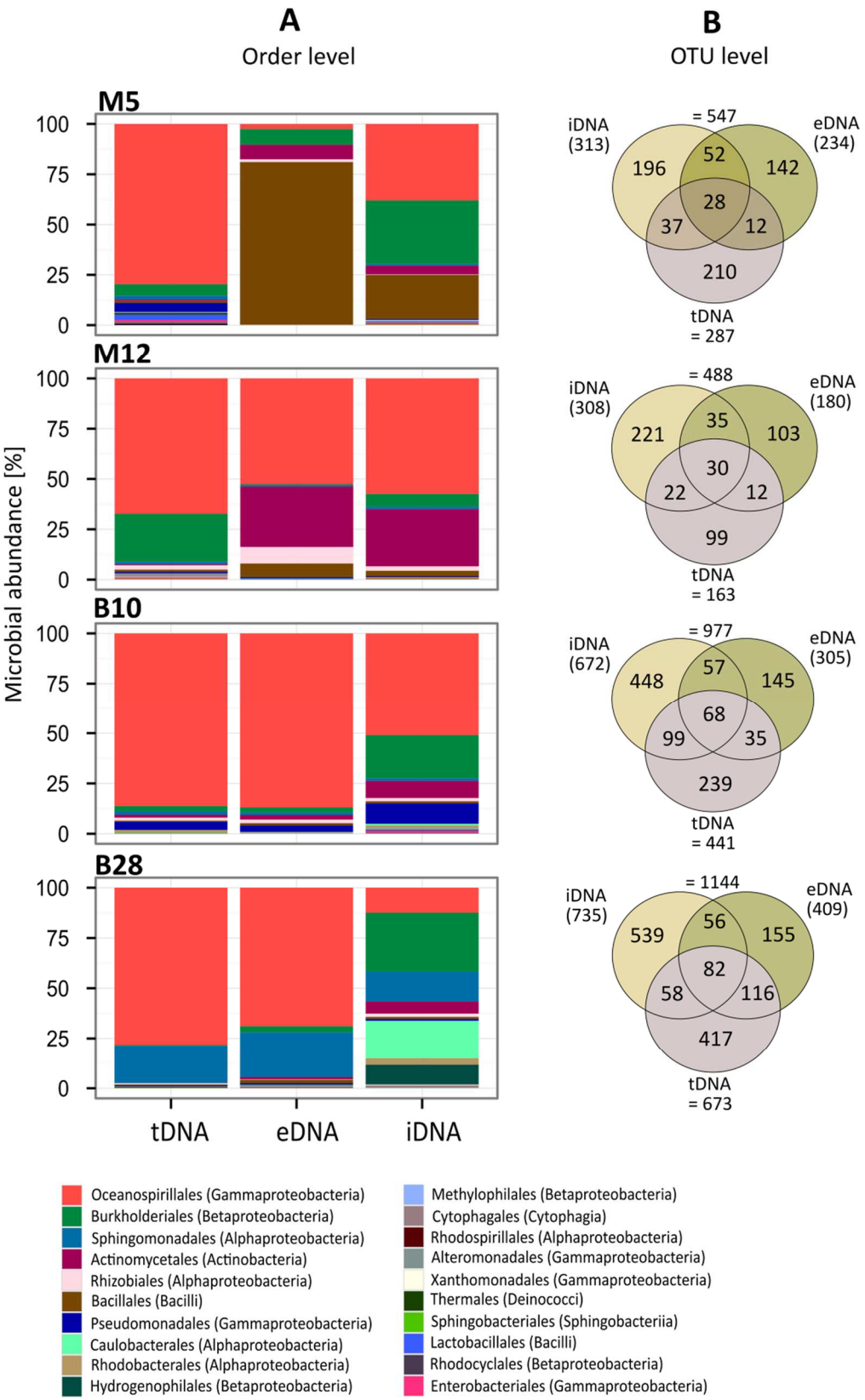

Figure 3.14: Taxonomic composition of the microbial community in El'gygytgyn deep lake sediments with (**A**) the relative abundance on phylogenetic order-level for the total (tDNA) as well as the extra- (eDNA) and intracellular (iDNA) DNA pool, and (**B**) the number of unique OTUs per DNA pool and the number of OTU-level taxonomic overlaps between the three DNA pools presented as Venn diagrams. The additional ten sediment samples analyzed in this study are summarized in Figure A.8.

To focus on the relative composition of the microbial community, we calculated the Cosine-distance (Cos_{dist}), showing a median distance of 24.1% between two DNA pools (Table 3.1 Cos_{dist}, emphasizing abundant taxa). On the basis of the relative distribution of the OTUs, we see considerable differences between the DNA pools (Cos_{dist_max} = 97.3%, Cos_{dist_min} = 0.2%). Again, the same 6 sediment depths show a distinct iDNA community composition, while the tDNA pool represents a similar distribution of OTUs as the eDNA pool (Cos_{dist} of eDNA and tDNA is near zero, Table 3.1, samples are highlighted in bold letters).

3.4 Environmental controls on microbial community composition and diversity

In this section, the correlations within the environmental data were examined prior to the visualization of the samples according to their microbial community composition in form of a non-metric multidimensional scaling analyses (NMDS). Additionally, to determine the environmental parameters that influence the different DNA pools, individual redundancy analyses (RDA) were performed.

Within the environmental data, we found a linear correlation pattern between the global marine isotope stack and the mean temperature of the warmest month (MTW) (positive correlation, R^2 = 0.62) and depth (anticorrelation, R^2 = 0.53), respectively. A positive exponential correlation was revealed between MTWM and the annual precipitation (PANN) (R^2 = 0.76), indicating warmer and wetter conditions in deeper and thereby older sediment samples. Moreover, there is a linear correlation between the sediment temperature and the sediment depth (linear temperature increase of 5 °C/100 m, Mottaghy et al. 2013, R^2 = 0.89). Cluster analysis did not reveal specific robust clusters within the environmental parameters, but the data show a gradient along the atmospheric temperatures and the sediment depth.

To determine the similarity in the bacterial community composition among the sediment samples, we performed non-metric multidimensional scaling analyses (NMDS) for the tDNA based (i) on the interglacial/glacial samples and (ii) on both sample series. Although, it was not possible to identify a statistically significant robust cluster in the NMDS plots, the microbial composition of different glacial/interglacial periods was more similar due to their age (and therefore consecutive MIS) than the mere affiliation with interglacial or glacial conditions (Figure 3.15). In the NMDS plot based on both sample series, the bacterial community pattern of the interglacial/glacial periods were separated from those of the Pliocene samples (Figure 3.16), which in turn formed three subgroups based on the main representative OTUs

and taxa richness. The first group of low-diversity samples consist of a *Halomonas*-rich community, the second group is characterized by a high abundance of *Comamonadaceae*-related sequences, and the last group consists of high diversity samples.

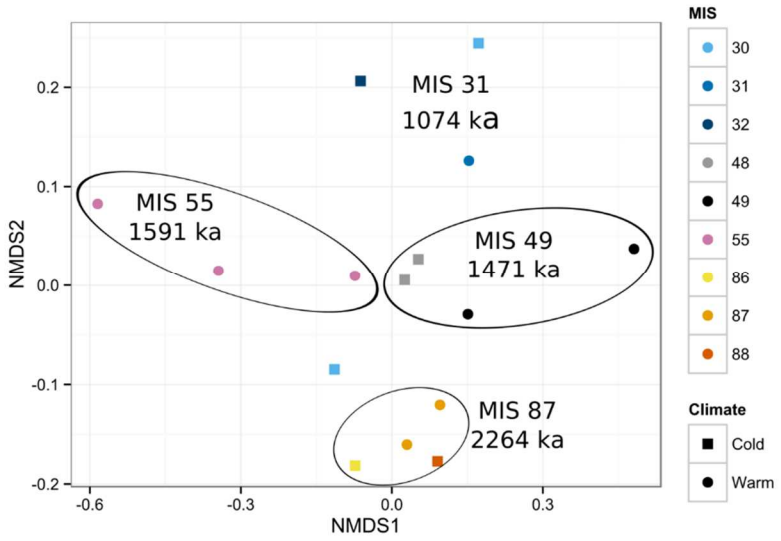

Figure 3.15: Non-metric multidimensional scaling plot (NMDS) of square root transformed Bray-Curtis distances within interglacial/glacial cycles of the Pleistocene based on the OTU composition in each sample. Interglacial stages are marked with circles; glacial stages are marked in squares. 2D Stress factor: 0.138.

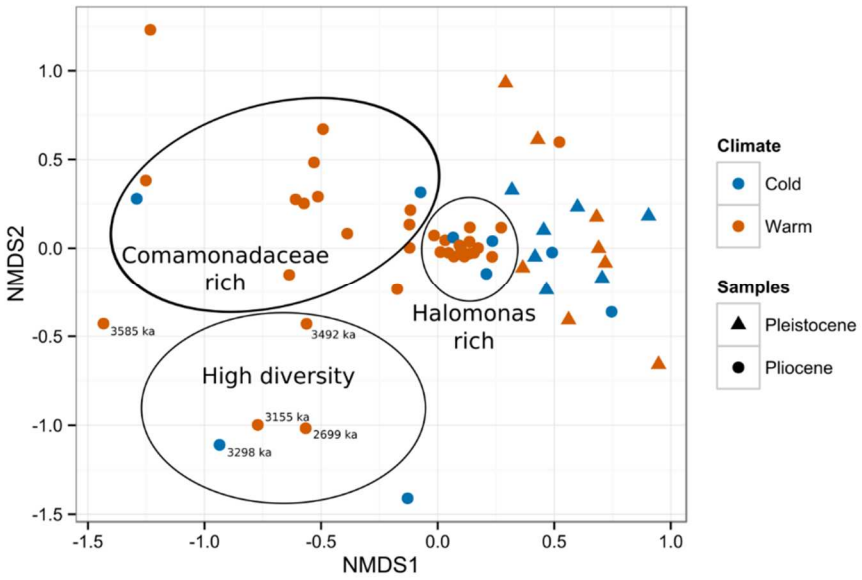

Figure 3.16: Non-metric multidimensional scaling plot (NMDS) of square root transformed Bray-Curtis distances within both samples series (interglacial/glacial cycles of the Pleistocene compared to Pliocene deposits) based on the OTU composition in each sample. Interglacial/glacial stages of the Pleistocene (triangles) are separated from Pliocene samples (circles). Stress factor: 0.161.

To identify the key environmental parameters influencing the bacterial community structure, we carried out forward selection using a redundancy analysis (RDA). The RDA plot for the tDNA pool shows the distribution of the samples according to their similarity as well as the orientation and weights of the influencing environmental parameters (Figure 3.17). Using a linear model, we were able to explain 20% of the total variance within the data; the first two axes account for 15.44% and 7.50%. The amount of biogenic silica and the sediment depth significantly influenced the distribution of the most abundant 20 OTUs in all of the samples (P_{Silica} = 0.001, P_{Depth} = 0.004). The grain size distribution seems to influence the microbial community composition and is included in the RDA plot, even if the statistical significance was not verifiable after the second forward selection step (P_{Clay} = 0.053, P_{Silt} = 0.077, P_{Sand} = 0.039). The RDA plot shows that the microbial community structure of the interglacial/glacial samples is highly shaped by the amount of silica, reflecting a higher in-lake primary production based on diatoms (Melles et al., 2012). Additionally, these samples were negatively correlated with depth (and therefore with age, MTWM, and PANN). Again, the taxa *Methylophilales*, *Rhizobiales*, and *Janthinobacterium lividum* were characteristic for the Pleistocene samples. Moreover, *Halomonas* was found in samples with a higher silica content as well as lower diversity and taxa evenness. In contrast, *Hydrogenophaga*, *Rhodobacter*, *Ramlibacter,* and 4 of 5 *Comamonadaceae*-related OTUs were mainly found within the deep sediments associated with low silica concentrations and a low amount of *Halomonas*. These OTUs seem to be affected by a higher proportion of sand and lower clay content, respectively. *Sphingomonas* represents a special position in the RDA plot, which seems to be negatively correlated with the silt amount and is significantly more abundant in the extreme Arctic warmth period (see Table A.1).

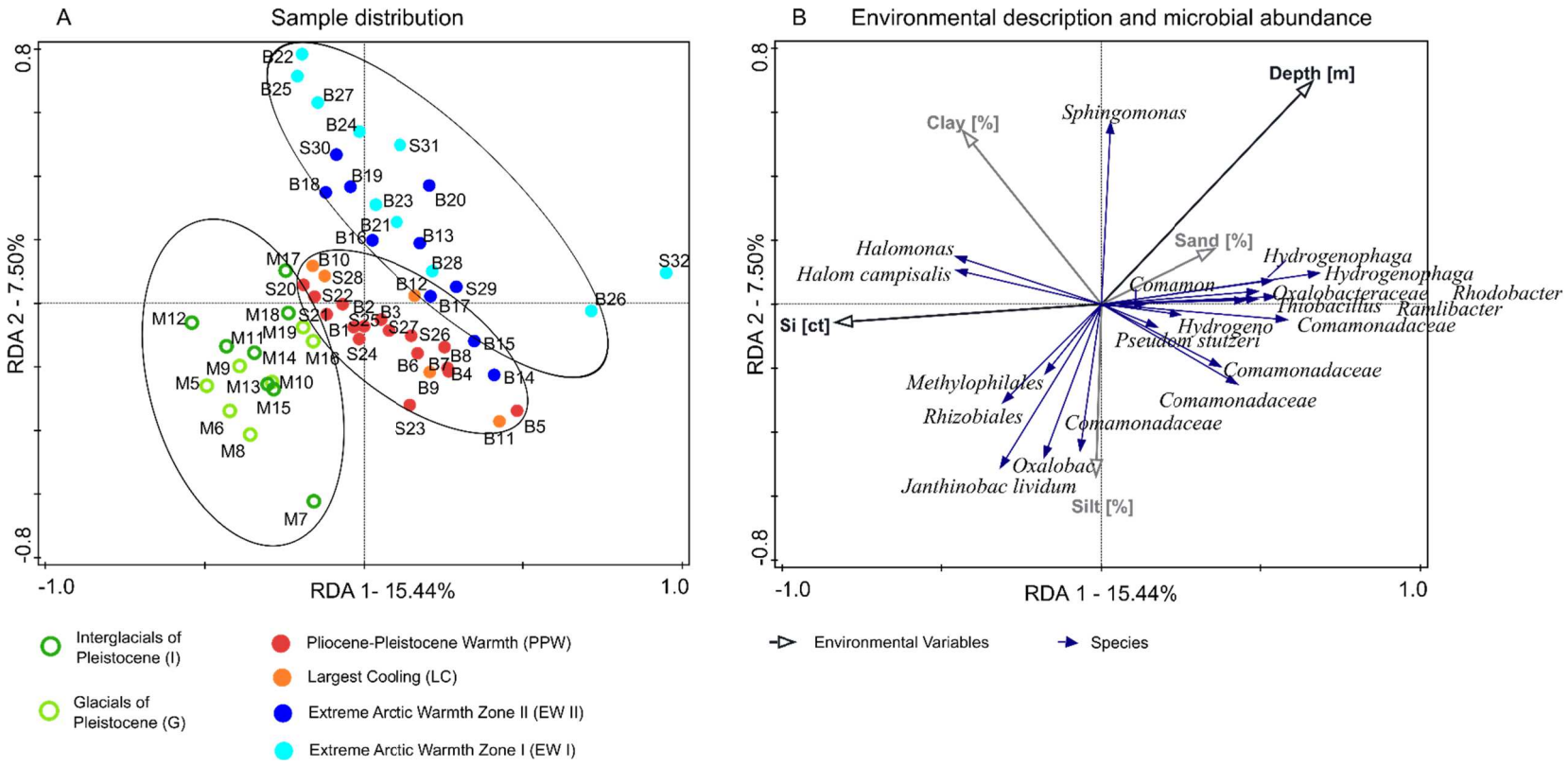

Figure 3.17: Ordination plot of redundancy analysis (RDA) for the 20 most abundant bacterial OTUs in the El'gygytgyn Crater Lake and the main environmental driver with (**A**) PCA loads of samples according to the similarity of their microbial composition, and (**B**) weights and orientation of the environmental descriptors (black arrows) and the 20 most abundant bacterial OTUs (blue arrows). Sediment samples are represented by circles (blue = Extreme Arctic Warmth deposits, orange = Largest Cooling in Pliocene, red = Pliocene-Pleistocene Warmth, open green = interglacial/glacial samples of Pleistocene). Significant environmental parameters (P_{Silica} = 0.001, P_{Depth} = 0.004) are indicated by black arrows, whereby the trends are shown in grey arrows (P_{Clay} = 0.053, P_{Silt} = 0.074, P_{Sand} = 0.039).

For both cell-separated DNA pools, individual RDA analyses were performed and subsequently compared with the tDNA pool. We identified significant differences between the three DNA pools and revealed that the tDNA pool is composed of mixed signals of the iDNA and eDNA pool (Figure 3.18B, C compared to Figure 3.18A).The individual RDA analyses of the cell-separated DNA pools explained not only a significantly higher value of variance of the microbial community (32.8% and 48.1%) compared to the tDNA pool (20%), but also demonstrated that the microbial community of the eDNA and iDNA pool are influenced by different environmental factors. Therefore, cell separation facilitates a much better analyses of the dependent environmental parameters. The community derived from the eDNA pool is mainly influenced by the sediment depth (P_{depth} = 0.001) and the amount of biogenic silica (P_{silica} = 0.039), which increases the binding and conservation probability of DNA (Boom et al., 1990). In contrast, the community derived from the iDNA pool is influenced – next to the sediment depth (P_{depth} = 0.001) – by live-depending parameters, such as the texture of the sedimentary matrix (P_{silt} = 0.009) and, as a trend, the water content and the predominant atmospheric temperature ($P_{water\ content}$ = 0.107, P_{d18O} = 0.274). A detailed analysis of the iDNA pool showed a strong carbon-dependency of the genera *Methylobacterium*, *Streptomyces*, *Kribella*, *Agrobacterium,* and *Nocardioides* (linear regression, R^2 = 0.78-0.56, p-value = <0.001-0.002) in the sediment samples, reinforcing the importance of live-depending parameter for the iDNA pool. For both cell-separated DNA pools the significance of the forcing environmental parameter on the microbial community is persistent even if we calculated the RDA based on all occurring OTUs (25.6% of adjusted explained variation for eDNA and 25.7% for iDNA), which indicates a robust data basis.

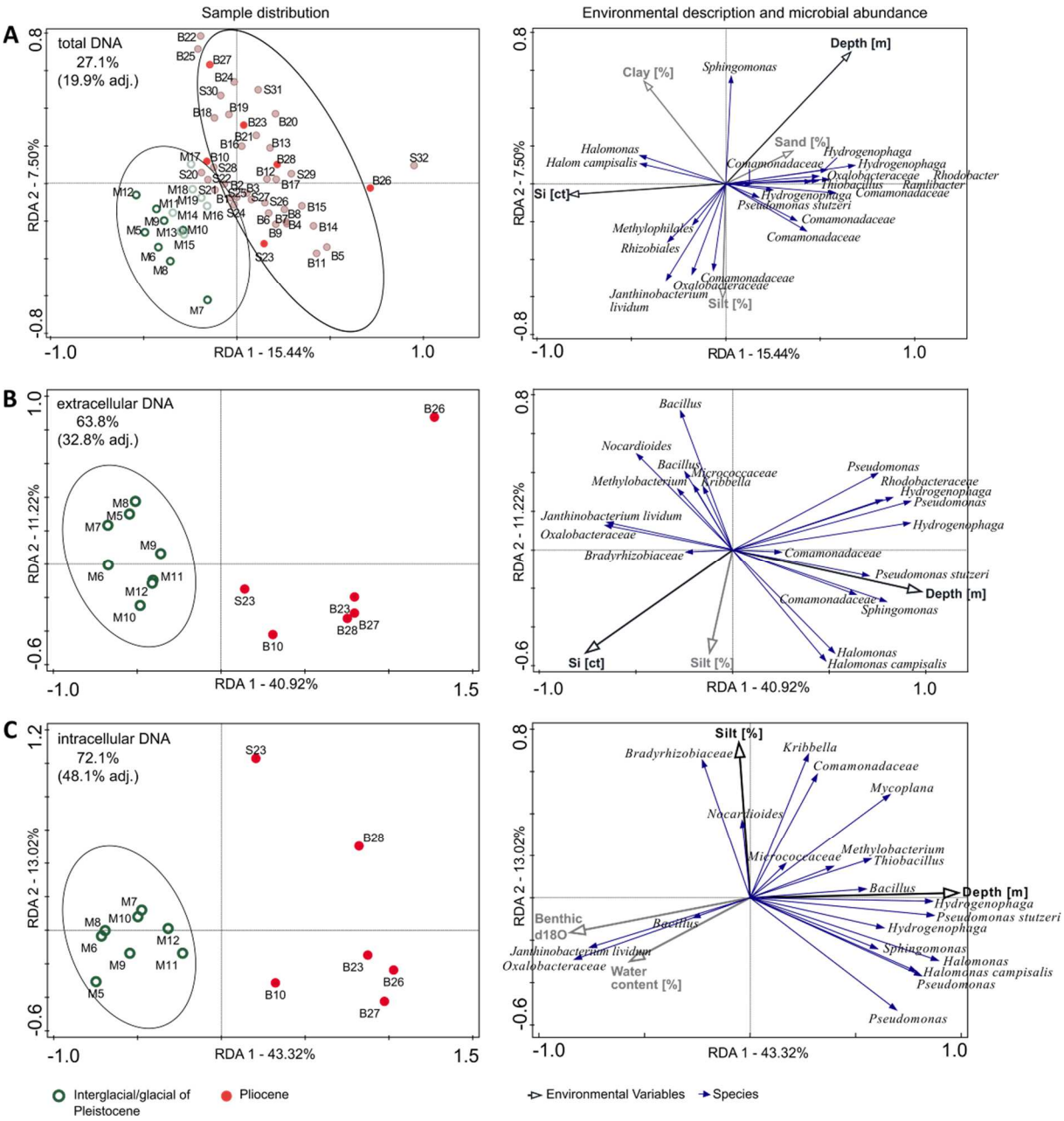

Figure 3.18: Ordination plot of redundancy analysis (RDA) for the 20 most abundant bacterial OTUs in the El'gygytgyn Crater Lake sediments and their main environmental drivers, separately shown for the total DNA pool (based on 57 sediment samples) (**A**), as well as the extracellular (**B**) and intracellular DNA pool (**C**) (obtained by cell separation according to Alawi et al., 2014). Left panel shows the PCA loads of samples; right panel shows the distribution of microbial abundance and environmental description. Sediment samples are represented by circles (green = interglacial/glacial samples of Pleistocene, red = Pliocene deposits). Black arrows indicate significant environmental parameters (p-value = 0.001-0.039), whereas trends are shown in grey arrows. The value of the explanatory variables (tDNA: 27.1%) and the adjusted explained variation (tDNA: 19.9%) are included in the left panel. The global marine isotope stack (benthic $\delta^{18}O$) was calculated by Lisiecki & Raymo, 2005 (Table A.3).

4 Synthesis and Conclusion

This chapter comprises three parts, the discussion of the results in comparison with the related work, the key insights of this thesis, as well as critical remarks about the underlying methods and an outlook on future work based on this thesis.

4.1 Discussion

This PhD thesis characterizes the microbial community of the El'gygytgyn Crater Lake, which was formed by a meteorite impact 3.6 Ma ago. Whereas former studies investigated only upper lacustrine sediments (e.g., He et al. 2012; Comeau et al. 2012; Crump et al. 2012), microbiological analyses on up to 317 m deep lake sediments constituting the oldest terrestrial climate record of the Arctic (Nolan and Brigham-Grette, 2007) were conducted here. The unique sediments span over the Pliocene and the Pleistocene, and include different climate phases, such as the Extreme Arctic Warmth (EW), the Largest Cooling of the mid-Pliocene (LC), the Northern Hemispheric Glaciation, the Pliocene-Pleistocene-Warmth (PPW), and different glacial/interglacial cycles (G/I) of the Pleistocene (Brigham-Grette et al., 2013; Melles et al., 2012). Hence, this study substantially contributes to the understanding of microbial life in the deep biosphere of lacustrine sediments by determining the main community-shaping environmental parameters including the paleoclimatic conditions in the time range of the last 3.6 Ma to 1.0 Ma.

The analyzed sediments pushed the established microbiological methods to their limits because of their substantial age, the low amounts of DNA, the PCR-inhibiting substances, and the overall limited amount of original samples. Nevertheless, a successful extraction and amplification of DNA from all investigated samples was performed, even from the oldest part of the sediment core (3.6 Ma old), which is almost devoid of pollen and other microfossils (Brigham-Grette et al., 2013). The DNA isolation is already a huge accomplishment because it has not been performed before in such old lake sediments. The results indicate that deep sediments are not only inhabited by a few extremophilic microorganisms but also by a complex ecosystem. This first DNA-based investigation of the lacustrine deep biosphere showed a surprisingly diverse and abundant microbial community in the El'gygytgyn sediments (Section 3.1 and 3.3). The bacterial abundance of the deep biosphere sediments was approximately two order of magnitudes higher (1.2×10^3 to 1.8×10^6 copies g^{-1} sediment ww) than the archaeal abundance (2.9×10^1 to 1.2×10^5 copies g^{-1} sediment ww), which is in line

with previous studies analyzing the microbial abundance in Arctic permafrost (Yergeau et al., 2010) or Arctic lake and wetland sediments (Stoeva et al., 2014). Interestingly, the archaeal and bacterial abundances of the Pleistocene sediments seem to follow the different glacial and interglacial periods (Section 3.1). The influence of changing climatic conditions on the microbial abundance could be demonstrated in a former study by analyzing younger sediments of the El'gygytgyn Crater Lake (Figure 1.1 in Section 1.1) (Görsch 2011). This investigation identified a strong positive influence of an algae bloom-driven enrichment of nutrients in the lake within interglacial periods that resulted in better growing conditions for the microbial community. Consequently, the microbial abundance of both bacteria and archaea was significantly increased during interglacial periods of MIS 11 and 9 (Figure 1.1D in Section 1.1).

In this thesis increasing gene copy numbers towards the deepest sediment layer (≈ 3.6 Ma) as well as a linear increase in the microbial diversity towards the sediment depth (OTU, Chao 1 index; Section 3.3) were additionally found. In particular, an approximately 2.5 times higher diversity in the Pliocene sediments compared to the Pleistocene sediments was observed (Section 3.1 and 3.3). Thus, this work indicates that a decrease in the microbial abundance and diversity with depth – as shown multiple times in the field of marine deep biosphere (e.g., Kallmeyer et al. 2012; Breuker & Schippers 2013) – is not omnipresent. Correlation analyses of the El'gygytgyn environmental parameters revealed that with increasing depth and age of the sediments also increasing paleo-temperatures, paleo- moistures, and in-situ sedimentary temperatures occur, whereby the parameters are known to positively affect the microbial diversity. The higher microbial diversity in the Pliocene is caused by a more intensive bioactivity, which is supported by elevated temperatures and increased precipitation during the time of sedimentation in the EW (3.6-3.4 Ma) together with long time-spans of open-water conditions (increased concentration of oxygen throughout the lake (Wennrich et al., 2014) by wind-driven mixing of the water column). The higher bioactivity is also indicated by the largest detected diatoms in EW II (3.39-3.34 Ma, Phillips 2013; Brigham-Grette et al. 2013), which leads to a longer and increased delivery of a variety of nutrients to the lake (Nolan and Brigham-Grette, 2007). Moreover, the warmer and wetter conditions of the Pliocene (before 2.7 Ma) benefit the formation of a diverse forest and tundra biome in the lake catchment area, which is dominated by cold deciduous forest, taiga, cool conifer forest, and cool mixed forest (Tarasov et al., 2013). As a result, the occurrence of a higher input of vegetation-driven organic-rich deposits into the lake is assumed during the warmer and wetter Pliocene, whereby this input is

expected to be much lower during the colder and drier Pleistocene interglacial/glacial periods characterized mainly by a permafrost-influenced tundra biome (Tarasov et al., 2013).

Using Illumina high-throughput analyses, a surprisingly high number of 6,910 OTUs at a 97% similarity threshold in the El'gygytgyn deep biosphere sediments was revealed. Thereby, the complex bacterial ecosystem is characterized by Shannon-Weaver diversity indices (H = 0.92-5.01; H_{mean} = 2) comparable to other polar lakes (H = 0.94-1.10 for maximal 40 m deep sediments, Bowman et al. 2000; H = 2.3-2.8 for water samples, Galand et al. 2008) or temperate lakes (H = 3.91-4.48 for water samples, Tang et al. 2009). The main abundant bacterial phyla were *Proteobacteria* (90.8%), followed by *Actinobacteria* (2.3%), *Bacteroidetes* (2.1%), and *Acidobacteria* (0.75%), which are affiliated with the families *Halomonadaceae*, *Sphingomonadaceae*, *Comamonadaceae*, *Oxalobacteriaceae,* and *Methylophilaceae*. The archaeal community (67 unique archaeal OTUs) consisted of species belonging to *Nitrososphaeraceae*, *Halobacteriaceae*, *Methanosarcinaceae,* and *Methanosaetaceae*. The main bacterial phyla of the El'gygytgyn deep biosphere could also be detected in Artic permafrost environments (Hinsa-Leasure et al., 2010; Steven et al., 2013, 2007; Yergeau et al., 2010) and in Arctic lake surface sediments (He et al., 2012). The presence of halotolerant or halophilic microbes in permafrost confirm our hypothesis that a major portion of the El'gygytgyn diversity is originated from the surrounding catchment area, most probably introduced by the 50 inflows, which today transport approximately 350 t sediment per year into the lake (Fedorov et al., 2013). Especially, the predominance of the halotolerant genus *Halomonas* (in average 60% of the total reads per sample) can be explainabled by its feasibility to survive in the deep subsurface due to its facultative anaerobic and heterotrophic features as well as its adaptation potential to low temperatures (Jadhav et al., 2013). The genus was also found pre-dominantly in a 1.8 km-deep subsurface Sandstone reservoir (Dong et al., 2014) and discovered in a wide range of lakes (Jiang et al., 2007; Joshi et al., 2007), in Antarctic fast ice (Reddy et al., 2003), and in the deep-sea (Kaye et al., 2011). Next to *Halomonas*, different halophilic archaea of the family *Halobacteriacea* were found.

In general, Lake El'gygytgyn sediments cover a diverse bacterial community with primary producers (e.g., *Chloroflexi*, *Cyanobacteria*, *Gammaproteobacteria*, *Epsilonprotobacteria*) as well as saprophytic microbes living on dead organic matter (e.g., *Bacteroidetes*, *Firmicutes*, *Actinomycetales*). During changing climate conditions the methane cycle (methane producers, methane oxidizers), the sulfur cycle, and the nitrogen cycle will be affected most and changes

in these may lead to an increased emission of greenhouse gases if the microbial community is stimulated, for example, by higher temperatures. Methanogens and methanotrophs were detected in the lake sediments and form a minor part of the total microbial community. Comparably, Bischoff et al. (Bischoff et al., 2014) revealed the methanogenic groups *Methanosarcinales* and *Methanomicrobiales* in Holocene deposits of a terrestrial permafrost core contiguous to Lake El'gygytgyn. These groups are in accordance with our findings in the deep lacustrine sediments (*Methanosarcina*, *Methanosaeta, Methanobacterium*). Additionally, our results are consistent with the methanogenic groups *Methanomicrobiaceae, Methanosarcinaceae,* and *Methanosaetaceae* identified in Siberian permafrost by Ganzert et al. 2007. Lake El'gygytgyn sediments contain common representatives of methanotrophic bacteria in Arctic environments, such as *Methylocystaceae* (including *Methylosinus* and *Methylophila*), *Verrucomicrobia* (*Methylacidiphilae*, restricted to the Pliocene samples), and *Beijerinckiaceae*, but did not include *Methylococcaceae*-related sequences, although these were always found in permafrost (He et al., 2012; Liebner et al., 2009). Representatives of the families *Methylophilaceae* and *Methylobacteriaceae* are highly abundant in MIS 55 (Figure 3.3) but also over the whole sediment core. They are obligate or strict facultative methylotrophic bacteria that use methanol and methylamine as carbon and energy sources. Furthermore, various taxa involved in sulfate reduction were identified. *Desulfosporosinus* was found in most sediment depths of the Pliocene, where *Desulfobulbaceae* and *Desulfococcus* were less abundant. It is remarkable that sequences of methanogens and sulfate-reducing bacteria (SRB) were not obtained from the Pleistocene glacial/interglacial periods. However, Bischoff et al. 2014 found methanogens in the overlaying lacustrine sediments within the MIS 9-11 by using a methanogenic-specific primer pair. Moreover, well-described species known for nitrification (e.g., ammonia-oxidizing bacteria: *Nitrospirae*, *Nitrosomonadacea* (*Nitrosovibrio*); and ammonia-oxidizing archaea: Candidatus *Nitrososphaera*) and denitrification (*Thiobacillus, Paracoccus, Pseudomonas*) were identified in the deep biosphere of Lake El'gygytgyn. The results show that representatives of all important biogeochemical cycles were found in the sediments.

The microbial community compositions strongly vary along the chronosequence. In general, all major climate phases (EW I and II, LC, PPW, and G/I) exhibit distinct compositions, whereby the largest difference were observed between the Pleistocene sediments and the Pliocene sediments. RDA analyses to examine the relationship between the composition of the microbial community and the environmental parameters were used. Approximately 20% of the variance

within the microbial community in the tDNA could be explained by the main community-shaping environmental parameters, the amount of biogenic silica and the sediment depth (P_{Silica} = 0.001, P_{Depth} = 0.004). Moreover, an influencing trend was shown for the texture of the sedimentary matrix (P_{Clay} = 0.053, P_{Silt} = 0.074, P_{Sand} = 0.039). It is assumed that the relatively small explainable variance of the environmental parameter is caused by an interference of signals of two microbial communities: First the living community (intact cells), and second the past microbial community mainly represented by the extracellular DNA. This assumption is supported by previous environmental studies that highlight a substantial portion of extracellular DNA in marine sediments and waters as well as deep sea ecosystems (Luna et al. 2002; Zweifel & Hagström 1995; Dell`Anno & Danovaro 2005). Thereby, significantly higher amounts of extractable eDNA than iDNA were found for lacustrine and marine environments. The eDNA/iDNA ratios in the El'gygytgyn Crater Lake of 12-26 (Section 3.3) are in accordance to earlier provided ratios of 36-68 in the Mediterranean Sea (Corinaldesi et al. 2014) or 6, 18, and 49 in the Barents Sea, the Baltic Sea, and the South Pacific Gyre, respectively (Alawi et al., 2014).

Because of the high amount of eDNA in the deep biosphere samples and the potential interference of signals of the living and the past microbial community, the focus of the second part of this thesis shifted towards the separation of DNA from living cells and extracellular DNA to consider the signals of the living and dead community individually. Due to the challenging El'gygytgyn sediments (e.g., several thousand to million year's old, small DNA content, PCR inhibiting substances), two newly methods were established/adapted: the PMA treatment and the cell separation protocol.

Firstly, a robust PMA treatment for methanogenic archaea was developed. Methanogenic archaea are key players in the carbon turnover of the Arctic (Allan et al., 2014) and contribute substantially to the emission of greenhouse gases to the atmosphere (Wuebbles and Hayhoe, 2000). The importance of archaeal methanogenesis was subject to different subsurface habitats (Newberry et al. 2004; Schippers et al. 2012; Ino et al. 2016) as well as to the upper El'gygytgyn sediments (Görsch 2011). Hence, an optimal PMA treatment for different strains of methanogenic archaea was developed based on different PMA concentrations (50-200 µM), light exposure times (0-10 min), and the comparison with a bacterial reference strain (*Pseudomonas fluorescens*). It was shown that intact membranes of methanogenic archaea are a natural barrier to PMA (50 and 130 µM, up to 20 min) and that PMA represents a useful

method to detect a lack of membrane integrity. Strain-specific differences in the efficiency of the PMA treatment were discovered between the genera *Methanosarcina* and *Methanobacterium* which are most probably a result of the texture of the cell structure (Section 3.2). Similar results were reported for Gram-positive and Gram-negative bacteria (Fittipaldi et al., 2012; Nkuipou-Kenfack et al., 2013; Nocker et al., 2006). Additionally, a protocol to simultaneously treat the domains of bacteria and archaea using 130 µM PMA and 5 min of photo-activation with blue LED light was successfully established. This protocol is a valuable asset for the examination of culture-based microbial survival rates under varying stress conditions, such as freeze/thaw cycles and long-term freezing (Morozova and Wagner, 2007), long-term desiccation (Schirmack et al., 2015), and the presence of perchlorate (Serrano, 2014) simulating different extreme environments, such as permafrost, the deep biosphere, or the planet Mars.

In another series of experiments, the limitation of the PMA treatment to distinguish between living cells and free DNA in particle-rich environmental samples was explored. It was confirmed that the applicability of PMA can only be guaranteed up to a certain particle load in the samples due to an increased inhibition of the light-induced cross-linking of PMA and free DNA (turbidity effect) (Section 3.2; Bae and Wuertz, 2009; Fittipaldi et al., 2012; Luo et al., 2010; Wagner et al., 2008). However, the maximal particle load significantly diverged from the previous studies (maximal particle-load of 0.68; 1; and 2 mg mL^{-1}, Liang and Keeley, 2012; Bae & Wuertz 2009; Taskin et al. 2011). This thesis revealed that the efficiency of the PMA treatment strongly depends on the soil texture (Section 3.2): Particle-rich samples with a sandy soil texture can be treated successfully up to a particle load of $\leq$ 200 mg mL^{-1}, whereas clay and silt-rich samples showed false positive results (i.e., free DNA is not completely shielded) in all used particle concentrations (0.6 to 1000 mg mL^{-1}).

Because the texture of El'gygytgyn sediments is rather fine-grained, a cell separation protocol was chosen over a PMA treatment to avoid the turbidity effect causing an overestimation of the living microbial community. The cell separation protocol of Alawi et al. (2014) was adapted to the El'gygytgyn sediments by adjusting the concentrations of the silica-particles to the actual DNA amounts and using a more efficient technique to extract the iDNA from the cell pellet, which includes thermal and chemical cell lysis (Section 1.4; Section 2.4). Additionally, this thesis contains the first validation of the applicability of next generation sequencing (Illumina MiSeq) on cell-separated DNA pools, which allows an in-depths description of the community

compositions of the iDNA and eDNA pools in complex and challenging environmental samples.

It is uncertain which part of a total DNA extract originates from the living community or might be an artifact of past communities or excreted DNA by active extrusion (Corinaldesi et al., 2011, 2005; Dell`Anno and Danovaro, 2005; Ogram et al., 1988). Therefore, the cell-separated DNA pools of 14 samples were compared with a total DNA (tDNA) pool obtained by a commercial extraction kit (Power Soil™ DNA Isolation Kit, MO BIO) to determine to which extent the tDNA pool covers the living and the potential past microbial communities (Section 3.3). Most importantly, it was found that the taxonomical composition between all three DNA pools significantly differs. First, one would expect that the tDNA pool covers both the microbial community of the iDNA and eDNA pool. However, it was shown that the cell-separated pools together contain almost double the extractable taxa than the tDNA pool (25% to 200% more OTUs). Second, the taxonomic disparity of the three DNA pools of each sample with two different dissimilarity indices (Jaccard and Cosine distance) were measured. It was observed that all three DNA pools share only a small number of common OTUs and contain a high number of unique OTUs (mainly rare biosphere). However, looking at the relative distribution of the taxa (emphasizing the most abundant taxa), the tDNA and eDNA pools are nearly similar for approximately half of the samples. Hence, the tDNA pool insufficiently covers the living community (iDNA pool) in those samples even at phylogenetic order-level and in particular at the phylogenetic OTU-level. These results show differences in the DNA extraction techniques (Section 4.3), but it can also be deduced that studies of old sediments that only rely on a total DNA extract have to be interpreted carefully in respect to the living community, because the tDNA pool probably resembles the eDNA (potential past microbial community) more than the living community.

The observation that the iDNA rather than the tDNA pool represents the living microbial community is supported by individual redundancy analysis (RDA) of the cell-separated DNA pools to determine the main influencing environmental parameters (Section 3.4). The RDA explained a higher value of variance within the microbial community composition of the cell-separated pools (32.8% and 48.1%) compared to the tDNA pool (20%). Moreover, the RDA analyses showed that the tDNA pool contains a mixed signal of the iDNA and eDNA community ($P_{Silica} = 0.001$, $P_{Depth} = 0.004$, $P_{Clay} = 0.053$, $P_{Silt} = 0.074$, $P_{Sand} = 0.039$), which lead to a poor expression of the environmental parameters shaping this pool. Further, the microbial

community of the eDNA and iDNA pool are forced by different environmental factors. Next to the depth (P_{Depth} = 0.001), which was identified as a main community-shaping factor for both cell-separated DNA pools, the community derived from the iDNA pool is influenced by live-depending parameters, such as the texture of the sedimentary matrix (P_{Silt} = 0.009) and as trend the water content ($P_{water\ content}$ = 0.107). A higher amount of silt indicates, for instance, a better supply of surface-bound nutrients. Additionally, a strong carbon-dependency of the genera *Methylobacterium*, *Streptomyces*, *Kribella*, *Agrobacterium,* and *Nocardioides* within the iDNA pool was found (linear regression, R^2 = 0.78-0.56). In conclusion, the iDNA most likely represents the active microbial community as a function of several life-depending parameters. In contrast, the composition of the eDNA communities is dependent on the biogenic silica content (P_{Silica} = 0.039), whereby a higher silica content on the one hand indicates an enhanced intra-lake bioproductivity based on algal blooms and therefore a higher nutrient supply. On the other hand, it represents an excellent surface for the attachment and long-term preservation of eDNA within the sedimentary matrix (Boom et al., 1990) . Former theoretical and empirical studies determined a long-term preservation of DNA for at least 50 ka to 1 Ma (Poinar et al. 1996; Willerslev & Cooper 2005). Supported by a distinct microbial community of the eDNA pools compared to the iDNA pools, this thesis proposes an even longer conservation time of eDNA in the El'gygytgyn Lake system. The long-time conservation of eDNA in the Crater Lake could be caused by a high level of negatively charged particles (e.g., silica particles, clay, humic acids). Extracellular DNA, which is attached to these particles is characterized by a lower bioavailability and a higher persistence against degradation (Paget et al., 1992; Pietramellara et al., 2009). Moreover, a low bioactivity and therefore low enzyme activity in the deep biosphere could be a reason for the accumulation and preservation of DNA over geological time scales.

In conclusion, this thesis describes the first microbiological investigation of lacustrine deep biosphere sediments and was able to identify the changes in the microbial distribution and abundance of the El'gygytgyn Crater Lake during the last 3.6 to 1.0 Ma. Using next generation sequencing, a large sequence data set was obtained, which can be used as an important comparative data basis for future microbiological studies on the deep biosphere of lacustrine sediments. Moreover, it was shown that the composition and diversity of the microbial community reflect the environmental changes within the Pliocene-Pleistocene transition and major climatic phases (EW I and II, LC, PPW and G/I). The microbial diversity mainly depends on the sedimentary temperature, an enhanced temperature-induced intra-lake bioproductivity, and the amount of organic-rich material originating from the catchment. Further, the microbial

richness can be used as a proxy for the climate of the El'gygytgyn Crater Lake as the microbial richness follows the general trends of the paleo-temperature and paleo-precipitation.

Focusing on the live/dead differentiation, which is extremely important when dealing with deep biosphere habitats due to the high potential for an accumulation of extracellular DNA, two methods were presented that proved to be very useful in the application: The PMA treatment was adapted for the differentiation between living cells and membrane-compromised (dead) cells of pure cultures of methanogenic archaea and sandy environmental samples. Further, the cell separation represents an extraordinarily good technique for the El'gygytgyn deep biosphere sediments (clay and silt-rich) and enables the separation of the microbial community of the intracellular and extracellular DNA. Thus, the pool of total DNA probably leads to an overestimation of the potential past community at the expense of the living microbial community of the deep lacustrine biosphere.

4.2 Key insights

Summarizing, the most important findings and achievements of this thesis are:

- Successful extraction and amplification of DNA from up to 3.6 Ma old lacustrine deep biosphere sediments were performed: Surprisingly diverse (6,910 OTUs, H = 0.92-5.01) and abundant microbial community (10^3-10^6 16S rRNA copies g^{-1}) was found in the El'gygytgyn sediments.
- Microbial community compositions varied strongly along the chronosequence and show distinct compositions for major climate phases (EW I and II, LC, PPW, and G/I).
- Microbial richness parameters follow general trends of the paleo-temperature and paleo-precipitation.
- Strong increase in the microbial diversity toward the sediment depth was detected (approximately 2.5 times higher diversity in Pliocene compared to Pleistocene sediments), which was caused by increased sedimentary temperatures and enhanced temperature-induced intra-lake bioproductivity as well as higher input of organic-rich material from the catchment.
- The applicability of the DNA-intercalating dye PMA to mask free DNA was successfully evaluated in different cultures of methanogenic archaea and in sandy environmental samples with a particle load of ≤ 200 mg mL^{-1}.
- The cell separation was successful adjusted for an in-depths characterization of the microbial community of the iDNA and eDNA in the El'gygytgyn deep biosphere and the DNA pools were compared with a commercial total DNA extraction (tDNA).
- Individual RDA analyses of cell-separated DNA pools better explained the correlation between the environmental parameters and the microbial community composition in the different sediment samples.
- Individual RDA analyses revealed that next to the main influencing factor of the sediment depth, the living community (iDNA pool) is mainly influenced by life-dependent parameters (e.g., grain size distribution, water availability), while the microbial community of the eDNA is dependent on the biogenic silica content.
- Previous community analyses in old environmental samples that are based on tDNA extraction might be biased due to co-extraction of eDNA (that most probably includes DNA from the past microbial community) and under-representation of the living microbial community.

4.3 Critical remarks and future work

In the field of microbiology, all results are dependent on the adaption of the underlying methods to the respective sample material and research question. In general, all information is based on the initial DNA extraction and DNA amplification. Therefore, it is not trivial to compare different environmental studies among each other if they differ in the DNA extraction approaches or in the choice of the primers. For instance, the observation that a species could not be detected by the chosen methods does not necessarily mean that the species does not occur in the habitat (e.g., false negative result). Any type of DNA extraction can differ in the composition of extractable species, depending on the strength of species bonding to the sedimentary matrix and the chemical and mechanical strength of an extraction method. Therefore, one should be aware that a DNA extract always reflects only a subset of the organisms contained in a sample. Differences in the extractable composition of the El'gygytgyn Crater Lake microorganisms could be determined, in particular, between a commercial DNA extraction kit (Power Soil™ DNA Isolation Kit, MO BIO) and a cell separation protocol. But also earlier studies demonstrated that the distribution of bacterial phyla depends on the selected extraction procedure (e.g., Williamson et al. 2011). In addition to the influence of the underlying extraction method, the revealed microbial assemblages of a certain habitat are also influenced by the specificity of the used oligonucleotide primers. Due to the preference of certain species by each primer pair, the relative abundance of the microbial community may vary between two analyses with different primer pairs (Baker et al., 2003).

Moreover, the specifications of the bioinformatics pipeline and the taxonomic assignment-underlying database may cause differences in the diversity analysis. Therefore, we have placed particular importance on the generation of the QIIME pipeline (Quantitative Insights Into Microbial Ecology, Caporaso et al. 2010b; Navas-Molina et al. 2013) and applied strict quality criteria for the sequences (e.g., no mismatch in the barcode or primer sequence; no contained ambiguous nucleotides; high Phred quality score of ≥ 25; de novo and reference-based chimera removal). The Illumina Miseq sequencing produces a relative short sequence lengths ($\approx$ 300 bp) in comparison to the expiring 454 pyrosequencing (up to 1000 bp), which could reduce the feasibility of a taxonomical assignment. However, here the V4 region of the bacterial and archaeal 16S rRNA gene was targeted, allowing to refer to an extensive database volume. Moreover, high-quality sequences based on the alignment of paired-end reads with a long overlapping area between the matching forward and reverse reads were generated.

Based on this work, a cell separation or another kind of live/dead differentiation in the field of environmental microbiology – and especially for deep biosphere research – as standard procedure is strongly suggested to avoid incorrect interpretations of the microbial function in the habitat and to be aware of the actual amount of extracellular DNA in a certain environmental sample. The relatively high amount of extracellular DNA in deep sediment samples is highlighted here and elsewhere (Corinaldesi et al. 2005; Alawi et al. 2014; Mao et al. 2014). Also, it is pointed out that the eDNA/iDNA ratio can differ significantly between one to another sample based on the sample characteristics. Influencing parameters are among others the amount of organic carbon, humic acids, biogenic silica, or cations as well as the temperature, pH and enzyme activity of the sample. Therefore, it is useful to apply the cell separation protocol to each sample under examination.

For future studies of the lacustrine deep biosphere, new ICDP drilling projects with dedicated microbiological objectives are desirable. To assess the influence of past climatic conditions on the microbial community, it is conceivable to sample, for instance, glacial and interglacial periods on a very high resolution and to apply functional primers in addition to general 16S rRNA gene primers. Moreover, the importance of multi proxy approaches and the combination of different techniques to validate the results among one another is highlighted. The DNA-based characterization of the living and dead microbial community could be coupled with FISH and RNA analysis (given adequate sample amount as well as time and procedure of storage) in order to derive the active microbial community. The combination of incubation and enrichment approaches, stable isotope probing (SIP), and the characterization of microorganisms represent desirable strategies to reveal insights into metabolic rates and microbial functions in a certain habitat and to extend the database representation of cultured and uncultured deep biosphere microbial communities which still is very limited.

References

Alawi, M., Schneider, B., Kallmeyer, J., 2014. A procedure for separate recovery of extra- and intracellular DNA from a single marine sediment sample. J. Microbiol. Methods 104, 36–42. doi:10.1016/j.mimet.2014.06.009

Allan, J., Ronholm, J., Mykytczuk, N.C.S., Greer, C.W., Onstott, T.C., Whyte, L.G., 2014. Methanogen community composition and rates of methane consumption in Canadian High Arctic permafrost soils. Environ. Microbiol. Rep. 6, 136–144. doi:10.1111/1758-2229.12139

Alonso, J.L., Amorós, I., Guy, R.A., 2014. Quantification of viable Giardia cysts and Cryptosporidium oocysts in wastewater using propidium monoazide quantitative real-time PCR. Parasitol. Res. 113, 2671–2678. doi:10.1007/s00436-014-3922-9

Andreev, A.A., Morozova, E., Fedorov, G., Schirrmeister, L., Bobrov, A.A., Kienast, F., Schwamborn, G., 2012. Vegetation history of central Chukotka deduced from permafrost paleoenvironmental records of the El'gygytgyn Impact Crater. Clim. Past 8, 1287–1300. doi:10.5194/cp-8-1287-2012

Andreev, A.A., Tarasov, P.E., Wennrich, V., Raschke, E., Herzschuh, U., Nowaczyk, N.R., Brigham-Grette, J., Melles, M., 2014. Late Pliocene and Early Pleistocene vegetation history of northeastern Russian Arctic inferred from the Lake El'gygytgyn pollen record. Clim. Past 10, 1017–1039. doi:10.5194/cp-10-1017-2014

Bae, S., Wuertz, S., 2012. Survival of host-associated Bacteroidales cells and their relationship with Enterococcus spp., Campylobacter jejuni, Salmonella enterica serovar Typhimurium, and Adenovirus in freshwater microcosms as measured by propidium monoazide-quantitative PCR. Appl. Environ. Microbiol. 78, 922–932. doi:10.1128/AEM.05157-11

Bae, S., Wuertz, S., 2009. Discrimination of viable and dead fecal Bacteroidales bacteria by quantitative PCR with propidium monoazide. Appl. Environ. Microbiol. 75, 2940–2944. doi:10.1128/AEM.01333-08

Bailey, N.J.L., Jabson, A.M., Rogers, M.A., 1973. Bacterial degradation of crude oil: Comparision of field and experimental data. Chem. Geol. 11, 203–221.

Baker, G.C., Smith, J.J., Cowan, D.A., 2003. Review and re-analysis of domain-specific 16S primers. J. Microbiol. Methods 55, 541–555. doi:10.1016/j.mimet.2003.08.009

Barbau-Piednoir, E., Mahillon, J., Pillyser, J., Coucke, W., Roosens, N.H., Botteldoorn, N., 2014. Evaluation of viability-qPCR detection system on viable and dead Salmonella serovar Enteritidis. J. Microbiol. Methods 103, 131–137. doi:10.1016/j.mimet.2014.06.003

Barbier, B. a, Dziduch, I., Liebner, S., Ganzert, L., Lantuit, H., Pollard, W., Wagner, D., 2012. Methane-cycling communities in a permafrost-affected soil on Herschel Island, Western Canadian Arctic: active layer profiling of mcrA and pmoA genes. FEMS Microbiol. Ecol. 82, 1–16. doi:10.1111/j.1574-6941.2012.01332.x

Barth, V.C., Cattani, F., Ferreira, C.A.S., de Oliveira, S.D., 2012. Sodium chloride affects

propidium monoazide action to distinguish viable cells. Anal. Biochem. 428, 108–110. doi:10.1016/j.ab.2012.06.012

Barton, L., 2005. Cell walls of Archaea, in: Barton, L.L. (Ed.), Structural and Functional Relationships in Prokaryotes. Springer Science & Business Media, New York, USA, pp. 116–117.

Biddle, J.F., Lipp, J.S., Lever, M.A., Lloyd, K.G., Sørensen, K.B., Anderson, R., Fredricks, H.F., Elvert, M., Kelly, T.J., Schrag, D.P., Sogin, M.L., Brenchley, J.E., Teske, A., House, C.H., Hinrichs, K.-U., 2006. Heterotrophic Archaea dominate sedimentary subsurface ecosystems off Peru. Proc. Natl. Acad. Sci. U. S. A. 103, 3846–3851. doi:10.1073/pnas.0600035103

Bischoff, J., Mangelsdorf, K., Heise, J., Lam, P., Rosen, P., Wennrich, V., Wagner, D., n.d. Glacial-interglacial microbial community dynamics in Middle to Late Pleistocene sediments in the Lake El'gygytgyn, Far East Russia. Prep. 1–23.

Bischoff, J., Mangelsdorf, K., Schwamborn, G., Wagner, D., 2014. Impact of lake-level and climate changes on microbial communities in a terrestrial permafrost sequence of the El'gygytgyn crater, far east Russian Arctic. Permafr. Periglac. Process. 25, 107–116. doi:10.1002/ppp.1807

Boom, R., Sol, C.J.A., Salimans, M.M.M., Jansen, C.L., Wertheim-van Dillen, P.M.E., van der Noordaa, J., 1990. Rapid and simple method for purification of nucleic acids. J. Clin. Microbiol. 28, 495–503.

Boone, D.R., Johnson, R.L., Liu, Y., 1989. Diffusion of the interspecies electron carriers H2 and formate in methanogenic ecosystems and its implications in the measurement of Km for H2 or formate uptake. Appl. Environ. Microbiol. 55, 1735–1741. doi:0099-2240/89/071735-07$02.00/0

Bowman, J.P., McCammon, S.A., Rea, S.M., McMeekin, T.A., 2000. The microbial composition of three limnologically disparate hypersaline Antarctic lakes. FEMS Microbiol. Lett. 183, 81–88. doi:10.1111/j.1574-6968.2000.tb08937.x

Breuker, A., Schippers, A., 2013. Data report: total cell counts and qPCR abundance of Archaea and Bacteria in shallow subsurface marine sediments of North Pond: gravity cores collected during site survey cruise prior to IODP Expedition 336. Proc. Integr. Ocean Drill. Progr. 336, 1–7. doi:10.2204/iodp.proc.336.201.2013

Brigham-Grette, J., Melles, M., Minyuk, P., Andreev, A., Tarasov, P., DeConto, R., Koenig, S., Nowaczyk, N., Wennrich, V., Rosén, P., Haltia, E., Cook, T., Gebhardt, C., Meyer-Jacob, C., Snyder, J., Herzschuh, U., 2013. Pliocene warmth, polar amplification, and stepped Pleistocene cooling recorded in NE Arctic Russia. Science 340, 1421–1427. doi:10.1126/science.1233137

Brown, J., Ferrians, O.J., J., Heginbottom, J.A., Melnikov, E.S., 1997. Circum-Arctic map of permafrost and ground-ice conditions. Washington, DC U.S. Geol. Surv. Coop. with Circum-Pacific Counc. Energy Miner. Resour.

Caporaso, J.G., Bittinger, K., Bushman, F.D., Desantis, T.Z., Andersen, G.L., Knight, R., 2010. PyNAST: A flexible tool for aligning sequences to a template alignment. Bioinformatics

26, 266–267. doi:10.1093/bioinformatics/btp636

Caporaso, J.G., Kuczynski, J., Stombaugh, J., Bittinger, K., Bushman, F.D., Costello, E.K., Fierer, N., Peña, A.G., Goodrich, J.K., Gordon, J.I., Huttley, G.A., Kelley, S.T., Knights, D., Koenig, J.E., Ley, R.E., Lozupone, C.A., McDonald, D., Muegge, B.D., Pirrung, M., Reeder, J., Sevinsky, J.R., Turnbaugh, P.J., Walters, W.A., Widmann, J., Yatsunenko, T., Zaneveld, J., Knight, R., 2010. QIIME allows analysis of high-throughput community sequencing data. Nat. Methods 7, 335–336. doi:10.1038/nmeth.f.303

Caporaso, J.G., Lauber, C.L., Walters, W.A., Berg-Lyons, D., Lozupone, C.A., Turnbaugh, P.J., Fierer, N., Knight, R., 2011. Global patterns of 16S rRNA diversity at a depth of millions of sequences per sample. Proc. Natl. Acad. Sci. U. S. A. 108, 4516–4522. doi:10.1073/pnas.1000080107

Chen, H., Boutros, P.C., 2011. VennDiagram: a package for the generation of highly-customizable Venn and Euler diagrams in R. BMC Bioinformatics 12, 35. doi:10.1186/1471-2105-12-35

Chen, M., Xiao, X., Wang, P., Zeng, X., Wang, F., 2005. Arthrobacter ardleyensis sp. nov., isolated from Antarctic lake sediment and deep-sea sediment. Arch. Microbiol. 183, 301–305. doi:10.1007/s00203-005-0772-y

Comeau, A.M., Harding, T., Galand, P.E., Vincent, W.F., Lovejoy, C., 2012. Vertical distribution of microbial communities in a perennially stratified Arctic lake with saline, anoxic bottom waters. Sci. Rep. 2, 1–10. doi:10.1038/srep00604

Corinaldesi, C., Barucca, M., Luna, G.M., Dell'Anno, A., 2011. Preservation, origin and genetic imprint of extracellular DNA in permanently anoxic deep-sea sediments. Mol. Ecol. 20, 642–654. doi:10.1111/j.1365-294X.2010.04958.x

Corinaldesi, C., Danovaro, R., Dell'Anno, A., 2005. Simultaneous recovery of extracellular and intracellular DNA suitable for molecular studies from marine sediments. Appl. Environ. Microbiol. 71, 46–50. doi:10.1128/AEM.71.1.46

Corinaldesi, C., Tangherlini, M., Luna, G.M., Dell'Anno, A., 2014. Extracellular DNA can preserve the genetic signatures of present and past viral infection events in deep hypersaline anoxic basins. Proc. R. Soc. B Biol. Sci. 281, 20133299. doi:10.1098/rspb.2013.3299

Crecchio, C., Stotzky, G., 1998. Binding of DNA on humic acids: effect on transformation of Bacillus subtilis and resistence to DNase. Soil Biol. Biochem. 30, 1061–1067.

Croudace, I.W., Rindby, A., Rothwell, R.G., 2006. ITRAX: Description and evaluation of a new multi-function X-ray core scanner. Geol. Soc. London, Spec. Publ. 267, 51–63. doi:10.1144/GSL.SP.2006.267.01.04

Crump, B.C., Amaral-Zettler, L.A., Kling, G.W., 2012. Microbial diversity in Arctic freshwaters is structured by inoculation of microbes from soils. ISME J. 6, 1629–1639. doi:10.1038/ismej.2012.9

D'Amico, S., Collins, T., Marx, J.-C., Feller, G., Gerday, C., 2006. Psychrophilic microorganisms: challenges for life. EMBO Rep. 7, 385–389. doi:10.1038/sj.embor.7400662

D'Hondt, S., Jørgensen, B.B., Miller, D.J., Batzke, A., Blake, R., Cragg, B.A., Cypionka, H., Dickens, G.R., Ferdelman, T., Hinrichs, K., Holm, N.G., Mitterer, R., Spivack, A., Wang, G., Bekins, B., Engelen, B., Ford, K., Gettemy, G., Rutherford, S.D., Sass, H., Skilbeck, C.G., House, C.H., Aiello, I.W., Gue, G., Inagaki, F., Meister, P., Naehr, T., Niitsuma, S., Parkes, R.J., Schippers, A., Smith, D.C., Teske, A., Wiegel, J., Padilla, C.N., Luz, J., Acosta, S., 2004. Distributions of microbial activities in deep subseafloor sediments. Science 306, 2216–2221.

D'Hondt, S., Rutherford, S., Spivack, A.J., 2002. Metabolic activity of subsurface life in deep-sea sediments. Science (80-.). 295, 2067–2070. doi:10.1126/science.1064878

De Lipthay, J.R., Johnsen, K., Albrechtsen, H.J., Rosenberg, P., Aamand, J., 2004. Bacterial diversity and community structure of a sub-surface aquifer exposed to realistic low herbicide concentrations. FEMS Microbiol. Ecol. 49, 59–69. doi:10.1016/j.femsec.2004.02.007

De Schepper, S., Head, M.J., Groeneveld, J., 2009. North Atlantic Current variability through marine isotope stage M2 (circa 3.3 Ma) during the mid-Pliocene. Paleoceanography 24, 1–17. doi:10.1029/2008PA001725

Dell`Anno, A., Danovaro, R., 2005. Extracellular DNA plays a key role in Deep-Sea ecosystem functioning. Science 309, 2179. doi:10.1126/science.1117475

DeSantis, T.Z., Hugenholtz, P., Larsen, N., Rojas, M., Brodie, E.L., Keller, K., Huber, T., Dalevi, D., Hu, P., Andersen, G.L., 2006. Greengenes, a chimera-checked 16S rRNA gene database and workbench compatible with ARB. Appl. Environ. Microbiol. 72, 5069–5072. doi:10.1128/AEM.03006-05

Dick, G.J., Anantharaman, K., Baker, B.J., Li, M., 2013. The microbiology of deep-sea hydrothermal vent plumes: ecological and biogeographic linkages to seafloor and water column habitats. Front. Microbiol. 4, 79–94.

Dieser, M., Nocker, A., Priscu, J.C., Foreman, C.M., 2010. Viable microbes in ice: Application of molecular assays to McMurdo Dry Valley lake ice communities. Antarct. Sci. 22, 470–476. doi:10.1017/S0954102010000404

Dlott, G., Maul, J.E., Buyer, J., Yarwood, S., 2015. Microbial rRNA:rRNA gene ratios may be unexpectedly low due to extracellular DNA preservation in soils. J. Microbiol. Methods 115, 112–120. doi:10.1016/j.mimet.2015.05.027

Dong, X., Chen, Z., 2012. Psychrotolerant methanogenic archaea: Diversity and cold adaptation mechanisms. Sci. China Life Sci. 55, 415–421. doi:10.1007/s11427-012-4320-0

Dong, Y., Kumar, C.G., Chia, N., Kim, P.-J., Miller, P.A., Price, N.D., Cann, I.K.O., Flynn, T.M., Sanford, R.A., Krapac, I.G., Locke, R.A., Hong, P.-Y., Tamaki, H., Liu, W.-T., Mackie, R.I., Hernandez, A.G., Wright, C.L., Mikel, M.A., Walker, J.L., Sivaguru, M., Fried, G., Yannarell, A.C., Fouke, B.W., 2014. Halomonas sulfidaeris-dominated microbial community inhabits a 1.8 km-deep subsurface Cambrian Sandstone reservoir. Environ. Microbiol. 16, 1695–1708. doi:10.1111/1462-2920.12325

Edgar, R.C., 2010. Search and clustering orders of magnitude faster than BLAST. Bioinformatics 26, 2460–2461. doi:10.1093/bioinformatics/btq461

Edgar, R.C., Haas, B.J., Clemente, J.C., Quince, C., Knight, R., 2011. UCHIME improves sensitivity and speed of chimera detection. Bioinformatics 27, 2194–2200. doi:10.1093/bioinformatics/btr381

Edwards, K.J., Becker, K., Colwell, F., 2012. The deep, dark energy biosphere: Intraterrestrial life on Earth. Annu. Rev. Earth Planet. Sci. 40, 551–568. doi:10.1146/annurev-earth-042711-105500

Eilers, H., Pernthaler, J., Glöckner, F.O., Amann, R., 2000. Culturability and in situ abundance of pelagic bacteria from the North Sea. Appl. Environ. Microbiol. 66, 3044–3051. doi:10.1128/AEM.66.7.3044-3051.2000

Fedorov, G., Nolan, M., Brigham-Grette, J., Bolshiyanov, D., Schwamborn, G., Juschus, O., 2013. Preliminary estimation of Lake El'gygytgyn water balance and sediment income. Clim. Past 9, 1455–1465. doi:10.5194/cp-9-1455-2013

Fittipaldi, M., Codony, F., Adrados, B., Camper, A.K., Morató, J., 2011. Viable real-time PCR in environmental samples: Can all data be interpreted directly? Microb. Ecol. 61, 7–12. doi:10.1007/s00248-010-9719-1

Fittipaldi, M., Nocker, A., Codony, F., 2012. Progress in understanding preferential detection of live cells using viability dyes in combination with DNA amplification. J. Microbiol. Methods 91, 276–289. doi:10.1016/j.mimet.2012.08.007

Fredrickson, J.K., Balkwill, D.L., 2006. Geomicrobial Processes and Biodiversity in the Deep Terrestrial Subsurface. Geomicrobiol. J. 23, 345–356. doi:10.1080/01490450600875571

Fredrickson, J.K., Zachara, J.M., Balkwill, D.L., Kennedy, D., Li, S.M.W., Kostandarithes, H.M., Daly, M.J., Romine, M.F., Brockman, F.J., 2004. Geomicrobiology of high-level nuclear waste-contaminated vadose sediments at the Hanford Site, Washington State. Appl. Environ. Microbiol. 70, 4230–4241. doi:10.1128/AEM.70.7.4230-4241.2004

Gagen, E.J., Huber, H., Meador, T., Hinrichs, K.-U., Thomm, M., 2013. Novel cultivation-based approach to understanding the miscellaneous crenarchaeotic group (MCG) archaea from sedimentary ecosystems. Appl. Environ. Microbiol. 79, 6400–6406. doi:10.1128/AEM.02153-13

Galand, P.E., Lovejoy, C., Pouliot, J., Garneau, M.-È., Vincent, W.F., 2008. Microbial community diversity and heterotrophic production in a coastal Arctic ecosystem: A stamukhi lake and its source waters. Limnol. Oceanogr. 53, 813–823. doi:10.4319/lo.2008.53.2.0813

Ganzert, L., Jurgens, G., Münster, U., Wagner, D., 2007. Methanogenic communities in permafrost-affected soils of the Laptev Sea coast, Siberian Arctic, characterized by 16S rRNA gene fingerprints. FEMS Microbiol. Ecol. 59, 476–488. doi:10.1111/j.1574-6941.2006.00205.x

Ganzert, L., Schirmack, J., Alawi, M., Mangelsdorf, K., Sand, W., Hillebrand-Voiculescu, A., Wagner, D., 2014. Methanosarcina spelaei sp. nov., a methanogenic archaeon isolated from a floating biofilm of a subsurface sulphurous lake. Int. J. Syst. Evol. Microbiol. 64, 3478–3484. doi:10.1099/ijs.0.064956-0

Gebhardt, A.C., Niessen, F., Kopsch, C., 2006. Central ring structure identified in one of the

world's best-preserved impact craters. Geology 34, 145–148. doi:10.1130/G22278.1

Gorham, E., 1991. Northern Peatlands: Role in the carbon-cycle and probable responses to climatic warming. Ecol. Appl. 1, 182–195.

Görsch, J., 2011. Zusammensetzung der Lebensgemeinschaft methanogener Archaeen im El'gygytgyn-Kratersee, NO-Sibiriens. Masterarbeit.

Graham, D.E., Wallenstein, M.D., Vishnivetskaya, T.A., Waldrop, M.P., Phelps, T.J., Pfiffner, S.M., Onstott, T.C., Whyte, L.G., Rivkina, E.M., Gilichinsky, D.A., Elias, D.A., Mackelprang, R., VerBerkmoes, N.C., Hettich, R.L., Wagner, D., Wullschleger, S.D., Jansson, J.K., 2012. Microbes in thawing permafrost: the unknown variable in the climate change equation. ISME J. 6, 709–712. doi:10.1038/ismej.2011.163

Gurov, E.P., Koeberl, C., Reimold, W.U., Brandstätter, F., Amare, K., 2005. Shock metamorphism of siliceous volcanic rocks of the El'gygytgyn impact crater (Chukotka, Russia). Geol. Soc. Am. 391–412.

He, R., Wooller, M.J., Pohlman, J.W., Quensen, J., Tiedje, J.M., Leigh, M.B., 2012. Shifts in identity and activity of methanotrophs in Arctic lake sediments in response to temperature changes. Appl. Environ. Microbiol. 78, 4715–4723. doi:10.1128/AEM.00853-12

Head, I.M., Jones, D.M., Larter, S.R., 2003. Biological activity in the deep subsurface and the origin of heavy oil. Nature 426, 344–352. doi:10.1038/nature02134

Heise, J., Nega, M., Alawi, M., Wagner, D., 2016. Propidium monoazide treatment to distinguish between live and dead methanogens in pure cultures and environmental samples. J. Microbiol. Methods 121, 11–23. doi:10.1016/j.mimet.2015.12.002

Hinsa-Leasure, S.M., Bhavaraju, L., Rodrigues, J.L.M., Bakermans, C., Gilichinsky, D.A., Tiedje, J.M., 2010. Characterization of a bacterial community from a Northeast Siberian seacoast permafrost sample. FEMS Microbiol. Ecol. 74, 103–113. doi:10.1111/j.1574-6941.2010.00945.x

Hodgson, D.A., Vyverman, W., Verleyen, E., Sabbe, K., Leavitt, P.R., Taton, A., Squier, A.H., Keely, B.J., 2004. Environmental factors influencing the pigment composition of in situ benthic microbial communities in east Antarctic lakes. Aquat. Microb. Ecol. 37, 247–263. doi:10.3354/ame037247

Hoehler, T.M., Jørgensen, B.B., 2013. Microbial life under extreme energy limitation. Nat. Rev. Microbiol. 11, 83–94. doi:10.1038/nrmicro2939

Hofreiter, M., Serre, D., Poinar, H.N., Kuch, M., Pääbo, S., 2001. Ancient DNA. Nat. Rev. Genet. 2, 353–359. doi:10.1038/35072071

Ino, K., Konno, U., Kouduka, M., Hirota, A., Togo, Y., Fukuda, A., Komatsu, D., Tsunogai, U., Tanabe, A.S., Yamamoto, S., Iwatsuki, T., Mizuno, T., Ito, K., Suzuki, Y., 2016. Deep microbial life in high-quality granitic groundwater from geochemically and geographically distinct underground boreholes. Environ. Microbiol. Rep. doi:10.1111/1758–2229.12379. doi:10.1111/1758-2229.12379

IPCC, 2013. Climate change 2013: The physical science basis. Contribution of working group I to the Fifth Assessment Report of the Intergovernmental Panel on Climate Change. Chapter 4 Observations: Cryosphere. Cambridge University Press.

doi:10.1017/CBO9781107415324.012

Jadhav, V.V., Pote, S.S., Yadav, A., Shouche, Y.S., Bhadekar, R.K., 2013. Extracellular cold active lipase from the psychrotrophic Halomonas sp. BRI 8 isolated from the Antarctic sea water. Songklanakarin J. Sience Technol. 35, 623–630.

Jansson, J.K., Taş, N., 2014. The microbial ecology of permafrost. Nat. Rev. Microbiol. 12, 414–425. doi:10.1038/nrmicro3262

Jeppesen, E., Meerhoff, M., Davidson, T.A., Trolle, D., Søndergaard, M., Lauridsen, T.L., Beklioğlu, M., Brucet, S., Volta, P., González-Bergonzoni, I., Nielsen, A., 2014. Climate change impacts on lakes: An integrated ecological perspective based on a multi-faceted approach, with special focus on shallow lakes. J. Limnol. 73, 84–107. doi:10.4081/jlimnol.2014.844

Jiang, H., Dong, H., Yu, B., Liu, X., Li, Y., Ji, S., Zhang, C.L., 2007. Microbial response to salinity change in Lake Chaka, a hypersaline lake on Tibetan plateau. Environ. Microbiol. 9, 2603–2621. doi:10.1111/j.1462-2920.2007.01377.x

Jørgensen, B.B., 2011. Deep subseafloor microbial cells on physiological standby. Proc. Natl. Acad. Sci. U. S. A. 108, 18193–18194. doi:10.1073/pnas.1115421108

Joshi, A.A., Kanekar, P.P., Kelkar, A.S., Sarnaik, S.S., Shouche, Y., Wani, A., 2007. Moderately halophilic, alkalitolerant Halomonas campisalis MCM B-365 from Lonar Lake, India. J. Basic Microbiol. 47, 213–221. doi:10.1002/jobm.200610223

Juggins, S., 2014. rioja: Analysis of quaternary science data, R package version (0.9-3).

Kallmeyer, J., Pockalny, R., Adhikari, R.R., Smith, D.C., D'Hondt, S., 2012. Global distribution of microbial abundance and biomass in subseafloor sediment. Proc. Natl. Acad. Sci. U. S. A. 109, 1–7. doi:10.1073/pnas.1203849109

Kallmeyer, J., Wagner, D., 2014. Microbial life of the deep biosphere. De Gruyter, Berlin, Boston. doi:10.1515/9783110300130

Kaye, J.Z., Sylvan, J.B., Edwards, K.J., Baross, J.A., 2011. Halomonas and Marinobacter ecotypes from hydrothermal vent, subseafloor and deep-sea environments. FEMS Microbiol. Ecol. 75, 123–133. doi:10.1111/j.1574-6941.2010.00984.x

Keller, M., Zengler, K., 2004. Tapping into microbial diversity. Nat. Rev. Microbiol. 2, 141–150. doi:10.1038/nrmicro819

Kerr, R.A., 2002. Deep life in the slow, slow lane. Science (80-.). 296, 1056–8.

Konings, W.N., Albers, S., Koning, S., Driessen, A.J.M., 2002. The cell membrane plays a crucial role in survival of bacteria and archaea in extreme environments. Antonie Van Leeuwenhoek 81, 61–72. doi:10.1023/A:1020573408652

Layer, P.W., 2000. Argon-40/argon-39 age of the El'gygytgyn impact event, Chukotka, Russia. Meteorit. Planet. Sci. 35, 591–599. doi:10.1111/j.1945-5100.2000.tb01439.x

Levy-Booth, D.J., Campbell, R.G., Gulden, R.H., Hart, M.M., Powell, J.R., Klironomos, J.N., Pauls, K.P., Swanton, C.J., Trevors, J.T., Dunfield, K.E., 2007. Cycling of extracellular DNA in the soil environment. Soil Biol. Biochem. 39, 2977–2991. doi:10.1016/j.soilbio.2007.06.020

Li, L., Mendis, N., Trigui, H., Oliver, J.D., Faucher, S.P., 2014. The importance of the viable but non-culturable state in human bacterial pathogens. Front. Microbiol. 5, 1–20. doi:10.3389/fmicb.2014.00258

Liang, Z., Keeley, A., 2012. Comparison of propidium monoazide-quantitative PCR and reverse transcription quantitative PCR for viability detection of fresh Cryptosporidium oocysts following disinfection and after long-term storage in water samples. Water Res. 46, 5941–5953. doi:10.1016/j.watres.2012.08.014

Liebner, S., Rublack, K., Stuehrmann, T., Wagner, D., 2009. Diversity of aerobic methanotrophic bacteria in a permafrost active layer soil of the Lena Delta, Siberia. Microb. Ecol. 57, 25–35. doi:10.1007/s00248-008-9411-x

Liebner, S., Wagner, D., 2007. Abundance, distribution and potential activity of methane oxidizing bacteria in permafrost soils from the Lena Delta, Siberia. Environ. Microbiol. 9, 107–117. doi:10.1111/j.1462-2920.2006.01120.x

Lisiecki, L.E., Raymo, M.E., 2005. A Pliocene-Pleistocene stack of 57 globally distributed benthic δ 18 O records. Paleoceanography 20, PA1003. doi:10.1029/2004PA001071

Lombard, N., Prestat, E., van Elsas, J.D., Simonet, P., 2011. Soil-specific limitations for access and analysis of soil microbial communities by metagenomics. FEMS Microbiol. Ecol. 78, 31–49. doi:10.1111/j.1574-6941.2011.01140.x

Lomstein, B.A., Langerhuus, A.T., D'Hondt, S., Jørgensen, B.B., Spivack, A.J., 2012. Endospore abundance, microbial growth and necromass turnover in deep sub-seafloor sediment. Nature 484, 101–104. doi:10.1038/nature10905

Luna, G.M., Manini, E., Danovaro, R., 2002. Large fraction of dead and inactive bacteria in coastal marine sediments: Comparison of protocols for determination and ecological significance. Appl. Environ. Microbiol. 68, 3509–3513. doi:10.1128/AEM.68.7.3509

Luo, J.-F., Lin, W.-T., Guo, Y., 2010. Method to detect only viable cells in microbial ecology. Appl. Microbiol. Biotechnol. 86, 377–384. doi:10.1007/s00253-009-2373-1

Mao, D., Luo, Y., Mathieu, J., Wang, Q., Feng, L., Mu, Q., Feng, C., Alvarez, P.J.J., 2014. Persistence of extracellular DNA in river sediment facilitates antibiotic resistance gene propagation. Environ. Sci. Technol. 48, 71–78.

McMurdie, P.J., Holmes, S., 2013. phyloseq: an R package for reproducible interactive analysis and graphics of microbiome census data. PLoS One 8, e61217. doi:10.1371/journal.pone.0061217

Melles, M., Brigham-Grette, J., Minyuk, P., Koeberl, C., Andreev, A., Cook, T., Fedorov, G., Gebhardt, C., Haltia-Hovi, E., Kukkonen, M., Nowaczyk, N., Schwamborn, G., Wennrich, V., 2011. The Lake El'gygytgyn scientific drilling project conquering Arctic challenges through continental drilling. Sci. Drill. 11, 29–40. doi:10.2204/iodp.sd.11.03.2011

Melles, M., Brigham-Grette, J., Minyuk, P.S., Nowaczyk, N.R., Wennrich, V., DeConto, R.M., Anderson, P.M., Andreev, A. a, Coletti, A., Cook, T.L., Haltia-Hovi, E., Kukkonen, M., Lozhkin, A. V, Rosén, P., Tarasov, P., Vogel, H., Wagner, B., 2012. 2.8 million years of Arctic climate change from Lake El'gygytgyn, NE Russia. Science 337, 315–320. doi:10.1126/science.1222135

Morozova, D., Wagner, D., 2007. Stress response of methanogenic archaea from Siberian permafrost compared with methanogens from nonpermafrost habitats. FEMS Microbiol. Ecol. 61, 16–25. doi:10.1111/j.1574-6941.2007.00316.x

Moser, D.P., Gihring, T., Fredrickson, J.K., Brockman, F.J., Balkwill, D., Dollhopf, M.E., Sherwood-Lollar, B., Pratt, L.M., Boice, E., Southam, G., Wanger, G., Welty, a T., Baker, B.J., Onstott, T.C., 2005. Desulfotomaculum and Methanobacterium spp. dominate a 4- to 5-kilometer-deep fault. Appl. Environ. Microbiol. 71, 8773–8783. doi:10.1128/AEM.71.12.8773

Mottaghy, D., Schwamborn, G., Rath, V., 2013. Past climate changes and permafrost depth at the Lake El'gygytgyn site: implications from data and thermal modeling. Clim. Past 9, 119–133. doi:10.5194/cp-9-119-2013

Nadkarni, M.A., Martin, F.E., Jacques, N.A., Hunter, N., 2002. Determination of bacterial load by real-time PCR using a broad-range (universal) probe and primers set. Microbiology 148, 257–266.

Navas-Molina, J.A., Peralta-Sánchez, J.M., González, A., McMurdie, P.J., Vázquez-Baeza, Y., Xu, Z., Ursell, L.K., Lauber, C., Zhou, H., Song, S.J., Huntley, J., Ackermann, G.L., Berg-Lyons, D., Holmes, S., Caporaso, J.G., Knight, R., 2013. Advancing our understanding of the human microbiome using QIIME. Methods Enzymol. 531, 371–444. doi:10.1016/B978-0-12-407863-5.00019-8

Newberry, C.J., Webster, G., Cragg, B.A., Parkes, R.J., Weightman, A.J., Fry, J.C., 2004. Diversity of prokaryotes and methanogenesis in deep subsurface sediments from the Nankai Trough, Ocean Drilling Program Leg 190. Environ. Microbiol. 6, 274–287. doi:10.1111/j.1462-2920.2004.00568.x

Niederberger, T.D., Steven, B., Charvet, S., Barbier, B., Whyte, L.G., 2009. Virgibacillus arcticus sp. nov., a moderately halophilic, endospore-forming bacterium from permafrost in the Canadian high Arctic. Int. J. Syst. Evol. Microbiol. 59, 2219–2225. doi:10.1099/ijs.0.002931-0

Nkuipou-Kenfack, E., Engel, H., Fakih, S., Nocker, A., 2013. Improving efficiency of viability-PCR for selective detection of live cells. J. Microbiol. Methods 93, 20–24. doi:10.1016/j.mimet.2013.01.018

Nocker, A., Camper, A.K., 2006. Selective removal of DNA from dead cells of mixed bacterial communities by use of ethidium monoazide. Appl. Environ. Microbiol. 72, 1997–2004. doi:10.1128/AEM.72.3.1997

Nocker, A., Cheung, C.-Y., Camper, A.K., 2006. Comparison of propidium monoazide with ethidium monoazide for differentiation of live vs. dead bacteria by selective removal of DNA from dead cells. J. Microbiol. Methods 67, 310–320. doi:10.1016/j.mimet.2006.04.015

Nocker, A., Sossa-Fernandez, P., Burr, M.D., Camper, A.K., 2007. Use of propidium monoazide for live/dead distinction in microbial ecology. Appl. Environ. Microbiol. 73, 5111–5117. doi:10.1128/AEM.02987-06

Nolan, M., Brigham-Grette, J., 2007. Basic hydrology, limnology, and meteorology of modern

Lake El'gygytgyn, Siberia. J. Paleolimnol. 37, 17–35. doi:10.1007/s10933-006-9020-y

Nolan, M., Liston, G., Prokein, P., Brigham-Grette, J., Sharpton, V.L., Huntzinger, R., 2002. Analysis of lake ice dynamics and morphology on Lake El'gygytgyn, NE Siberia, using synthetic aperture radar (SAR) and Landsat. J. Geophys. Res. 108, 8162. doi:10.1029/2001JD000934

Nowaczyk, N.R., Haltia, E.M., Ulbricht, D., Wennrich, V., Sauerbrey, M.A., Rosén, P., Vogel, H., Francke, A., Meyer-Jacob, C., Andreev, A.A., Lozhkin, A. V., 2013b. Chronology of Lake El'gygytgyn sediments. Clim. Past Discuss. 9, 3061–3102. doi:10.5194/cpd-9-3061-2013

Nowaczyk, N.R., Haltia, E.M., Ulbricht, D., Wennrich, V., Sauerbrey, M.A., Rosén, P., Vogel, H., Francke, A., Meyer-Jacob, C., Andreev, A.A., Lozhkin, A. V., 2013a. Chronology of Lake El'gygytgyn sediments – a combined magnetostratigraphic, palaeoclimatic and orbital tuning study based on multi-parameter analyses. Clim. Past 9, 2413–2432. doi:10.5194/cp-9-2413-2013

Ogram, A., Sayler, G.S., Barkay, T., 1987. The extraction and purification of microbial DNA from sediments. J. Microbiol. Methods 7, 57–66.

Ogram, A., Sayler, G.S., Gustin, D., Lewis, R.J., 1988. DNA adsorption to soils and sediments. Environ. Sci. Technol. 22, 982–984. doi:10.1021/es00173a020

Oksanen, J., Blanchet, F.G.K.R., Legendre, P., Minchin, P.R., O'Hara, R.B., Simpson, G.L., Solymos, P., Stevens, M.H.H., Wagner, H., 2014. vegan: Community ecology package. R package version 2.2-0.

Okshevsky, M., Meyer, R.L., 2015. The role of extracellular DNA in the establishment, maintenance and perpetuation of bacterial biofilms. Crit Rev Microbiol 41, 341–352. doi:10.3109/1040841x.2013.841639

Paget, E., Monrozier, L.J., Simonet, P., 1992. Adsorption of DNA on clay minerals: protection against DNase I and influence on gene transfer. FEMS Microbiol. Lett. 97, 31–40.

Parkes, R.J., Cragg, B.A., Bale, S.J., Getliff, J.M., Goodmann, K., Rochelle, P.A., Fry, J.C., Weightman, A.J., Harvey, S.M., 1994. Deep bacterial biosphere in pacific ocean sediments. Nature 371, 410–413.

Parmesan, C., Yohe, G., 2003. A globally coherent fingerprint of climate change impacts across natural systems. Nature 421, 37–42. doi:10.1038/nature01286

Peeters, K., Verleyen, E., Hodgson, D.A., Convey, P., Ertz, D., Vyverman, W., Willems, A., 2012. Heterotrophic bacterial diversity in aquatic microbial mat communities from Antarctica. Polar Biol. 35, 543–554. doi:10.1007/s00300-011-1100-4

Perkins, D.M., McKie, B.G., Malmqvist, B., Gilmour, S.G., Reiss, J., Woodward, G., 2010. Chapter 5 - Environmental warming and biodiversity–ecosystem functioning in freshwater microcosms: Partitioning the effects of species identity, richness and metabolism, in: Research, G.W.B.T.-A. in E. (Ed.), Integrative Ecology: From Molecules to Ecosystems. Academic Press, pp. 177–209. doi:http://dx.doi.org/10.1016/B978-0-12-385005-8.00005-8

Phillips, K., 2013. Size variation of planktonic diatoms on glacial-interglacial time scales in the

sediment record of Lake El'gygytgyn, north-east Russia. pp 34.

Pietramellara, G., Ascher, J., Borgogni, F., Ceccherini, M.T., Guerri, G., Nannipieri, P., 2009. Extracellular DNA in soil and sediment: fate and ecological relevance. Biol. Fertil. Soils 45, 219–235. doi:10.1007/s00374-008-0345-8

Poinar, H.N., Höss, M., Bada, J.L., Pääbo, S., 1996. Amino acid racemization and the preservation of ancient DNA. Science 272, 864–866.

Price, M.N., Dehal, P.S., Arkin, A.P., 2009. FastTree: Computing large minimum evolution trees with profiles instead of a distance matrix. Mol. Biol. Evol. 26, 1641–1650. doi:10.1093/molbev/msp077

Price, P.B., Sowers, T., 2004. Temperature dependence of metabolic rates for microbial growth, maintenance, and survival. Proc Natl Acad Sci USA 101, 4631–4636.

Quayle, W.C., Peck, L.S., Peat, H., Ellis-Evans, J.C., Harrigan, P.R., 2002. Extreme responses to climate change in Antartic lakes. Science (80-.). 295, 645. doi:10.1126/science.1064074

Reddy, G.S.N., Raghavan, P.U.M., Sarita, N.B., Prakash, J.S.S., Nagesh, N., Delille, D., Shivaji, S., 2003. Halomonas glaciei sp. nov. isolated from fast ice of Adelie Land, Antarctica. Extremophiles 7, 55–61. doi:10.1007/s00792-002-0295-2

Rosén, P., Vogel, H., Cunningham, L., Reuss, N., Conley, D.J., Persson, P., 2009. Fourier transform infrared spectroscopy, a new method for rapid determination of total organic and inorganic carbon and biogenic silica concentration in lake sediments. J. Paleolimnol. 43, 247–259. doi:10.1007/s10933-009-9329-4

Schippers, A., Kock, D., Höft, C., Köweker, G., Siegert, M., 2012. Quantification of microbial communities in subsurface marine sediments of the Black Sea and off Namibia. Front. Microbiol. 3, 1–11. doi:10.3389/fmicb.2012.00016

Schippers, A., Köweker, G., Höft, C., Teichert, B.M.A., 2010. Quantification of microbial communities in forearc sediment basins off Sumatra. Geomicrobiol. J. doi:10.1080/01490450903456798

Schirmack, J., Alawi, M., Wagner, D., 2015. Influence of Martian regolith analogs on the activity and growth of methanogenic archaea, with special regard to long-term desiccation. Front. Microbiol. 6, 1–12. doi:10.3389/fmicb.2015.00210

Schirmack, J., Mangelsdorf, K., Ganzert, L., Sand, W., Hillebrand-Voiculescu, A., Wagner, D., 2014. Methanobacterium movilense sp. nov., a hydrogenotrophic, secondary-alcohol-utilizing methanogen from the anoxic sediment of a subsurface lake. Int. J. Syst. Evol. Microbiol. 64, 522–527. doi:10.1099/ijs.0.057224-0

Schulze-Makuch, D., Kennedy, J.F., 2000. Microbiological and chemical characterization of hydrothermal fluids at Tortugas Mountain Geothermal Area, southern New Mexico, USA. Hydrogeol. J. 8, 295.

Schuur, E.A.G., Abbott, B.W., Bowden, W.B., Brovkin, V., Camill, P., Canadell, J.G., Chanton, J.P., Chapin, F.S., Christensen, T.R., Ciais, P., Crosby, B.T., Czimczik, C.I., Grosse, G., Harden, J., Hayes, D.J., Hugelius, G., Jastrow, J.D., Jones, J.B., Kleinen, T., Koven, C.D., Krinner, G., Kuhry, P., Lawrence, D.M., McGuire, A.D., Natali, S.M.,

O'Donnell, J.A., Ping, C.L., Riley, W.J., Rinke, A., Romanovsky, V.E., Sannel, A.B.K., Schädel, C., Schaefer, K., Sky, J., Subin, Z.M., Tarnocai, C., Turetsky, M.R., Waldrop, M.P., Walter Anthony, K.M., Wickland, K.P., Wilson, C.J., Zimov, S.A., 2013. Expert assessment of vulnerability of permafrost carbon to climate change. Clim. Change 119, 359–374. doi:10.1007/s10584-013-0730-7

Schwartzman, D., 1999. Life, temperature, and the Earth: The self-organizing biosphere.

Serrano, P., 2014. Methanogens from Siberian permafrost as models for life on mars. Doctoral thesis.

Shindell, D.T., Faluvegi, G., Koch, D.M., Schmidt, G.A., Unger, N., Bauer, S.E., 2009. Improved attribution of climate forcing to emissions. Science (80-.). 326, 716–718.

Simankova, M. V, Kotsyurbenko, O.R., Lueders, T., Nozhevnikova, A.N., Wagner, B., Conrad, R., Friedrich, M.W., 2003. Isolation and characterization of new strains of methanogens from cold terrestrial habitats. Syst. Appl. Microbiol. 26, 312–318. doi:10.1078/072320203322346173

Smith, L.C., Sheng, Y., MacDonald, G.M., Hinzman, L.D., 2005. Disappearing Arctic lakes. Science (80-.). 308, 1429. doi:10.1126/science.1108142

Smol, J.P., Wolfe, A.P., Birks, H.J.B., Douglas, M.S. V, Jones, V.J., Korhola, A., Pienitz, R., Rühland, K., Sorvari, S., Antoniades, D., Brooks, S.J., Fallu, M.-A., Hughes, M., Keatley, B.E., Laing, T.E., Michelutti, N., Nazarova, L., Nyman, M., Paterson, A.M., Perren, B., Quinlan, R., Rautio, M., Saulnier-Talbot, E., Siitonen, S., Solovieva, N., Weckström, J., 2005. Climate-driven regime shifts in the biological communities of arctic lakes. Proc. Natl. Acad. Sci. U. S. A. 102, 4397–4402. doi:10.1073/pnas.0500245102

Stahl, D.A., Amann, R., 1991. Development and application of nucleic acid probes. In Nucleic acid techniques in bacterial systematics., in: Stackebrandt, E., Goodfellow, M. (Eds.), Nucleic Acid Techniques in Bacterial Systematics. John Wiley & Sons Ltd., Chichester, United Kingdom, pp. 205–248.

Steinberg, L.M., Regan, J.M., 2008. Phylogenetic comparison of the methanogenic communities from an acidic, oligotrophic fen and an anaerobic digester treating municipal wastewater sludge. Appl. Environ. Microbiol. 74, 6663–6671. doi:10.1128/AEM.00553-08

Steven, B., Briggs, G., McKay, C.P., Pollard, W.H., Greer, C.W., Whyte, L.G., 2007. Characterization of the microbial diversity in a permafrost sample from the Canadian high Arctic using culture-dependent and culture-independent methods. FEMS Microbiol. Ecol. 59, 513–523. doi:10.1111/j.1574-6941.2006.00247.x

Steven, B., Lionard, M., Kuske, C.R., Vincent, W.F., 2013. High bacterial diversity of biological soil crusts in water tracks over permafrost in the High Arctic polar desert. PLoS One 8, e71489. doi:10.1371/journal.pone.0071489

Stoeva, M.K., Aris-Brosou, S., Chételat, J., Hintelmann, H., Pelletier, P., Poulain, A.J., 2014. Microbial community structure in lake and wetland sediments from a high Arctic polar desert revealed by targeted transcriptomics. PLoS One 9, e89531. doi:10.1371/journal.pone.0089531

Taberlet, P., Homme, S.M.P., Campione, E., Roy, J., Miquel, C., Shehzad, W., Gielly, L., Rioux, D., Choler, P., Clément, J.-C., Melodelima, C., Pompanon, F., Coissac, E., 2012. Soil sampling and isolation of extracellular DNA from large amount of starting material suitable for metabarcoding studies. Mol. Ecol. 21, 1816–1820. doi:10.1111/j.1365-294X.2011.05317.x

Takai, K.E.N., Moser, D.P., Flaun, M.D.E., Onstott, T.C., Fredrickson, J.K., 2001. Archaeal diversity in waters from deep South African gold mines. Appl. Environ. Microbiol. 67, 5750–5760. doi:10.1128/AEM.67.21.5750

Tang, X., Gao, G., Qin, B., Zhu, L., Chao, J., Wang, J., Yang, G., 2009. Characterization of bacterial communities associated with organic aggregates in a large, shallow, eutrophic freshwater lake (Lake Taihu, China). Microb. Ecol. 58, 307–322. doi:10.1007/s00248-008-9482-8

Tarasov, P.E., Andreev, A.A., Anderson, P.M., Lozhkin, A. V., Leipe, C., Haltia, E., Nowaczyk, N.R., Wennrich, V., Brigham-Grette, J., Melles, M., 2013. A pollen-based biome reconstruction over the last 3.562 million years in the Far East Russian Arctic – new insights into climate–vegetation relationships at the regional scale. Clim. Past 9, 2759–2775. doi:10.5194/cp-9-2759-2013

Tarnocai, C., Canadell, J.G., Schuur, E.A.G., Kuhry, P., Mazhitova, G., Zimov, S., 2009. Soil organic carbon pools in the northern circumpolar permafrost region. Global Biogeochem. Cycles 23, 1–11. doi:10.1029/2008GB003327

Taskin, B., Gozen, A.G., Duran, M., 2011. Selective quantification of viable Escherichia coli bacteria in biosolids by quantitative PCR with propidium monoazide modification. Appl. Environ. Microbiol. 77, 4329–4335. doi:10.1128/AEM.02895-10

Taylor, M.J., Bentham, R.H., Ross, K.E., 2014. Limitations of using propidium monoazide with qPCR to discriminate between live and dead Legionella in biofilm samples. Microbiol. Insights 7, 15–24. doi:10.4137/MBI.S17723.RECEIVED

Ter Braak, C.J.F., Šmilauer, P., 2012. CANOCO reference manual and user's guide: software for ordination (version 5).

Torti, A., Lever, M.A., Jørgensen, B.B., 2015. Origin, dynamics, and implications of extracellular DNA pools in marine sediments. Mar. Genomics 24, 185–196. doi:doi:10.1016/j.margen.2015.08.007

Tzedakis, P.C., 2010. The MIS 11 – MIS 1 analogy, southern European vegetation, atmospheric methane and the "early anthropogenic hypothesis." Clim. Past 6, 131–144. doi:10.5194/cp-6-131-2010

Van Everdingen, R., 2005. Multi-language glossary of permafrost and related ground-ice terms. National Snow and Ice Data Center/World Data Center for Glaciology. Boulder, Colorado, USA.

Vincent, W.F., Hobbie, J.E., Laybourn-Parry, J., 2008. Introduction to the limnology of high-latitude lake and river ecosystems, in: Vincent, W.., Laybourn-Parry, J. (Eds.), Polar Lakes and Rivers -Limnology of Arctic and Antarctic Aquatic Ecosystems. Oxford University Press, p. 346.

Wagner, A.O., Malin, C., Knapp, B.A., Illmer, P., 2008. Removal of free extracellular DNA from environmental samples by ethidium monoazide and propidium monoazide. Appl. Environ. Microbiol. 74, 2537–2539. doi:10.1128/AEM.02288-07

Wagner, D., Liebner, S., 2009. Permafrost Soils, Chapter 15: Global warming and carbon dynamics in permafrost soils: methane production and oxidation, Soil Biology, Soil Biology. Springer Berlin Heidelberg, Berlin, Heidelberg. doi:10.1007/978-3-540-69371-0

Wagner, D., Schirmack, J., Ganzert, L., Morozova, D., Mangelsdorf, K., 2013. Methanosarcina soligelidi sp. nov., a desiccation- and freeze-thaw-resistant methanogenic archaeon from a Siberian permafrost-affected soil. Int. J. Syst. Evol. Microbiol. 63, 2986–2991. doi:10.1099/ijs.0.046565-0

Walsh, J.E., Anisimov, O., Hagen, J.O.M., Jakobsson, T., Oerlemans, J., Prowse, T.D., Romanovsky, V., Savelieva, N., Shiklomanov, A., Shiklomanov, I., Solomon, S., Arendt, A., Atkinson, D., Demuth, M.N., Dowdeswell, J., Dyurgerov, M., Glazovsky, A., Koerner, R.M., Meier, M., Sigur, O., Steffen, K., Truffer, M., 2005. Cryosphere and Hydrology, in: ACIA Scientific Report, Chapter 6. pp. 183–242.

Wennrich, V., Minyuk, P.S., Borkhodoev, V., Francke, A., Ritter, B., Nowaczyk, N.R., Sauerbrey, M.A., Brigham-Grette, J., Melles, M., 2014. Pliocene to Pleistocene climate and environmental history of Lake El'gygytgyn, Far East Russian Arctic, based on high-resolution inorganic geochemistry data. Clim. Past 10, 1381–1399. doi:10.5194/cp-10-1381-2014

Whitman, W.B., Coleman, D.C., Wiebe, W.J., 1998. Prokaryotes : The unseen majority. Proc. Natl. Acad. Sci. U. S. A. 95, 6578–6583.

Willerslev, E., Cooper, A., 2005. Ancient DNA. Proc. R. Soc. London B 272, 3–16. doi:10.1098/rspb.2004.2813

Williams, K.H., Bargar, J.R., Lloyd, J.R., Lovley, D.R., 2013. Bioremediation of uranium-contaminated groundwater: A systems approach to subsurface biogeochemistry. Curr. Opin. Biotechnol. 24, 489–497. doi:10.1016/j.copbio.2012.10.008

Williamson, K.E., Kan, J., Polson, S.W., Williamson, S.J., 2011. Optimizing the indirect extraction of prokaryotic DNA from soils. Soil Biol. Biochem. 43, 736–748. doi:10.1016/j.soilbio.2010.04.017

Wuebbles, D.J., Hayhoe, K., 2000. Atmospheric methane: Trends and impacts., in: van Ham, J., Baede, A.P.M., Meyer, L.A., Ybema, R. (Eds.), Non-CO2 Greenhouse Gases: Scientific Understanding, Control and Implementation. Kluwer Academic Publishers, The Netherlands, pp. 1–44. doi:10.1007/978-94-015-9343-4_1

Yáñez, M.A., Nocker, A., Soria-Soria, E., Múrtula, R., Martínez, L., Catalán, V., 2011. Quantification of viable Legionella pneumophila cells using propidium monoazide combined with quantitative PCR. J. Microbiol. Methods 85, 124–130. doi:10.1016/j.mimet.2011.02.004

Yergeau, E., Hogues, H., Whyte, L.G., Greer, C.W., 2010. The functional potential of high Arctic permafrost revealed by metagenomic sequencing, qPCR and microarray analyses. ISME J. 4, 1206–1214. doi:10.1038/ismej.2010.41

Zhang, J., Kobert, K., Flouri, T., Stamatakis, A., 2014. PEAR: A fast and accurate Illumina Paired-End reAd mergeR. Bioinformatics 30, 614–620. doi:10.1093/bioinformatics/btt593

Zweifel, U.L., Hagström, Å., 1995. Total counts of marine bacteria include a large fraction of non-nucleoid-containing bacteria (ghosts). Appl. Environ. Microbiol. 61, 2180–2185. doi:0099-2240/95/$04.0010

Acknowledgements

I am grateful to the German Research Foundation (DFG) who funded this thesis as part of the priority program SPP 1006/18 under the grants WA-1554/14-1 and WA-1554/14-2. Moreover, I thank the German Research Centre for Geosciences (GFZ) and the University of Potsdam (UP) for giving me the opportunity to conduct this thesis.

I thank Prof. Dr. Dirk Wagner for his supervision, valuable discussions, and continuous support during my time as a PhD student. I am pleased that he has encouraged me to participate in two international conferences. Furthermore, I would like acknowledge Prof. Dr. Elke Dittmann and Prof. Dr. Dirk Schulze-Makuch for the evaluation of my dissertation.

Many thanks to Prof. Dr. Susanne Liebner for proofreading this thesis as well as to all of my co-authors and the reviewers of the manuscripts who helped to improve the manuscripts a lot.

Special thanks goes to Marcella Nega for all the enthusiastic work she did during her master thesis.

I am thankful to all former and current members of the “Geomics”. I won´t list everybody, please feel addressed in any case, but I would like to name in special Juliane Bischoff, Felizitas Bajerski, Janosch Schirmack, Mashal Alawi, Susanne Liebner, Fabian Horn, Jens Kallmeyer, Beate Schneider, Marcella Nega, Susann Kämpf, Julia Magritz, Nadja Torres Reyes, Steffi Genderjahn, Sizhong Yang, Roman Osudar, Andrea Kiss, Oliver Burckhardt, Anke Saborowski, Axel Kitte and Sybille Hahmann for working side by side in the laboratory, all the scientific discussions, friendly words, and support whenever necessary.

I am particularly grateful for the lab assistance of Ute Kuschel (AWI), Dyke Scheidemann (AWI), and Oliver Burckhardt (GFZ), as well as for the help during their student worker time of Julia Magritz, Marcella Nega, and Patryk Krauze.

I extend my deepest gratitude to the German Academic Exchange Service (DAAD), to Prof. Dr. Carsten Suhr Jacobson, and Jana Voříšková for the opportunity of my research visit in Denmark. Scientifically, I was very well supported and I have felt very comfortable with all of

you. A big thank to all of my Danish colleagues, namely to Jana Voříšková, Carsten Suhr Jacobsen, Morten Nielsen, Toke Bang-Andreasen, Jeppe Nielsen, Mads Bolander, Karen Cameron, Pia Jakobsen, Merian Haugwitz, Karen Bjerre, Nikoline Olsen, and Ernesto Kettner.

Specifically, I thank for the financial support of the University of Potsdam/Coordination Office for Equal Opportunities (Brückenprogramm zur Förderung des Promotionsabschlusses) within the final period of my dissertation.

Moreover, I am grateful for the opportunity to be a mentee of the Mentoring Plus Program 2015-2016 of the Potsdam Graduate School (PoGS), an individual career development program for highly qualified women.

I thank the Potsdam Graduate School (PoGS), the Federation of European Microbiological Society (FEMS) and the Association for General and Applied Microbiology (VAAM) for their financial travel support to attend to national and international conferences.

A big thank to Anna Maria Przybycin, Christin Lubitz, and Tobias Weber. Your enthusiastic work during your and my time as PhD representative leads to a wonderful friendship. Thank you for making life on and off the Telegrafenberg much more pleasant.

My most sincere gratitude to my family, and in particular to my parents, always believing in me and supporting me with positive energy and lots of heartiness.

Finally, I want to thank my husband Arvid for being in any situation my tower of strength, for all his support and unbroken encouragement during my time as PhD candidate. Without you I would not have managed it.

Selbstständigkeitserklärung

Die vorliegende Dissertation wurde von mir am Deutschen GeoForschungsZentrum in Potsdam angefertigt und in englischer Sprache geschrieben.

Hiermit versichere ich an Eides statt, dass die vorliegende Arbeit selbstständig und unter Verwendung keiner anderen als der angegebenen Hilfsmittel verfasst wurde. Die Dissertation wurde bei keiner anderen Hochschule zur Begutachtung eingereicht.

(Janine Heise)	(Potsdam, Februar 2017)
Unterschrift	Ort, Datum

Appendix A

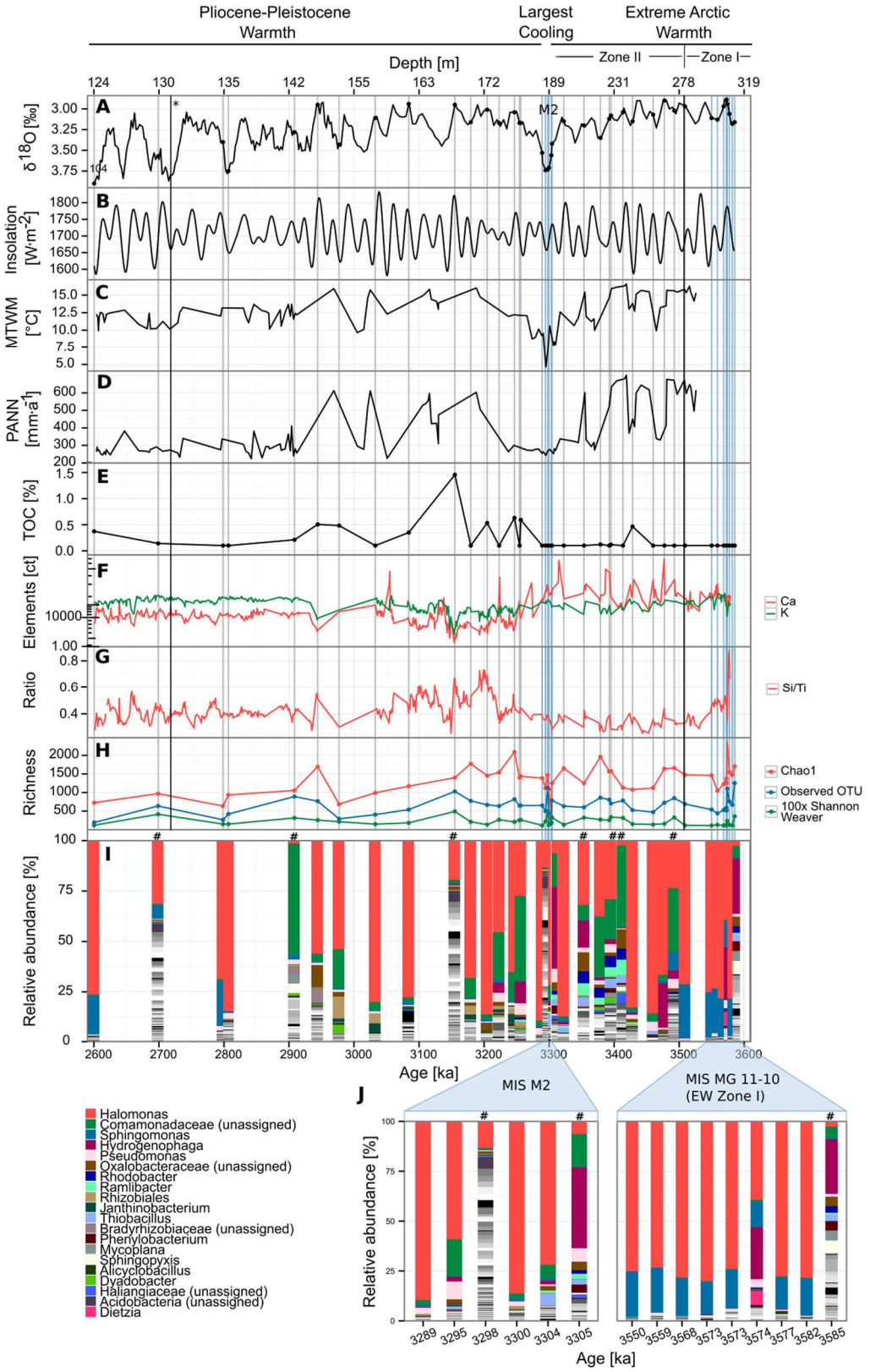

Figure A.1: Complete version of Figure 3.2: Mid- to late-Pliocene: Comparison of the microbial diversity and community composition, the reconstructed paleo-climatological conditions and other influencing environmental parameter with (**A**) global marine isotope stack in ‰ ($\delta^{18}O$, Lisiecki & Raymo (2005), M2 = Largest cooling in

Pliocene, * = onset of northern hemisphere glaciation, 104 = first glacial, (**B**) 65°N summer insolation in W m^{-2} (Laskar et al., 2004), (**C**, **D**) reconstructed mean temperature of the warmest month (MTWM) in °C and annual precipitation (PANN) in mm a^{-1} based on pollen spectra (Tarasov et al., 2013, within first 20 ka no pollen could be detected and therefore no reconstruction of the MTWM and PANN is available), (**E**) total organic carbon (TOC) in %, (**F**, **G**) calcium and potassium composition as well as Mn/Fe and Si/Ti ratio measured with XRF laser scanning (Wennrich et al., 2014), (**H**) microbial diversity measurements expressed as the number of observed OTU, the Chao1 richness estimates, and the evenness-emphasizing Shannon-Weaver index (multiplied by 100), (**I**) relative abundance of microbial taxa (> 0.1% abundance; legend is sorted by frequency and shows the most abundant 20 taxa in color; additional taxa are shown in shades of grey), and (**J**) expanded view into microbial community of the extreme Arctic warmth Zone I (MIS MG 10-11) and the largest cooling in Pliocene (MIS M2). Please note that all parameters are mapped to the age incorporating the specific sedimentation rates (up to 1 order of magnitude difference) of the age-depth model by Nowaczyk et al., 2013. Sediment layers with a Shannon-Weaver index above 3 and therefore an outstandingly high number of abundant OTUs (55-175 taxonomic categories above 0.1% of the total relative abundance) are indicated by pound signs.

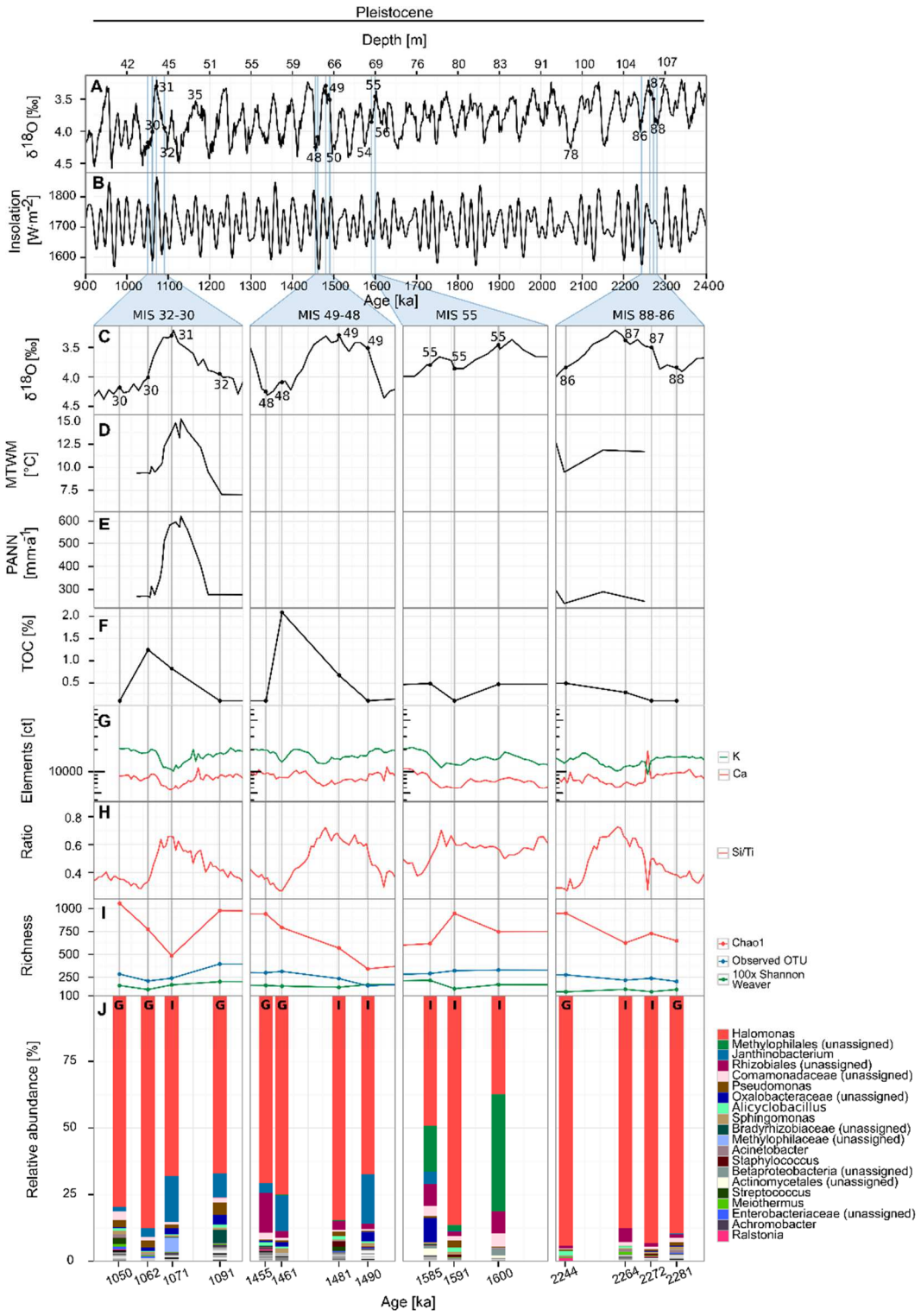

Figure A.2: Complete version of Figure 3.3: Interglacial/glacial cyclicity of the Pleistocene (super interglacial MIS 31, 49, 55, 87): Comparison of the microbial diversity and community composition, the reconstructed paleo-climatological conditions and other influencing environmental parameter with (**A**) global marine isotope stack in ‰ ($\delta^{18}O$, Lisiecki & Raymo (2005), (**C**) detailed view in global marine isotope stack in ‰, (**D, E**) reconstructed mean temperature of the warmest month (MTWM) in °C and annual precipitation (PANN) in mm a^{-1}, not determined for MIS 65-48, (**F**) total organic carbon (TOC) in %, (**G, H**) calcium and potassium composition as well as Mn/Fe and Si/Ti ratio measured with XRF laser scanning (Wennrich et al., 2014), (**I**) microbial diversity measurements expressed as the number of observed OTU, the Chao1 richness estimator, and the evenness-

emphasizing Shannon-Weaver index (multiplied by 100), and (**J**) relative abundance of microbial taxa (> 0.1% abundance; legend is sorted by frequency and shows the most abundant 20 taxa in color; additional taxa are shown in shades of grey). Please note that all parameter are mapped to the age incorporating the specific sedimentation rates (up to 1 order of magnitude difference) of the age-depth model by Nowaczyk et al., 2013. G: Glacial period, I: Interglacial period

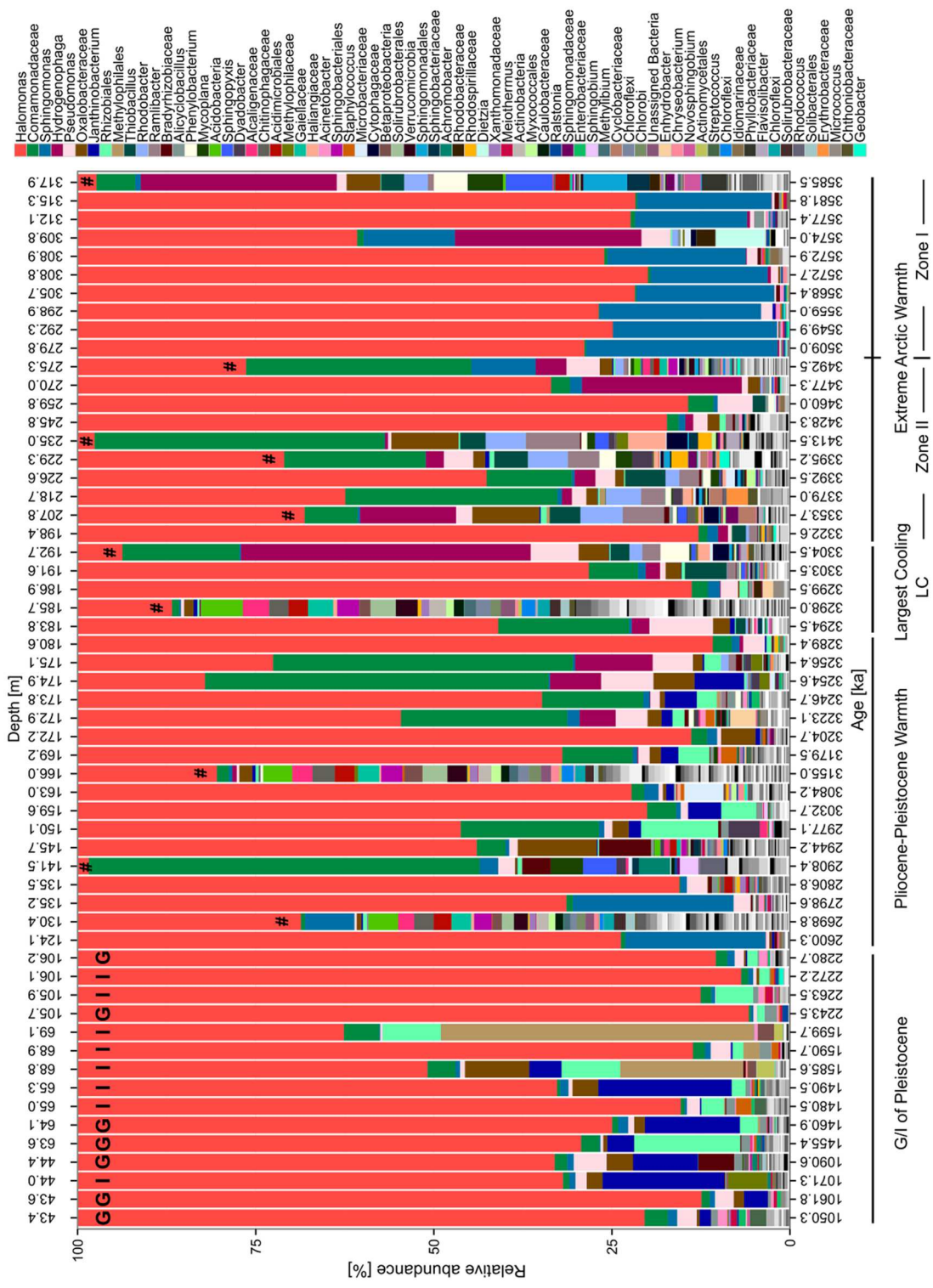

Figure A.3: Relative abundance of phylogenetic taxa in dependence of the sediment depth (visible are all taxa with a relative abundance above 0.1%). Legend is sorted by frequency and shows the most abundant 70 taxa in color. Additional taxa are shown in shades of gray to indicate the high degree of microbial diversity. Sediment layers with a Shannon-Weaver index above 3 and therefore an outstandingly high number of abundant OTUs (55-175 taxonomic categories above 0.1% of the total relative abundance) are indicated by pound signs. G: Glacial period, I: Interglacial period.

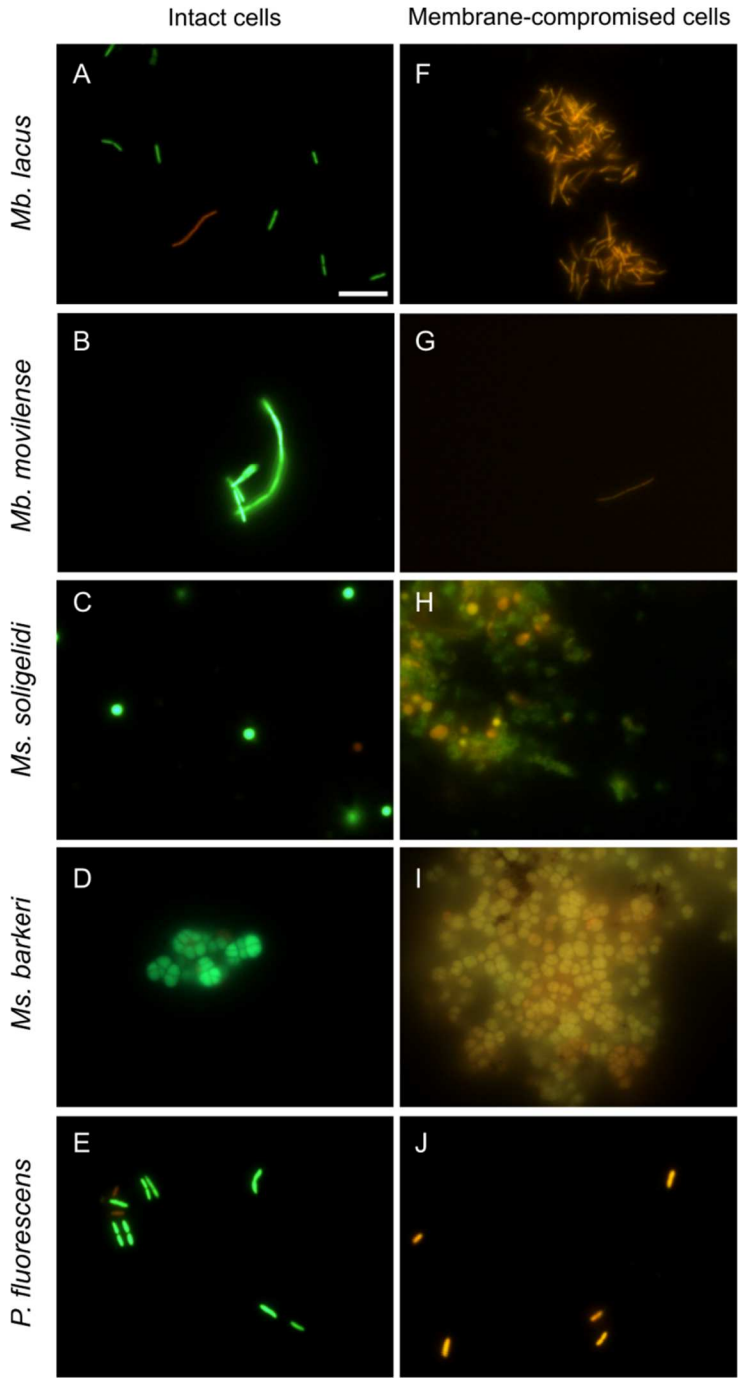

Figure A.4: Staining of methanogenic archaeal strains with the LIVE/DEAD® BacLight™ kit (filter system FI/RH, Leica) in comparison to the bacterial reference strain. Intact and membrane-compromised cells of *Methanobacterium lacus* (**A, F**), *Methanobacterium movilense* (**B, G**), *Methanosarcina soligelidi* (**C, H**), *Methanosarcina barkeri* (**D, I**), and the γ-*Proteobacteria Pseudomonas fluorescens* as a reference strain (**E, J**). SYTO 9 (green) stained all of the bacterial or archaeal cells, whereas PI (red) only penetrated cells with damaged membranes. After isopropanol killing, both strains of *Methanosarcina* formed a dense aggregate of cells and medium components. Bar, 10 µm.

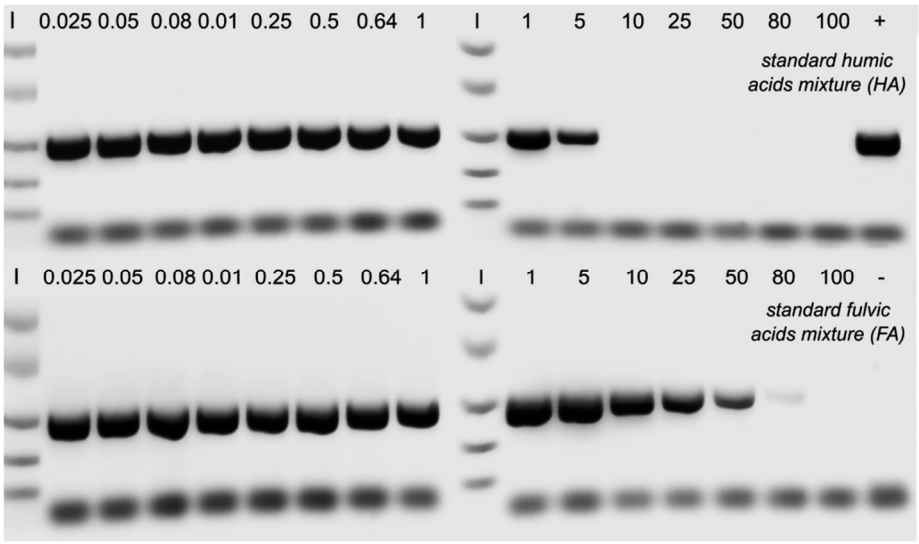

Figure A.5: Inhibition of the iTaq polymerase activity in dependence to an increasing concentration of humic substances (range of 0.025 and 100 µg mL^{-1}). The PCR amplicons in the agarose gel indicate that the effect on the polymerase is smaller for fulvic acids (no amplification for 100 µg mL^{-1}) than for humic acids (no amplification between 10 and 100 µg mL^{-1}). Ladder: Easy Ladder I (Bioline).

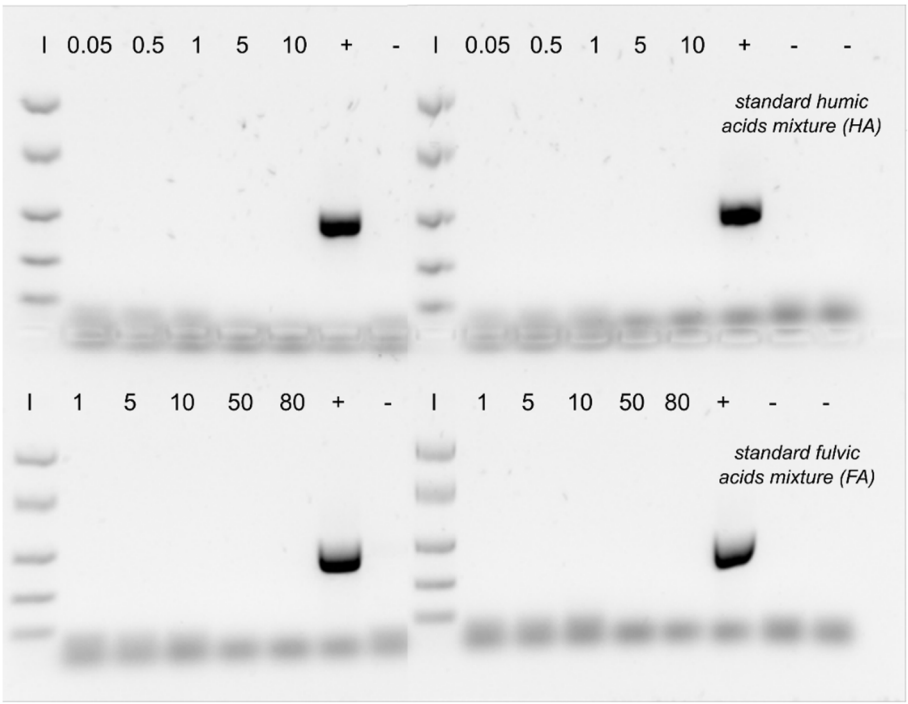

Figure A.6: The PCR amplicons in the agarose gel indicate no influence of different concentrations of humic substances (HA: 0.05 to 10 µg mL-1, FA: 1 to 80 µg mL-1) on a PMA treatment. The 10 ng μL^{-1} of free DNA was successfully suppressed by PMA for all concentrations of humic and fulvic acids. Ladder: Easy Ladder I (Bioline).

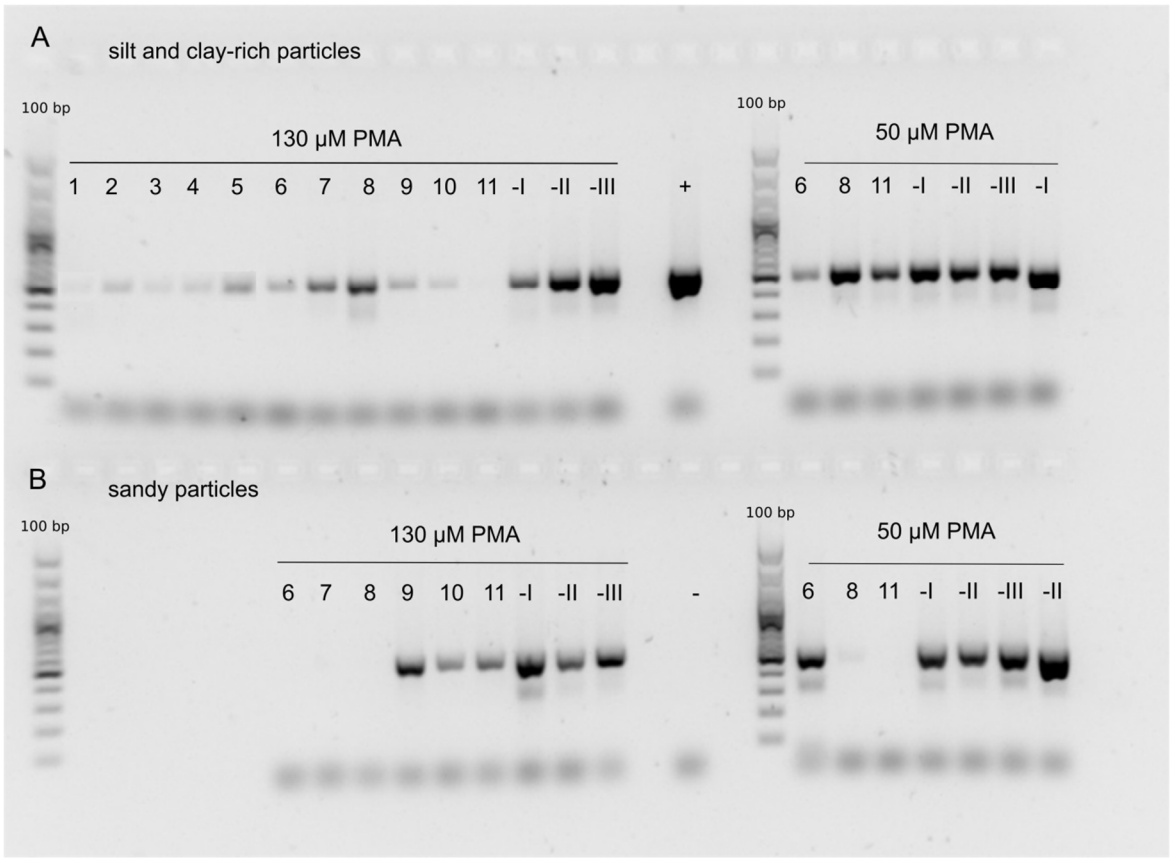

Figure A.7: Influence of sediment/soil matrix on a PMA treatment. Agarose gel of PCR amplicons, whereby different concentrations of silt and clay-rich sediment (**A**) or sandy soil (**B**) were added prior PMA treatment (50 µM, 130 µM) to a 10 ng/µL DNA mixture. Increasing Arabic numerals indicate higher concentrations of double autoclaved material (1 to 11: 0.6, 1, 5, 10, 25, 50, 100, 200, 500, 600, 1000 mg mL-1) per reaction. A PMA concentration of 50 µM was not sufficient to inhibit the DNA. For 130 µM PMA, an amplification of DNA was mainly shown for the silt and clay-rich sediments, whereas a sufficient inhibition of free DNA was possible in sandy soil up to 200 mg mL-1 (No. 8). Roman numerals are controls, where PMA does not inhibit the amplification of free DNA (-I: without PMA and light, -II: without light but with PMA addition, -III: without PMA but with light exposure).

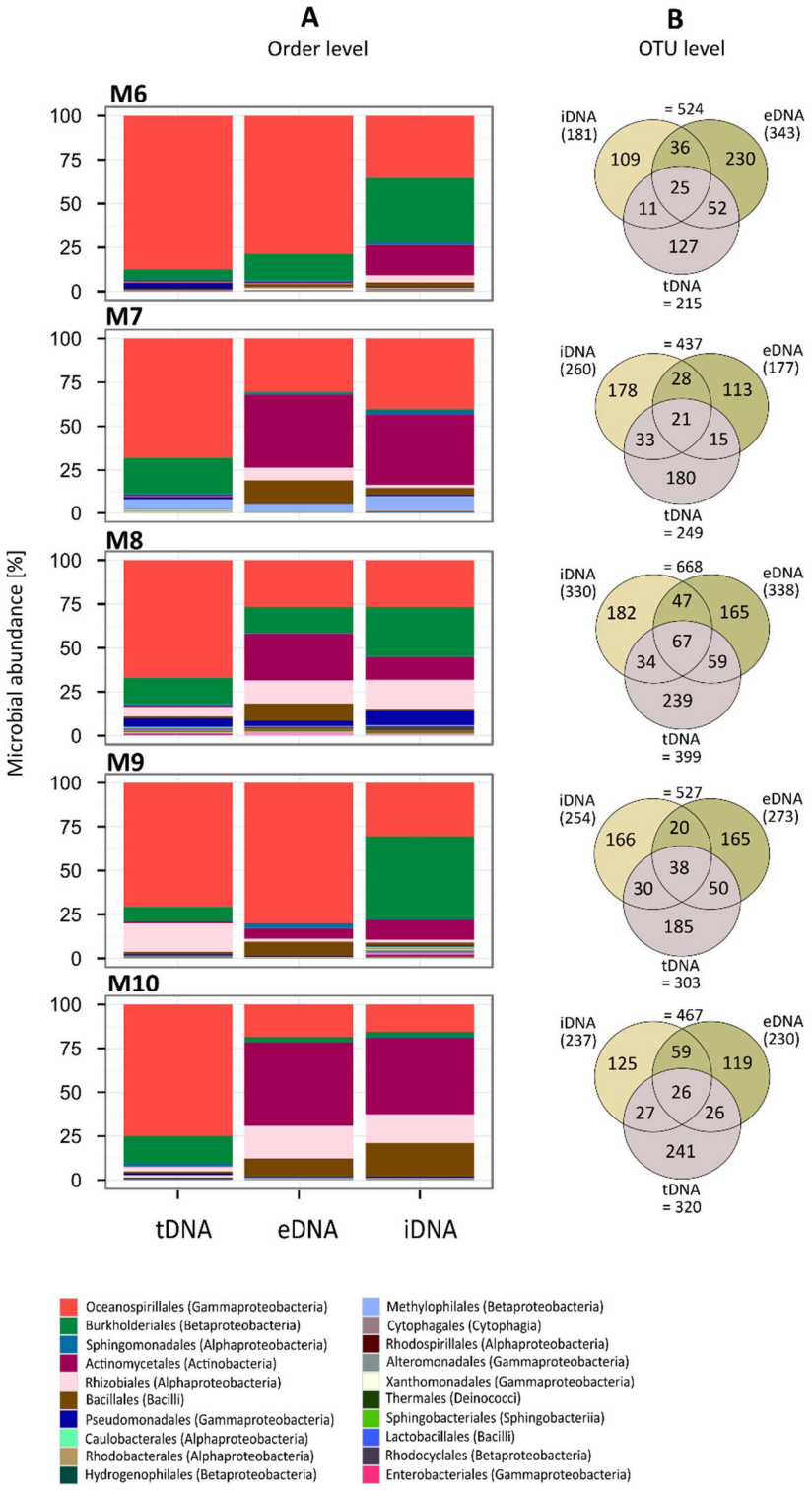

Figure A.8: Additional investigated El'gygytgyn sediments beyond Figure 3.14: Taxonomic composition of the microbial community in El'gygytgyn deep lake sediments with (**A**) the relative abundance on phylogenetic order-level for the total (tDNA) as well as the extra- (eDNA) and intracellular (iDNA) DNA pool, and (**B**) the number of unique OTUs per DNA pool and the number of OTU-level taxonomic overlaps between the three DNA pools presented as Venn diagrams.

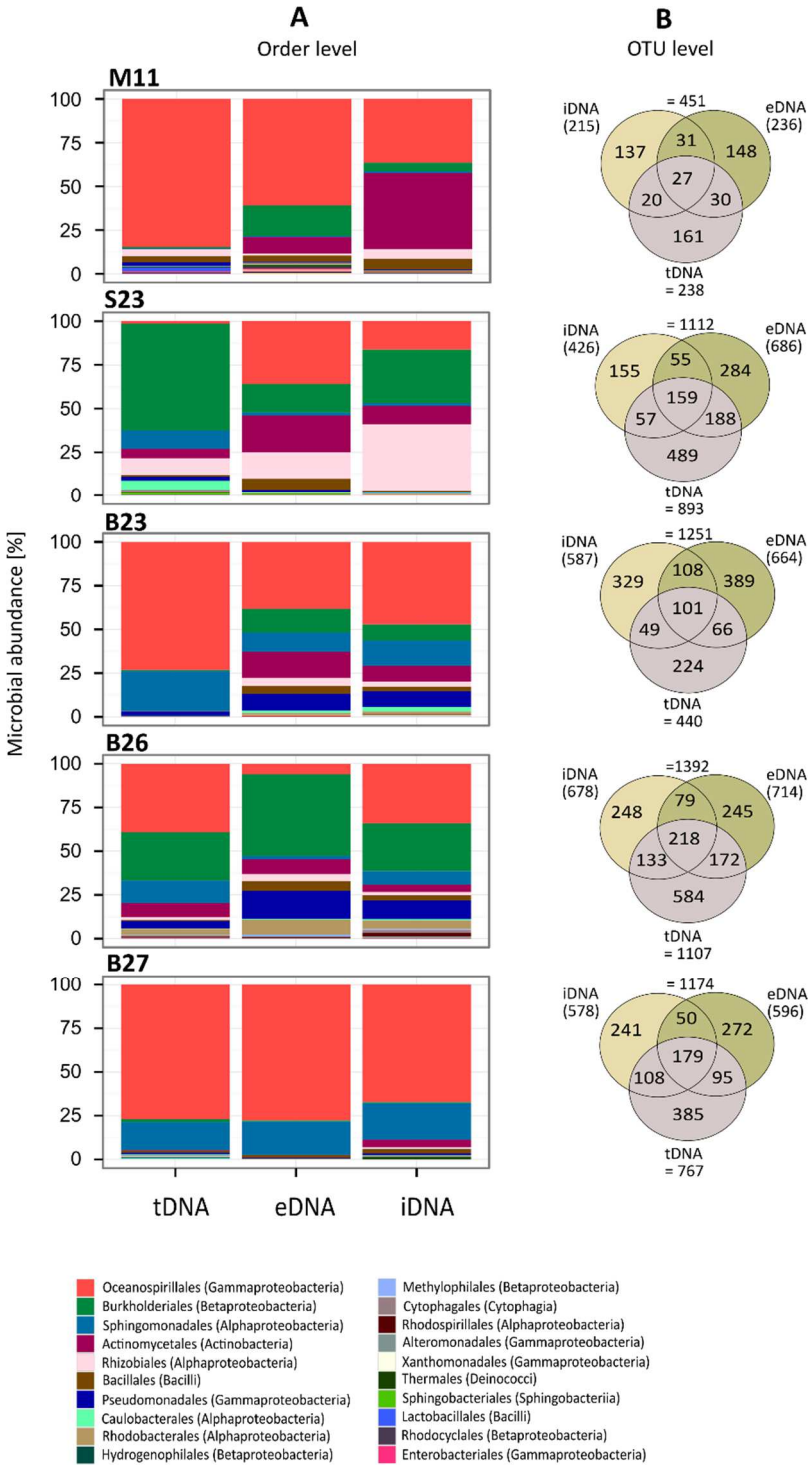

Figure A.9: Continued

Table A.1: Phylogenetic assignment of the 20 most abundant bacterial OTUs according to the Greengenes database (13_8-release; DeSantis et al., 2006, used in QIIME pipeline), as well as to the NCBI blast (BLASTN 2.2.30+, nucleotide collection, January 2015). Mean relative abundance is calculated within all samples and highlighted in colors within the different geological timescales (dark red = >50%, >bright red > bright green > dark green = 0%). Cover: Query Cover, RA: mean relative abundance, SD: Standard deviation, EW: Extreme arctic warmth, LC: Largest cooling in Pliocene, PPW: Pliocene-Pleistocene warmth, G: Glacial periods, I: Interglacial periods. Statistical significant differences in relative abundance among different climatic conditions are indicated with different letters (t-test, $p < 0.005$).

	Greengenes				NCBI blast					Abundance							
OTU number	**Best idenified hit**	**Class**	**Order**	**Family**	**Best idenified hit (accession number)**	**Cover (%)**	**E-value**	**Similarity [%]**	**Source**	**RA [‰]**	**SD [‰]**	**EW**	**LC**	**PPW**	**G**	**I**	
OTU_1815	Halomonas campisalis	γ-Proteob.	Oceanospirillales	Halomonadaceae	Halomonas campisalis strain BMEN3 16S ribosomal RNA gene, partial sequence (**KC480069.1**)	98	2,00E-143	99	Saline-alkali lake [1]	488.5	214.9	bc	bc	c	b	bc	ubiquitous
OTU_23248	Halomonas	γ-Proteob.	Oceanospirillales	Halomonadaceae	Halomonas sp. JSM 102054 16S ribosomal RNA gene, partial sequence (**KM093735.1**)	98	2,00E-148	99	Dehang Canyon	115.1	54.1	b	c	c	b	b	
OTU_53875	Rhizobiales	α-Proteob.	Rhizobiales	Methylocystaceae	Methylocystis sp. enrichment culture clone PPN M1.20 16S ribosomal RNA gene, partial sequence (**KJ657742.1**)	98	2,00E-143	99	Endophytic aerobic methanotrophs isolated from Sphagnum	14.1	29.2	c	b	abc	abc	a	highly abundant in G/I
OTU_6506	Janthinobacterium lividum	β-Proteob.	Burkholderiales	Comamonadaceae	Janthinobacterium sp. MsC-03-4CB3-01 gene for 16S rRNA, partial sequence (**AB991685.1**)	98	2,00E-143	99	Glacier ice worm [2]	16.8	37.4	c	bc	b	b	b	
OTU_52410	Methylophilales	β-Proteob.	Methylophilales	Methylophilaceae	Uncultured Methylophilus sp. clone S206 16S ribosomal RNA gene, partial sequence (**JN217077.1**)	98	2,00E-138	99	Anaerobic culture [3]	11.5	62.1	bc	bc	b	bc	c	
OTU_55992	Comamonadaceae	β-Proteob.	Burkholderiales	Comamonadaceae	Acidovorax ebreus 16S ribosomal RNA gene, partial sequence (**KM287569.1**)	98	2,00E-143	99	Active sludge	7.5	10.8	c	b	b	b	b	
OTU_34519	Sphingomonas	α-Proteob.	Sphingomonadales	Sphingomonadaceae	Sphingomonas sp. Lor54 16S ribosomal RNA gene, partial sequence (**KJ016215.1**)	98	2,00E-143	99	Lichen substances, China	46.3	77.6	c	b	b	b	b	more abundant in deep biosphere
OTU_20144	Pseudomonas stutzeri	γ-Proteob.	Pseudomonadales	Pseudomonadaceae	Pseudomonas sp. GMCo37 16S ribosomal RNA gene, partial sequence (**KM370370.1**)	98	2,00E-143	99	Coastal & marine ecosystems	8.9	13.3	b	c	bc	b	b	
OTU_34393	Oxalobacteraceae	β-Proteob.	Burkholderiales	Oxalobacteraceae	Undibacterium sp. MsC-14-4CH2-11 gene for 16S rRNA, partial sequence (**AB991658.1**)	98	5,00E-145	99	Glacier ice worm [2]	6.5	16.2	c	b	bc	b	b	
OTU_41489	Comamonadaceae	β-Proteob.	Burkholderiales	Comamonadaceae	Polaromonas sp. MsC-08-1CB1-02 gene for 16S rRNA, partial sequence (**AB991680.1**)	98	5,00E-146	99	Glacier ice worm [2]	19.9	69.0	bc	c	bc	b	bc	
OTU_23867	Comamonadaceae	β-Proteob.	Burkholderiales	Comamonadaceae	Acidovorax defluvii strain RK 16S ribosomal RNA gene, partial sequence (**KJ643429.1**)	98	2,00E-148	99	Contaminated aerated sediment	17.4	35.2	c	b	b	bc	bc	
OTU_46908	Comamonadaceae	β-Proteob.	Burkholderiales	Comamonadaceae	Ramlibacter sp. WSR16 16S ribosomal RNA gene, partial sequence (**KC485331.1**)	98	1,00E-146	99	Endophyte Bacteria from JiDong wild soybean	5.1	11.3	bc	c	bc	b	b	
OTU_976	Comamonadaceae	/	/	/	Uncultured bacterium partial 16S rRNA gene, isolate Mineral.top.2.1.6_18288 (**LN541625.1**)	98	1,00E-146	99	Sand filters for groundwater treatment [4]	24.9	57.8						
OTU_26244	Hydrogenophaga	β-Proteob.	Burkholderiales	Comamonadaceae	Hydrogenophaga sp. IDSBO-1 16S ribosomal RNA gene, partial sequence (**KM199760.1**)	98	2,00E-143	99	Contaminated mine sediments	20.7	51.2						not present in G/I
OTU_37985	Thiobacillus	β-Proteob.	Hydrogenophilales	Hydrogenophilaceae	Uncultured Thiobacillus sp. clone PS107 16S ribosomal RNA gene, partial sequence (**KF517403.1**)	98	2,00E-143	99	Shrimp culture pond sediment, India	5.9	14.5						
OTU_27115	Hydrogenophaga	β-Proteob.	Methylococcales	Methylococcaceae	Antarctic bacterium R-9284 partial 16S rRNA gene, strain R-9284 (**AJ441011.1**)	98	2,00E-148	99	Microbial mats from ten Antarctic lakes [5]	3.4	13.7						
OTU_16240	Rhodobacter	α-Proteob.	Rhodobacterales	Rhodobacteraceae	Uncultured Gemmobacter sp. clone C2_313 16S ribosomal RNA gene, partial sequence (**KP016245.1**)	98	2,00E-143	99	Surface layer sediment from Jiaojiang Estuary	5.5	14.4						
OTU_54541	Oxalobacteraceae	Betaproteobacteria	Burkholderiales	Oxalobacteraceae	Herminiimonas sp. S3H39 partial 16S rRNA gene, isolate S3H39 (**HE814796.2**)	98	2,00E-143	99	Arctic plants from low arctic fell tundra [6]	5.4	16.1						
OTU_12536	Ramlibacter	β-Proteob.	Burkholderiales	Comamonadaceae	Caenimonas sp. TSX9-5 16S ribosomal RNA gene, partial sequence (**HM156151.1**)	98	2,00E-143	99	Soil from glacier forefield	5.6	14.1						
OTU_53072	Hydrogenophaga	β-Proteob.	Burkholderiales	Comamonadaceae	Hydrogenophaga sp. AT08-09 16S ribosomal RNA gene, partial sequence (**KM349947.1**)	98	1,00E-145	99	UV-C resistant microorganisms from manganese deposits in desert	6.1	33.6						

[1] Yan Gua et al. Heterotrophic nitrification and aerobic denitrification by a novel Halomonas campisalis [2013]. Biotechnol Lett. 2013 Dec;35(12):2045-9. doi: 10.1007/s10529-013-1294-3. Epub 2013 Aug 2.

[2] Murakami et al 2015 Census of bacterial microbiota associated with the glacier ice worm Mesenchytraeus solifugus. FEMS microbiology ecology

[3] Liu J et al Molecular characterization of a microbial consortium involved in methane oxidation coupled to denitrification under micro-aerobic conditions. Microb Biotechnol. 2014 Jan;7(1):64-76. doi: 10.1111/1751-7915.12097. Epub 2013 Nov 19.

[4] Gülay et al. 2014. Internal porosity of mineral coating supports microbial activity in rapid sand filters for groundwater treatment. Appl Environ Microbiol. 2014 Nov;80(22):7010-20. doi: 10.1128/AEM.01959-14. Epub 2014 Sep 5.

[5] Trappen et al 2002 Diversity of 746 heterotrophic bacteria isolated from microbial mats from ten Antarctic lakes. Syst Appl Microbiol. 2002 Dec;25(4):603-10.

[6] Nissinen et al 2012 Endophytic bacterial communities in three arctic plants from low arctic fell tundra are cold-adapted and host-plant specific. FEMS Microbiol Ecol. 2012 Nov;82(2):510-22. doi: 10.1111/j.1574-6941.2012.01464.x. Epub 2012 Aug 2

Table A.2: Overview of the total read numbers, total OTU numbers, and Shannon-Weaver and Chao1 indices of all Pleistocene and Pliocene sediment samples.

	MIS	Depth [m]	Sample Age [ka]	Total Reads*	Total OTUs*,§	Shannon-Weaver Index£	Chao1
Pleistocene	30	43.5	1050.3	37661	287	1.60	1057
	30	43.6	1061.8	25543	215	1.17	775
	31	43.9	1071.3	37816	249	1.67	484
	32	44.4	1090.6	51909	399	2.03	978
	48	63.6	1455.4	45602	303	1.62	943
	48	64.1	1460.9	47443	320	1.54	793
	49	65.0	1480.5	29143	238	1.42	569
	49	65.3	1490.5	18467	163	1.69	343
	55	68.8	1585.6	35988	295	2.16	618
	55	69.0	1592.6	48828	328	1.26	947
	55	69.1	1603.9	51542	332	1.70	748
	86	105.7	2243.5	36386	282	0.92	949
	87	106.0	2263.5	24052	222	1.18	625
	87	106.1	2272.2	39679	247	0.93	729
	88	106.2	2280.7	28985	207	1.17	648
	104	124.1	2600.3	36713	193	1.17	725
Pliocene	G5	130.4	2698.8	35818	655	4.15	969
	G10	135.2	2798.6	36633	270	1.50	636
	G10	135.5	2806.8	72696	421	1.49	935
	G15	141.5	2908.4	141458	893	3.15	1054
	G17	145.7	2944.2	137096	780	2.56	1694
	G18	150.1	2977.1	70133	293	2.13	685
	G21	159.5	3032.7	92450	409	1.48	991
	K1	163.0	3084.2	131599	569	1.82	1169
	KM3	166.0	3155.0	98476	1052	4.91	1399
	KM4	169.2	3179.5	144631	783	2.11	1771
	KM5	172.2	3204.7	127491	668	1.35	1453
	KM6	173.0	3223.1	115327	640	2.67	1541
	M1	174.0	3246.7	160674	818	2.07	2087
	M1	175.0	3254.6	181350	651	2.56	1398
	M1	175.1	3256.4	124423	653	2.63	1438
	M1	180.6	3289.4	157316	651	1.13	1385
	M2	183.8	3294.5	76817	502	2.21	1117
	M2	185.7	3298.0	130701	1165	5.01	1466
	M2	186.9	3299.5	95926	441	1.25	1084
	M2	191.6	3303.5	3972	172	1.93	355
	M2	192.7	3304.5	115492	799	3.24	1252
	MG1	198.3	3322.6	134124	638	1.32	1652
	MG3	207.8	3353.7	72363	604	3.24	1248
	MG4	218.7	3379.0	148030	864	2.70	1958
	MG5	226.6	3392.5	135108	813	2.54	1566
	MG5	229.2	3395.2	105306	708	3.37	1574

	MG5	235.0	3413.5	169452	793	3.16	1132
	MG5	245.8	3428.3	121718	535	1.51	1076
	MG6	259.8	3460.0	99453	472	1.37	1125
	MG7	270.0	3477.3	165537	729	1.58	1638
	MG7	275.3	3492.5	103257	865	3.27	1660
	MG7	279.8	3509.0	130881	696	1.16	1476
	MG10	292.3	3549.9	117952	543	1.12	1460
	MG10	299.0	3559.0	103068	440	1.29	1047
	MG11	305.7	3568.4	125547	533	1.12	1222
	MG11	308.8	3572.7	157755	591	1.15	1372
	MG11	308.9	3572.9	105505	518	1.37	1254
	MG11	309.7	3574.0	207788	1107	2.34	2360
	MG11	312.1	3577.4	225569	767	1.29	1548
	MG12	315.3	3581.8	176916	673	1.12	1473
	MG12	317.9	3585.5	140485	1272	3.57	1706
		177.0 [Ø]	2841.0 [Ø]	98106 [Ø]	557 [Ø]	2.00 [Ø]	65985 [Ø]

[*]after stringent quality filtering and removing of singletons
[§]OTU threshold at a 97% similarity level, clustering using de-novo UCLUST algorithm (Edgar et al., 2010) selection of representative sequences with cluster seed method
[£]calculated in R statistical environment (R Development Core Team, r-project.org) using function *estimate_richness*
[Ø] mean value

Table A.3: Overview of the sediment characteristics of the 14 El'gygytgyn Crater Lake sediments used for cell separation.

	Sample_ID	MIS	Depth [m]	Sample Age [ka]	Benthic d18O (‰)#	TOC [%]	TC [%]	TN [%]	Water content [%]	Sand [%]	Silt [%]	Clay [%]
Pleistocene	M5	30	43.5	1050.3	4.23	< 0.10	0.25	< 0.10	36.1	26.1	53.0	20.9
	M6	30	43.6	1061.8	4.01	1.246	1.59	< 0.10	36.1	19.2	57.7	23.1
	M7	31	43.9	1071.3	3.28	0.824	1.18	0.104	58.3	24.1	62.1	13.7
	M8	32	44.4	1090.6	3.98	< 0.10	0.28	< 0.10	38.3	24.1	58.0	17.9
	M9	48	63.6	1455.4	4.26	< 0.10	0.26	< 0.10	30.5	16.7	60.9	22.4
	M10	48	64.1	1460.9	4.09	2.089	2.10	< 0.10	23.0	20.9	58.4	20.7
	M11	49	65.0	1480.5	3.42	0.674	0.95	< 0.10	48.3	28.1	55.3	16.7
	M12	49	65.3	1490.5	3.64	< 0.10	0.25	< 0.10	40.0	27.4	55.6	17.0
Pliocene	S23	G15	141.5	2908.4	3.28	0.211	0.38	< 0.10	16.4	17.4	71.6	11.0
	B10	M2	186.9	3299.5	3.72	< 0.10	0.19	< 0.10	31.1	18.3	66.6	15.1
	B23	MG10	299.0	3559.0	3.13	< 0.10	0.26	< 0.10	29.5	30.1	58.1	11.8
	B26	MG11	309.7	3574.0	2.93	< 0.10	0.27	< 0.10	15.0	43.9	47.1	8.9
	B27	MG11	312.1	3577.4	3.06	< 0.10	0.44	< 0.10	30.0	23.3	50.8	25.9
	B28	MG12	315.3	3581.8	3.17	< 0.10	0.33	< 0.10	18.0	24.6	67.1	8.2
			Ø 143	Ø 2.190	Ø 3.6	Ø 0.43	Ø 0.6	Ø < 0.1	Ø 32	Ø 25	Ø 59	Ø 17

Table A.4: Overview of the total read numbers, OTU numbers (for Bacteria, Archaea and unassigned OTUs), as well as Shannon-Weaver and Chao1 indices of the different DNA pools (total DNA; extra- and intracellular DNA) of the 14 El'gygytgyn Crater Lake sediments.

	Sample_ID	Total Reads*			Bacteria OTUs*,§			Archaea OTUs*,§			Unassigned OTUs*,§			Shannon-Weaver Index£			Chao1£		
		tDNA	eDNA	iDNA	tDNA	eDNA	iDNA	tDNA	eDNA	iDNA	tDNA	eDNA	iDNA	tDNA	eDNA	iDNA	tDNA	eDNA	iDNA
Pleistocene	M5	37661	62654	40913	285	230	309	0	1	1	2	3	3	1.6	1.0	2.0	1057.4	492.1	977.9
	M6	25543	46706	14220	210	338	170	1	2	2	4	3	9	1.2	1.4	2.2	774.8	918.1	425.2
	M7	37816	34519	39232	240	170	252	4	2	4	5	5	4	1.7	2.3	2.1	484.5	509.0	827.7
	M8	51909	45849	40234	396	335	324	1	1	4	2	2	2	2.0	2.8	2.7	978.5	890.9	788.4
	M9	45602	45478	36715	300	269	250	2	3	2	1	1	2	1.6	1.4	2.3	943.5	683.6	512.2
	M10	47443	39861	45064	315	222	230	3	6	5	2	2	2	1.5	2.3	2.4	793.6	730.6	699.0
	M11	29143	27156	35396	236	232	208	0	2	2	2	2	5	1.4	2.0	2.1	569.1	880.7	652.0
	M12	18467	27121	34168	157	176	300	3	0	4	3	4	4	1.7	2.0	1.9	342.9	468.8	800.8
Pliocene	S23	141458	95954	89909	890	684	425	3	2	0	0	0	1	3.2	2.8	2.2	1053.9	1310.1	956.1
	B10	95926	38835	129483	436	302	671	4	2	0	1	1	1	1.3	1.2	2.4	1084.2	879.5	1602.1
	B23	103068	170398	147569	437	661	585	0	1	0	3	2	2	1.3	2.5	2.4	1047.3	1527.3	1319.8
	B26	207788	158584	126949	1102	711	677	1	2	0	4	1	1	2.3	2.7	2.7	2360.4	1221.5	1843.0
	B27	225569	190837	131348	758	595	574	5	0	3	4	1	1	1.3	1.1	1.6	1548.3	1534.4	1367.2
	B28	176916	89594	151282	671	405	729	1	4	2	1	0	4	1.1	1.4	2.9	1473.4	1145.4	1238.6
		Ø 88879	Ø 76682	Ø 75892	Ø 460	Ø 381	Ø 407	Ø 2	Ø 2	Ø 2	Ø 2	Ø 2	Ø 3	Ø 2	Ø 2	Ø 2	Ø 1037	Ø 942	Ø 1001

Pliocene-Pleistocene stack of δ18O records (LR04 stack) by Lisiecki & Raymo, 2005

*after stringent quality filtering and removing of global singletons

§OTU threshold at a 97% similarity level, clustering using de-novo UCLUST algorithm (Edgar, 2010) selection of representative sequences with cluster seed method

£calculated in R statistical environment (R Development Core Team, r-project.org) using function estimate_richness (phyloseq package, McMurdie & Holmes, 2013)

Ø mean value

Supplementary file/Dataset (.xls):

Dataset 1: OTU abundance table of 57 El'gygytgyn deep biosphere sediments, representing the data basis of all plots as well as further analyses of this study. The absolute abundances of all detected OTUs are shown for each sediment sample.

Dataset 2**:** OTU abundance table of 14 deep sediment samples of the El'gygytgyn Crater Lake, separately for the total DNA pool (tDNA) as well as the extracellular (eDNA) and intracellular (iDNA) pool. The OTU table includes the absolute number of all detected OTUs for each sediment sample and DNA pool.